New inhibitory pathways in CD8 T cell function

Dissertation

zur

Erlangung des Doktorgrades (Dr. rer. nat.)

der

Mathematisch-Naturwissenschaftlichen Fakultät

der

Rheinischen Friedrich-Wilhelms-Universität Bonn

vorgelegt von

Julita Mikulec

aus

Konin, Polen

Bonn 2015

Angefertigt mit Genehmigung der Mathematisch-Naturwissenschaftlichen Fakultät der Rheinischen Friedrich-Wilhelms-Universität Bonn

1. Gutachter: Prof. Linda Diehl, PhD

2. Gutachter: Prof. Dr. rer. nat. Thorsten Lang

Tag der Promotion: 11.02.2016

Erscheinungsjahr: 2016

Erklärung

Diese Dissertation wurde im Sinne von § 6 der Promotionsordnung der Mathematisch-Naturwissenschaftlichen Fakultät der Rheinischen Friedrich-Wilhelms-Universität Bonn vom 03.06.2011 im Zeitraum von August 2011 bis Dezember 2014 von Frau Prof. Linda Diehl betreut.

Eidesstattliche Erklärung

Hiermit versichere ich, dass

- die vorgelegte Arbeit – abgesehen von den ausdrücklich bezeichneten Hilfsmitteln – persönlich, selbständig und ohne Benutzung anderer als der angegebenen Hilfsmittel angefertigt wurde,
- die aus anderen Quellen direkt oder indirekt übernommenen Daten und Konzepte unter Angabe der Quelle kenntlich gemacht sind,
- die vorgelegte Arbeit oder ähnliche Arbeiten nicht bereits anderweitig als Dissertation eingereicht worden ist bzw. sind, sowie eine Erklärung über frühere Promotionsversuche und deren Resultate,
- für die inhaltlich-materielle Erstellung der vorgelegten Arbeit keine fremde Hilfe, insbesondere keine entgeltliche Hilfe von Vermittlungs- bzw. Beratungsdiensten (Promotionsberater oder andere Personen) in Anspruch genommen wurde sowie keinerlei Dritte vom Doktoranden unmittelbar oder mittelbar geldwerte Leistungen für Tätigkeiten erhalten haben, die im Zusammenhang mit dem Inhalt der vorgelegten Arbeit stehen.

Bonn, den 12.10.2015

To My Family

Auszüge dieser Arbeit gingen in folgende Publikation ein:

Kaczmarek J., Homsi Y., van Üum J., Metzger C., Knolle P.A., Kolanus W., Lang T., Diehl L. (2014). Liver sinusoidal endothelial cell-mediated CD8 T cell priming depends on co-inhibitory signaling integration over time. PLoS One *9*, e99574.

Table of contents

Abstract **1**

1 Introduction **2**

1.1 The immune system **2**

1.2 T cell-mediated immunity **3**

1.2.1 Antigen presentation 3

1.2.2 The immunological synapse 4

1.2.3 T cell activation 7

1.2.4 T cell tolerance 8

1.3. The role of B7-CD28 superfamily in T cell activation and tolerance **11**

1.3.1 Co-stimulatory molecules 11

1.3.2 Co-inhibitory molecules 12

1.4 Liver as immunological organ **15**

1.4.1 Liver microarchitecture 16

1.4.2 Antigen-presenting cells in the liver 17

1.4.3 Antigen presentation to CD8 T cells by liver sinusoidal endothelial cells 19

1.5. Small GTPases **20**

1.5.1 Arf family of small GTPases 21

1.5.2 Small GTPase exchange factors 22

1.5.3 Arl4 family 23

2 Objectives **25**

3 Material and Methods **26**

3.1 Material **26**

3.1.1 Equipment 26

3.1.2 Chemical and Reagents 27

3.1.3 Antibodies 28

3.1.4 Beads 30

3.1.5 Kits 31

3.1.6 Enzymes 31

3.1.8 Buffers 32

3.1.9 Animals 35

3.1.10 Recombinant viruses 35

3.1.11 Primers 36

3.1.12 Software 36

3.2 Methods **37**

3.2.1 Isolation of primary cells 37

3.2.2 Magnetic cell separation (MACS) 39
3.2.3 Cell culture 39
3.2.4 Antigen-specific stimulation of CD8 T cells *in vivo* 41
3.2.5 Flow cytometry 41
3.2.6 ELISA 43
3.2.7 Microscopy 43
3.2.8 Gene expression array 45
3.2.9 Western Blot 46
3.2.10 Real-time PCR 46
4 Results 47
4.1 The immunological synapse formed by CD8 T cells and LSEC is not affected by PD-L1/PD-1 interaction 47
4.1.1 Contact of CD8 T cell with LSEC results in multifocal immunological synapse formation 47
4.1.2 PD-L1/PD-1 signaling rapidly interferes with TCR signal transduction 47
4.1.3 LSEC-mediated PD-L1 signals do not affect TCRβ and CD11a cluster formation 51
4.2. PD-L1/PD-1 signaling represses IL-2 production by LSEC-stimulated CD8 T cells .. 54
4.3 Co-stimulatory CD28 signaling does not prevent LSEC-mediated CD8 T cell non-responsiveness after prolonged co-inhibitory PD-L1/PD-1 signaling 55
4.4 Expression of small GTPase Arl4d in LSEC-primed CD8 T cells is PD-L1-dependent 57
4.5 The Arl4d knockout mouse serves as a proper tool to study small GTPase function 59
4.6 Arl4d deficiency leads to enhanced anti-viral CD8 T cell immune response 62
4.6.1 Arl4d dampens IL-2 production in CD8 T cells *in vitro* 62
4.6.2 Arl4d attenuates primary anti-viral CD8 T cell immunity *in vivo* 62
5 Discussion 73
5.1 LSEC-CD8 T cell interaction results in multifocal synapse formation 73
5.3 LSEC-primed CD8 T cell state depends on the integration of co-inhibitory signaling over a certain period of time 77
5.4 PD-L1-dependent expression of newly discovered small GTPase in CD8 T cells 78
5.5 Composition of the peripheral lymphoid compartment in the absence of Arld4 81
5.6 Function of Arl4d via regulation of IL-2 production 82
5.7 Future perspectives 84
6 References 86
7 Abbreviations 96
Table of Figures 100
Acknowledgements 101

Abstract

An adaptive immune response is initiated upon recognition of antigen presented on the surface of antigen-presenting cell (APC) by T cells. CD8 T cells primed in the liver by antigen-presenting liver sinusoidal endothelial cells (LSECs) develop into nonresponsive cells with a memory-phenotype. Liver-primed CD8 T cells are not terminally committed to this unique differentiation state but develop into effector cells upon infection. The adaptive immune response is balanced by co-stimulatory and co-inhibitory signals. LSEC-primed CD8 T cells require co-inhibitory PD-L1 signals delivered by LSECs to develop into a nonresponsive/memory state. In this study we investigated the relation between PD-L1/PD-1 signaling at early time-points and formation of an immune synapse, which may play a role in further development of effector function in T cells.

Upon antigen-specific interaction of APC and T cell, an immunological synapse is formed at their interface that is required for signaling exchanged between these cells. In this study, we demonstrate that LSEC-CD8 T cell interaction results in multifocal immune synapse formation. Furthermore, although the development of nonresponsive state of liver-primed CD8 T cells requires co-inhibitory PD-L1/PD-1 signaling, the formation and phenotype of the immune synapse did not. Not only the absence of PD-L1 signaling, but also delivery of CD28 co-stimulatory signals can prevent differentiation of CD8 T cells into nonresponsiveness after priming by LSEC. Interestingly, we found that co-stimulation via CD28 was able to overcome this unique differentiation program when introduced between 0 and 36 hours of LSEC-CD8 T cell coculture, indicating that co-inhibitory PD-1 signaling is required to be integrated during this time to induce typical liver-primed non-responsive memory like T cells.

Gene expression analysis identified the small GTPase ADP-ribosylation factor 4D (Arl4d) to be overexpressed in LSEC-primed CD8 T cells, compared to DC-primed CD8 T cells. More interestingly, Arl4d expression in CD8 T cells during LSEC-priming is dependent on PD-L1/PD-1 signaling. Similar to T cells activated in the presence of co-inhibitory PD-1 signaling, in the presence of Arl4d expression IL-2 production by CD8 T cells is attenuated *in vitro* and *in vivo*. In addition, Arl4d restricts effector CD8 T cell development and expansion on viral infection. Taken together, this study reveals a new as-yet undiscovered inhibitory function of Arl4d in modulating T cell immunity most likely via the regulation of IL-2 availability. Therefore, Arl4d might act downstream of co-inhibitory PD-1 signaling and thus play role in the regulation of CD8 T cell immunity.

1 Introduction

1.1 The immune system

The human body is under constant assault from pathogens. There exist two types of immunity that protect the host from infection: innate and adaptive immunity. Most of the microorganisms, encountered daily in the life of healthy individuals, are detected and destroyed within minutes or hours by the mechanisms of innate immunity, which serve as the first line of defense (Mueller et al., 2013; Iwasaki and Medzhitov, 2010; Murphy, 2012). Innate immunity relies on a limited number of germ-line encoded receptors, called pattern recognition receptors (PRRs) that recognize molecules typical of a microorganism, called pathogen-associated molecular patterns (PAMPs). The innate immune cells bearing these receptors, like macrophages, dendritic cells (DCs), mast cells, neutrophils and natural killer cells (NK) mature upon an inflammatory response and are capable of eradicating pathogens. However, in some cases, the innate immune system is unable to deal with an infection, requiring the involvement of the adaptive immune system. In contrast to the innate immunity, the adaptive immunity can provide specific recognition of antigens, because of a great variability and rearrangement of receptor gene segments (Janeway and Medzhitov, 2002; Murphy, 2012). The adaptive immune response has two goals: to provide functional effector cells in order to augment innate immune response, and to provide immunological memory, capable of mounting a quicker and more robust response to the same pathogen upon a second encounter (Hamilton and Jameson, 2007). The adaptive immune system is composed of B and T lymphocytes (Iwasaki and Medzhitov, 2010). B cells produce antibodies that destroy extracellular microorganisms in order to prevent intracellular infections, whereas T cells recognize intracellular antigens, generated either from extracellular antigens ingested by other cells or from proteins in situ. T cells are able to directly kill the cell infected with intracellular pathogens such as viruses, or to “help” in response to extracellular pathogens by interacting with B cells (Murphy, 2012).

1.2 T cell-mediated immunity

T cells initiate and regulate adaptive immunity to infections and cancer and play an important role in autoimmunity, allergy and transplantation. T cell function relies on binding of the T cell receptor (TCR) to antigens, which are short peptides presented on major histocompatibility complex (MHC) molecules on the surface of antigen-presenting cell (APC) (Lever et al., 2014).

CD8 T cells are the key effector cells of the adaptive immune system. Upon antigen encounter, they differentiate into mature cytotoxic T lymphocytes (CTLs) that then kill antigen-bearing target cells (Parish and Kaech, 2009). CTL responses are necessary to control variety of bacterial and viral infections. They migrate to the site of infection and specifically target the infected cells (Williams and Bevan, 2007).

CD4 T cells are crucially involved in immune responses. They regulate macrophage function, help B cells to produce antibodies, enhance and control CD8 T cell responses, arrange immune responses against diversity of pathogens. In addition, CD4 T cells regulate suppression to control autoimmunity and to adjust magnitude and persistence of the infection (Zhu et al., 2010). Importantly, CD4 T cells are key components of immunological memory. Without the help of CD4 T cells, the generation of B cell memory and the maintenance and secondary expansion of memory CD8 T cells are impaired (Tokoyoda et al., 2009; Sun and Bevan, 2003; Sun et al., 2004).

1.2.1 Antigen presentation

Naïve T cells recirculate between the lymph nodes, blood and spleen. They do not directly encounter antigens in the periphery but rely on professional APCs, mostly DCs, but also B cells and macrophages that present antigens to T cells (Heath and Carbone, 2001). DCs are located in lymphoid and non-lymphoid peripheral tissue where they constitutively sample the microenvironment and phagocytose microbial products and apoptotic cells. In most tissues, DCs are present in an immature state. At sites of infection they take up pathogens, leading to activation of their Toll-like receptors (TLRs), and become mature. Mature DCs show increased expression of MHC class I (MHC I) and class II (MHC II) molecules and co-stimulatory molecules, which enable them to prime T cells. During infection, tissue antigen-bearing DCs acquire migratory properties and travel into draining lymph nodes, where antigen presentation to T cells

occur (Arens and Schoenberger, 2010; Mellman and Steinman, 2001; Murphy, 2012). Recognition of antigens, which are presented to specific T cell receptors (TCRs) on MHC molecules of APCs, is crucial for T cell activation. CD8 T cells recognize protein-derived peptides on MHC I, whereas CD4 T cells recognize peptides bound to MHC II (Vyas et al., 2008; Blum et al., 2013; Lever et al., 2014). These peptides have a different origin: MHC I molecules present endogenous (cytosolic) antigens, whereas MHC II molecules present exogenous antigens. Interestingly, exogenous antigens can be presented on MHC I molecules, in a process called cross-presentation, which is crucial for the initiation of immune response against viruses that do not infect APCs (Neefjes et al., 2011). Furthermore, under non-inflammatory self-antigens are also cross-presented, however this leads to deletion of self-reactive CTLs in a process called cross-tolerance (Kurts et al., 2010).

1.2.2 The immunological synapse

1.2.2.1 Structural diversity

Recognition of antigens is a physical process that requires formation of a cell-cell junction between T cells and APCs. This interaction takes place through the formation of a specific structure at the interface: immunological synapse (IS) (Depoil and Dustin, 2014; Yokosuka et al., 2005). The IS was originally described to be formed between T cells and B cells or T cells and planar bilayers. Confocal microscopy revealed that the structure of the IS consists of two rings of molecules, which were named supramolecular activation clusters (SMAC) (Monks et al., 1998; Grakoui et al., 1999; Alarcon et al., 2011). The central SMAC (cSMAC) includes TCR-pMHC interactions together with the signaling molecule protein kinase C (PKC-θ), whereas adhesion molecule interactions, between lymphocyte function-associated antigen (LFA-1) and ICAM-I, surround the cSMAC and form the peripheral SMAC (pSMAC) (Monks et al., 1998; Thauland and Parker, 2010). This IS has a typical bull's-eye pattern and is called a classical IS (Fig. 1A). Further studies showed that there is a more peripheral region than pSMAC, called distal SMAC (dSMAC) containing large molecules like CD43 and CD45, which are firstly recruited to the cSMAC but later translocate to the dSMAC (Alarcon et al., 2011; Delon et al., 2001; Allenspach et al., 2001; Freiberg et al., 2002; Saito and Yokosuka, 2006).

Apart from the bull's-eye classical type, other non-classical IS forms have been identified: the multifocal synapse and the kinapse. The multifocal synapse is characterized by small TCR-pMHC interaction clusters at the T cell:APC interface, in contrast to classical IS where they are concentrated in the center of the interface (Fig. 1B). The kinapse is formed between two motile cells and is characterized by crescent-shaped accumulation of LFA-1-ICAM-1 in the middle of the cell (lamella) pointing towards the direction of migration, whereas TCR-pMHC clusters accumulate in trailing uropod (Fig. 1C) (Thauland and Parker, 2010).

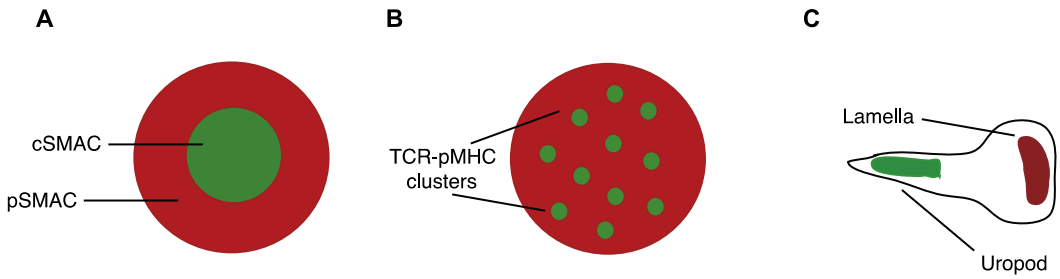

Figure 1. Immunological synapse structures

A: Bull's eye-classical IS. **B:** Multifocal IS. **C:** Immunological kinapse. TCR-pMHC and LFA-1-ICAM interactions are shown in green and red, respectively (Thauland and Parker, 2010; modified).

Why does the IS structure show such diversity? Firstly, the T cell differentiation state has a profound effect on IS structure (Thauland and Parker, 2010). Double-positive (DP) thymocytes interacting with either thymic epithelial cells or planar bilayers form a multifocal synapse, whereas mature T cells form classical IS. Thus, it was suggested that low TCR expression in immature thymocytes regulates synapse formation (Hailman et al., 2002; Lee et al., 2003). Furthermore, it is suggested that apart from TCR signal strength also other conditions play here a role in the IS formation, like antigen dosage (Thauland and Parker, 2010). For instance, type 1 and type 2 T helper cells (Th1 and Th2) cells form different IS type with planar bilayers. Th2 cells usually form a multifocal IS, however at decreased antigen dosage, the pMHC-TCR interactions are located in the center. Interestingly, ICAM-LFA-1 did not form a pSMAC in this case. In contrast, Th1 cells did not change IS structure with decreasing antigen concentration (Thauland et al.,

2008). Thus, IS synapse formation does not always depend on TCR signal strength, because T cell differentiation state plays here also an important role.

Secondly, the type of APC can affect IS structure. Interaction between DC and naïve CD4, CD8 and activated CD4 T cell results in multifocal synapse formation (Brossard et al., 2005; Fisher et al., 2008; Alarcon et al., 2011). In contrast, interaction of CD4 T cells with B cells results in a formation of a central ring rich in TCR-pMHC clusters surrounded by the ring of adhesion molecules (Grakoui et al., 1999; Yuseff et al., 2013; Duchez et al., 2011).

Furthermore, it is suggested that the IS is formed for function. The classical bull's eye IS is formed mostly by CTLs and Th1 cells, thought to facilitate the directed release of effector cytokines and cytolytic granules (Thauland et al., 2008; Stinchcombe and Griffiths, 2003). In contrast, the classical IS is not required for thymic selection, T-cell priming or Th2 function, at least under some conditions, suggesting that IS structure is linked to the function (Thauland and Parker, 2010).

1.2.2.2 Function of immunological synapse

The IS can be considered to have three functional layers, depending on receptor interactions, signal transduction and cytoskeletal transport.

The receptor interaction layer includes TCRs, adhesion molecules, co-stimulatory and co-inhibitory molecules, and co-receptors (Dustin and Depoil, 2011). TCR-CD3 microclusters are formed at the initial contact site with pMHC, as early as 5 seconds. After 1-2 min T cells expand the contact area, more microclusters are formed and accumulate at the periphery (expansion phase) and after reaching a maximum of cell spreading they move toward a center and create cSMAC after 5 min (Yokosuka et al., 2005; Campi et al., 2005). Adhesion molecules are important components of the receptor interaction layer. LFA-1 is essential for IS formation, because its engagement of ICAM-1 facilitates TCR-pMHC interactions. The co-stimulatory (CD28-CD80/86) and co-inhibitory (CTLA-4-CD80/86 and PD-1-PD-L1) complexes are located at the TCR microcluster where they modulate the TCR signal in order to increase or decrease the T cell activation (Tseng et al., 2008; Fooksman et al., 2010; Pentcheva-Hoang et al., 2004; Yokosuka et al., 2012).

The signaling layer contains lymphocyte-specific protein tyrosine kinase (Lck), non-receptor tyrosine kinase ζ-associated protein of 70 kDa (ZAP-70), phospolipase Cγ (PLCγ) and protein kinase (PKCθ). Although the TCR has no intrinsic catalytic activity, it forms a multisubunit complex with CD3, containing immunoreceptor tyrosine-based activation motifs (ITAMs). Upon antigen recognition, the tyrosine kinase Lck phosphorylates ITAMs. Further, ZAP-70 is recruited and phosphorylates several adaptor proteins, such as the linker for activation of T cells (LAT) and Src homology 2 (SH2) domain-containing leukocyte phosphoprotein of 76 kDa (SLP-76). Phosphorylation of LAT is essential for PLCγ activation and increases the level of intracellular Ca^{2+} (Dustin and Depoil, 2011; Saito and Yokosuka, 2006; Yokosuka et al., 2005). The initiation of TCR signaling takes place in the microcluster of the d- and pSMAC, whereas signal termination and TCR degradation take place in the cSMAC. Moreover, it has been shown that a member of the endosomal sorting complex required for transport (ESCRT) of proteins, TSG-101 is required for cSMAC formation and dephosphorylation of TCR signaling (Lee et al., 2003; Varma et al., 2006; Fooksmann et al., 2010; Vardhana et al., 2010). The signaling layer is integrated within cytoskeletal layer to this extent that adhesion and TCR signaling events require filamentous actin (F-actin) polarization and reorganization (Dustin and Depoil, 2011).

The cytoskeletal layer is assembled around three filament-forming proteins: actin, myosin II and tubulin (Dustin and Depoil, 2011). Actin polarization is not only crucial for microcluster transport but also for the tyrosine phosphorylation events within the clusters leading to sustained Ca^{2+} signaling. Myosin IIA activity maintains the radial symmetry and overall organization of IS (Babich et al., 2012), whereas the microtubule network position microtubule organization center (MTOC) organizes the alignment of secretory organelles in the IS enabling direct release of cytokines toward the APC (Huse, 2012).

1.2.3 T cell activation

To be effectively activated T cells require three signals: signal 1, 2 and 3. Signal 1 (antigen recognition) is mediated by binding of peptide MHC (pMHC) to a specific TCR. The most proximal event is the tyrosine phosphorylation of ITAMs (described in detail in 1.2.2.2), followed by the activation of several signaling pathways. Signal 2 (co-

stimulation) is mediated mostly by binding of CD28 on naïve T cells with CD80/86 on APCs. Together, TCR engagement and co-stimulation lead to T cell activation, expansion and acquisition of effector function. When only signal 1 is delivered, T cells become anergic, therefore signal 1 and 2 are required for T cell activation. For the full activation, T cells need signal 3, the production of cytokines by APCs at distinct stages of a T cell response. The particular cytokine combination will then drive the T cell differentiation to specific types of effector cells (Lichtenstein et al., 2012; Goral, 2011).

Upon specific antigen recognition, naïve CD4 T cells develop into T helper (Th) cells, classified into Th1, Th2 and Th17. Th1 and Th17 control inflammatory responses, effective for anti-viral and anti-bacterial immunity, whereas Th2 cells control antibody responses required for anti-viral and anti-parasitic immunity (Lichtenstein et al., 2012). Signal 3 plays the central role in fate determination of Th cells. Th1 cells develop in the presence of interleukin 12 (IL-12) and interferon-gamma (IFNγ), Th2 cells develop in the presence of IL-2 and IL-4 and Th17 differentiate in the presence of transforming growth factor-beta (TGF-β), IL-6 and IL-21 (Zhu et al., 2010).

Encounter of antigen by naïve CD8 T cells leads to their expansion and differentiation into effector CTLs, which kill target cells. Following the clearance of the infection, most (>90%) of the antigen-specific CD8 T cells die by apoptosis and only a few cells survive as long-lived memory T cells (Kaech et al., 2002; Boyman and Sprent, 2012). It has been shown that type I interferons (IFN-α/β) and IL-12 play an important role in the differentiation of effector CD8 T cells upon infection. IFN-α/β promote DC maturation and their ability to cross-prime CD8 T cells. In addition, IFN-α promotes clonal expansion and IFNγ production by CD8 T cells. Importantly, in the presence of IFN-α/β and IL-12 CD8 T cells upregulate mRNA expression of the effector proteins granzyme B and perforin, which are important for the killing of target cells (Curstinger et al., 2005).

1.2.4 T cell tolerance

The immune system is balanced between self-antigen-driven tolerance and pathogen-driven immunity. A shift towards extreme ends of both, i.e., lack of response (immunodeficiency) or an inappropriate, excessive response (autoimmunity or allergy), leads to pathophysiology. Self-tolerance is maintained firstly by the development and selection of T cells in the thymus (central tolerance) and secondly by suppression,

deletion and anergy of mature T cells in the nonlymphoid and lymphoid organs (peripheral tolerance) (Kyewski and Klein, 2006).

1.2.4.1 Central tolerance

Elimination of autoreactive T cells in the thymus is an important part of T cell development to avoid the potentially pathological state of autoimmunity. Subsequent to positive selection and CD4 and CD8 T cell commitment, thymocytes translocate to the thymic medulla, where negative selection occurs. Expression of tissue-restricted antigens (TRAs) on medullary thymic epithelial cells (mTECs) plays an essential role in central tolerance: TRAs represent virtually all parenchymal organs, thereby mirroring peripheral-self. TRAs are directly presented by mTECs or cross-presented by thymic DCs to the thymocytes (Anderson, 2002; Redmond and Shermann, 2005; Klein et al., 2009; Hogquist et al., 2005). If the recognition of these antigens on MHC complexes is too strong, those autoreactive thymocytes will be negatively selected and die by apoptosis (Venanzi et al., 2004). The transcription factor AIRE (autoimmune regulator) plays an important role in turning on TRAs and its mutation or absence leads to autoimmune disorders (Metzger and Anderson, 2011; Peterson, 2008).
Despite central tolerance effectiveness, other tolerance mechanisms are required for self-reactive T cell silencing because many self-antigens may not access the thymus or are expressed at insufficient levels for thymocytes with low-avidity TCR to being recognized. Moreover, the human body is constant exposed to the nonpathogenic antigens both from the environment and diet to which it should remain tolerant (Steinman and Nussenzweig, 2002; Redmond and Shermann, 2005).

1.2.4.2. Peripheral tolerance

As thymic selection is not a perfect process many low-avidity, autoreactive T cells can be found in the periphery. To control these cells in the periphery, tolerance is achieved by various mechanisms including clonal ignorance, anergy and clonal deletion (Parish and Heath, 2008; Srinivasan and Frauwirth, 2009).
Immunological ignorance occurs when antigens do not enter lymphoid organs at sufficient levels and thereby can not induce an efficient immune response or when

antigens are located in privileged sites, such as the central nervous system or the eye, to which T cells do not have access (Ochsenbein et al., 1999; Ohashi, 1991; Srinivasan and Frauwirth, 2009). Furthermore, tolerance due to ignorance may occur in low-avidity T cells because the TCR/MHC affinity needed for T cell activation in the periphery is higher than in the thymus. Therefore, such low-avidity self-reactive naïve T cells interacting with self-pMHC will not be activated (Parish and Heath, 2008; Srinivasan and Frauwirth, 2009; Mescher et al., 2007).

As described above (see 1.2.1), mature DCs drive immunity, whereas immature DCs induce tolerance. The mechanism of T cell tolerance induced by immature DCs involves programmed cell death 1 (PD-1) and cytotoxic T lymphocyte antigen 4 (CTLA-4) (co-inhibitory molecules are described in detail in 1.3.2). Thus, CD8 T cells lacking PD-1 and CTLA-4 are primed but not tolerized by immature DCs (Probst et al., 2005).

Anergic T cells are antigen experienced and remain alive for an extended period of time. However, they neither proliferate nor produce IL-2 upon restimulation (Lutz and Schuler, 2002; Schwartz, 2003; Srinivasan and Frauwirth, 2009). Gene expression analysis revealed that PD-1 upregulation is important for induction of both anergy and deletion. Furthermore, autoreactive T cells undergoing deletion are characterized by excessive upregulatation of the proapoptotic BH3-only Bcl-2 family member Bim and downregulation of the anti-apoptotic Bcl-2 family proteins, granzyme B (GzmB), Ly6C and the IL-7α chain (Parish et al., 2009; Davey, 2002). Why do some autoreactive T cells become anergic and why are others deleted? There is evidence that strength of TCR-pMHC interaction can play a role. Some studies show that the continuous exposure of a clonal T cell line to high versus low doses of antigen induced anergy or deletion, respectively (Redmond and Shermann, 2005; Redmond et al., 2005).

Apart from anergy and deletion, additional tolerance mechanisms exist, which are mediated by $CD4^+CD25^+Foxp3^+$ T cells, called T regulatory cells (Tregs). Natural Tregs (nTregs) originate in the thymus during thymocytes maturation, whereas induced Tregs (iTregs) develop in secondary lymphoid organs from peripheral naïve $CD4^+CD25^-$ T cells upon antigen stimulation by DCs. iTreg generation occurs mainly in bacterial or viral infection, in tumors or in mucosal tissues in the context of oral tolerance (Sakaguchi et al., 2009; Tang and Bluestone, 2008; Piccirillo and Shevach, 2004; Bilate and Lafaille, 2012; Goldstein et al., 2013). Tregs suppress proliferation of naïve T cells, their differentiation into effector cells and cytokine production via cell-cell contact or

production of anti-inflammatory cytokines. Thus, interaction of Tregs with DCs causes down modulation of their function (downregulation of CD80/86 expression and production of proinflammatory IL-6 and TNFα) (Sakaguchi et al., 2008; Belkaid and Tarbel, 2009; Sakaguchi et al., 2009). Furthermore, it is reported that IL-10 and TGFβ produced by Tregs control colitis and inhibits differentiation of activated T cells to Th1 or Th2 effector cells, respectively (Liu et al., 2003; Schmitt et al., 2012; Chaudhry et al., 2011; Wan and Flavell, 2007).

1.3. The role of B7-CD28 superfamily in T cell activation and tolerance

Interaction of co-signaling molecules between T cells and APCs is an early event for transmitting signals to control T cell growth, differentiation, activation and tolerance (Tsushima et al., 2007). Function of co-signaling molecules entirely depends on TCR signals (signal 1). Co-stimulators enhance TCR-mediated responses, whereas co-inhibitors inhibit TCR-mediated responses (Chen, 2004). In the absence of sufficient TCR signaling, co-signaling molecules lose their function or function aberrantly. Following antigen recognition, they are one of the earliest responding elements of the immune system. These molecules are members of the immunoglobin and tumor-necrosis factor (TNF) superfamilies (Chen, 2004). The B7-CD28 superfamily is crucial in regulating activation and tolerance of T cells (Sharpe and Freeman, 2002).

1.3.1 Co-stimulatory molecules

1.3.1.1 CD28

CD28 is constitutively expressed on the surface of naive CD4 and CD8 T cells and plays a major role in co-stimulation in the initial activation of T cells. Engagement of the TCR and CD28 ligation results in initiation of T-cell–mediated immunity (Gardner et al., 2014). CD28 interacts with two ligands on APC: B7-1 (CD80) and B7-2 (CD86), providing co-stimulatory signaling. In contrast, CD80 and CD86 ligation with CTLA-4 provides co-inhibitory signaling (see 1.3.2.1). CD86 is constitutively expressed at low levels on DC and upregulated rapidly upon activation, whereas CD80 expression is induced later after activation. Both CD80 and CD86 are crucial in regulating T cell activation and tolerance (Sharpe and Freeman, 2002; Sotomayor et al., 1999). Binding

of CD80/CD86 to CD28 leads to association of phosphatidylinositol 3-kinase (PI3K) and its phosphorylation, further inducing IL-2 mRNA production and enhanced T cell survival (Rudd et al., 2009; Sharpe and Freeman, 2002). The main function of CD28 co-stimulation is to augment and sustain T-cell responses initiated by antigen-receptor signaling, by promoting T cell survival and therefore enabling cytokines to initiate T-cell differentiation and expansion (Sharpe and Freeman, 2002).

1.3.2 Co-inhibitory molecules

1.3.2.1 CTLA-4

CTLA-4 (cytotoxic T lymphocyte antigen 4) engagement of CD80/CD86 delivers negative signal, which inhibits TCR- and CD28-mediated signal transduction (Sharpe and Freeman, 2002). In contrast to CD28, CTLA-4 is expressed at low levels on naive T cells, but rapidly upregulated after activation. If the interaction between CTLA-4 and CD80/86 is blocked, it will result in enhancement of T-cell responses against foreign- and self-antigens. T cells deficient for CTLA-4 show greater cell expansion and cytokine production after adoptive transfer into wild-type mice. In addition, CTLA-4-deficient mice spontaneously develop CD28-dependent autoimmune responses, which indicates that CD28 co-stimulation is actively suppressed by CTLA-4 (Chen, 2004; Sharpe and Freeman, 2002). Furthermore, *in vivo* CTLA-4 blockade with monoclonal antibodies confirmed its inhibitory function of T cell responses and the role in augmenting antitumor immunity (Sotomayor et al., 1999; Leach et al., 1996; Sharpe and Freeman, 2002). Interestingly, recent studies revealed that CTLA-4 acts as an inhibitor on $CD4^+CD25^+$ T cells via transendocytosis of CD80 and CD86. In this way, CTLA-4 promotes removal and degradation of CD80/CD86 from the APC, preventing access of CD28 to its ligands (Gardner et al., 2014; Quereshi et al., 2011).

1.3.2.2 PD-1

PD-1 (programmed cell death 1) acts as a co-inhibitory receptor during B- and T-cell responses. It was first cloned from a T cell hybridoma undergoing programmed cell death (Chen, 2004). PD-1 is induced on activated $CD4^+$ and $CD8^+$ T cell, B cells and monocytes (Chen 2004; Greenwald et al., 2005). Interestingly, PD-1 is upregulated in CD8 T cells interacting with liver sinusoidal endothelial cells (LSECs), which is

correlated with PD-L1 upregulation in LSECs, inducing a unique quiescent state in CD8 T cells (in details described in 1.4.3).

PD-1 is monomeric and its cytoplasmic domain has two tyrosines: one constitutes an immunoreceptor tyrosine-based inhibition motif (ITIM), and the other an immunoreceptor tyrosine- based switch motif (ITSM) (Chen 2004; Greenwald et al., 2005). It is suggested that PD-1 phosphorylation of the cytoplasmic tyrosine domain of PD-1 recruits SRC homology 2 (SH2)-domain-containing protein tyrosine phosphatase (SHP-2). SHP-2 then dephosphorylates TCR associated CD3ζ and ZAP-70 resulting in inhibition of downstream signaling (Dai et al., 2014). This leads to the attenuation of the PI3K and Akt pathways, resulting in decreased proliferation, survival and IL-2 production (Francisco et al., 2010). PD-1 blockade by antibody treatment results in rapid expansion of antigen-specific CD8 T cells and improves their effector function upon viral infection (Velu et al., 2009). Furthermore, PD-1 blockade inhibits tumor growth by enhanced recruitment and proliferation of effector T cells at the tumor sites (Iwai et al., 2004). PD-1-deficient mice spontaneously develop lupus-like proliferative arthritis and glomerulonephritis with IgG deposition (C57BL/6 background) and autoimmune dilated cardiomyopathy or sudden death by congestive heart failure (BALB/c background). Moreover, these mice have a high serum titer of IgG autoantibodies specific for cardiac troponin I protein, indicating the role of PD-1 in the maintenance of peripheral tolerance (Chen, 2004).

Importantly, PD-1 is highly expressed on exhausted CD8 T cells upon chronic LCMV infection as well as upon infection with the human immunodeficiency virus (HIV) (Barber et al., 2006, Day et al., 2006). In addition, PD-1 expression observed in HIV-specific CD8 T cells predicts disease progression, thus it correlates positively with viral load (Day et al., 2006). Blocking the interaction of PD-1 with its ligand by administration of blocking antibodies can restore the ability of exhausted CD8 T cell to proliferate and produce cytokines (Barber et al., 2006; Petrovas et al., 2006; Freeman et al., 2006). PD-1 is highly induced on tumor infiltrating and circulating tumor-specific T cells and inhibits their activation and tumor cell killing (Ji et al., 2015). Checkpoint inhibitors are a novel cancer therapy that targets these inhibitory signals and augument antitumor T cell responses. Both, PD-1 and CTLA-4 checkpoint inhibitors are lately approved agents in melanoma and lung cancer therapy (Brahmer and Pardoll, 2013; Pennock and Chow, 2015).

1.3.2.3 PD-L1

PD-ligand 1 (PD-L1, also known as B7H1) and PD-ligand 2 (PD-L2) are ligands for PD-1. Within the immune system, PD-L1 expression is mostly restricted to macrophages, activated B cells, activated T cells and mature DCs. Furthermore, it can be found on the surface of nonhematopoietic cells including microvascular endothelial cells and nonlymphoid organs like heart, lung, pancreas, muscle and placenta (Greenwald, 2005; Bazhin et al., 2014). PD-L1 is also expressed on liver sinusoidal endothelial cells, where it plays a pivotal role in LSEC-CD8 T cell priming (see 1.4.3). Importantly, PD-L1 mRNA can be found in various human tissues but abundance of mRNA does not correlate with protein expression. Experimental evidence showed that PD-L1 can act as co-stimulatory and co-inhibitory molecule (Chen, 2004). On one hand, application of blocking monoclonal PD-L1 antibodies prevented development of experimental colitis in mice in association with decreased expansion of pathogenic T cells, indicating a co-stimulatory function of PD-L1 (Kanai et al., 2003). On the other hand, it increased the incidence of autoimmune diabetes in non-obese diabetic (NOD) mice and hapten-induced hyperreactivity, indicating co-inhibitory function (Chen, 2004). Recent studies characterize in detail the influence of PD-L1 deficiency *in vivo*. In PD-L1-deficient mice NK, NKT cells and $Gr1^{+}CD11b^{+}$ myeloid cells are decreased. Moreover, the percentages of pDCs but not cDCs are increased in PD-L1-deficient mice. In the T-cell compartment PD-L1 deficiency resulted in an increased amount of Tregs and a decreased amount of conventional CD4 T cells (T conv), however, which showed an increase in percentages of activated T cells, suggesting that in the absence of PD-L1 the immune system tries to maintain its stimulatory/suppressory balance by engaging more Tregs (Bazhin et al., 2014).

1.3.2.4 PD-L1/PD-1 inhibitory pathway

The PD-L1/PD-1 pathway controls the balance between peripheral tolerance and immunity in several ways. PD-L1/PD-1 interactions inhibit the expansion of naïve self-reactive T cells and/or their differentiation into effector cells (Francisco et al., 2010). It has been shown that peripheral CD8 T cell tolerance depends on PD-1 signals, as the absence of PD-1 resulted in conversion of tolerance into priming induced by resting DCs

upon LCMV infection (Probst et al., 2005). Moreover, tissue-specific expression of PD-L1 has a key role in protection against self-reactive T cells within pancreas and inhibits development of autoimmune diabetes (Keir et al., 2006). Endothelial antigen presentation to CD8 T cells is an important step in the pathogenesis of allograft rejection and can be involved in organ-specific autoimmunity as PD-L1 expression is induced on human and mouse endothelial cells inhibiting CD8 T cell effector responses to endothelial antigen presentation (Rodig et al., 2003). Taken together, PD-L1/PD-1 interactions play an important role in the induction of tissue tolerance.

PD-L1 expression is also induced on LSECs. Priming of naïve CD8 T cells by LSECs leads to development of antigen-experienced CD8 T cells that are unable to perform effector functions (Limmer et al., 2000). Interestingly, this LSEC-mediated unresponsiveness of CD8 T cells is PD-1/PD-L1 dependent (Diehl et al., 2008) and requires the integration of co-inhibitory signaling over time (Kaczmarek et al., 2014).

The PD-L1/PD-1 pathway plays an important role in exhaustion of CD8 T cells. These cells are generated under chronic antigen stimulus and express activation/memory markers ($CD44^{high}$ $CD62L^{lo}$), however they are unable to perform effector functions (Zajac et al., 1998). Interestingly, studies investigating CD8 T cell responses upon chronic LCMV and HIV infection revealed that exhausted CD8 T cells strongly upregulate PD-1 and the blockade of the PD-L1/PD-1 pathway had a beneficial effect on antigen-specific impaired CD8 T cells, restoring their ability to proliferate, to produce cytokines and to perform cytotoxic activity (Barber et al., 2006; Petrovas et al., 2006; Freeman et al., 2006). Therefore, these findings indicate the PD-1/PD-L1 pathway as a therapeutic target to augment not only the immune responses during chronic viral infections. Importantly, PD-1 checkpoint pathway is the target in the novel immunotherapy (as mentioned in 1.3.2.3).

1.4 Liver as immunological organ

The liver is an organ that fulfills diverse functions in the metabolism of carbohydrates, proteins and lipids. Moreover, it plays an important role in the clearance of toxins and pathogens. Unique hepatic regulatory mechanisms prevent induction of immunity against antigens from gastrointestinal duct, damaged cells and neo-antigens that arise during metabolic processes. Although most of the pathogens reaching the liver via the

blood are cleared, certain pathogens like *Plasmodium spp* sporozites, causing malaria, hepatitis B and C virus have evolved multiple strategies to escape the T cell-mediated immunity and to establish hepatic infection (Thompson and Knolle, 2010; Protzer et al., 2012; Knolle and Thimme, 2014). The tolerogenic properties of the liver are exemplified by its role in oral tolerance, the immunological mechanism whereby the mucosal immune system maintains unresponsiveness to antigens that might induce undesired immune responses, and portal venous tolerance, the induction of the peripheral tolerance following portal vein delivery of antigen. Furthermore, the liver exemplifies its tolerogenic properties by the persistence of infections and tumor metastases, as well as by immune tolerance against hepatic transplants (Crispe, 2003; Thomson and Knolle, 2010).

1.4.1 Liver microarchitecture

Blood is delivered to the liver via the portal vein, which is enriched in nutrients and bacterial degradation products, and via the hepatic artery, which also supplies large amounts of blood continuously to the liver (Knolle and Thimme, 2014). About 30% of the total blood passes through the liver every minute and it carries about 10^8 lymphocytes in 24 hours (Racanelli and Rehermann, 2006). In Figure 2, the schematic overview of the hepatic microarchitecture is shown. Hepatocytes are separated from the blood stream by LSECs. The slow blood flow within and the narrow diameter of hepatic sinusoid facilitates the interaction of lymphocytes with LSEC, the main antigen presenting cells in the liver, and promotes lymphocytes extravasation (Racanelli and Rehermann, 2006; Knolle and Thimme, 2014). The space of Disse, located between LSECs and hepatocytes, is filled with extracellular matrix and is populated with stellate cells (HSC), which are immune-sensing cells involved in liver fibrosis (Protzer et al., 2012). Blood plasma passes from the sinusoids into the space of Disse, where lymph is collected and flows through lymphatic vessels further into portal tracts to the draining lymph nodes. In contrast to LSECs, hepatocytes have no direct contact to the blood flow but they can directly interact with T cells via LSEC fenestrations (Knolle and Thimme, 2014; Crispe, 2003).

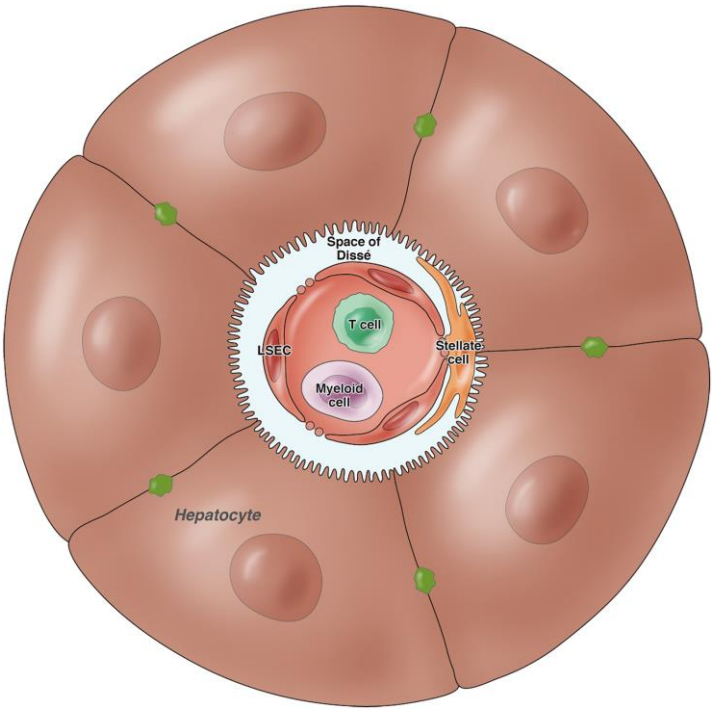

Figure 2. Schematic overview of liver microarchitecture.

LSECs line the liver sinusoids and together with stellate cells separate hepatocytes from blood passing through the liver (adapted from Knolle and Thimme, 2014).

1.4.2 Antigen-presenting cells in the liver

Liver dendritic cells

Liver DCs are located around central veins and portal tracts and can be divided into myeloid DCs (mDCs) ($CD11c^+CD8\alpha^-CD11b^+$), $CD8\alpha^+$ DCs ($CD11c^+CD8\alpha^+CD11b^-$) and plasmocytoid DCs (pDCs) ($CD11c^{low}B220^+Ly6C^+CD11b^-SIGLECH^+$). Immature DCs express the CC-chemokine receptor 1 (CCR1) and CCR5 and are recruited into the liver via interaction with Kupffer cells expressing CC-chemokine ligand 3 (CCL3). After maturation DCs lose CCR1 and CCR5 expression and upregulate CCR7, with which they gain responsiveness to CCL19 and CCL21 produced by lymphoid tissue. Murine liver bulk DCs or purified mDCs are less mature, in phenotype and function, than lymphoid tissue DCs. They express MHC II at lower levels, secrete less IL-12 and preferentially produce IL-10 and IL-27. Freshly isolated liver mDCs are tolerant to lipopolysaccharide (LPS), called „endotoxin tolerance“. Also liver pDCs express low levels of MHC class II molecules and CD40, CD80 and CD86. In response to microbial TLR stimulation, they produce less IFNα, IL-6, IL-12 and TNF than splenic pDCs. It is suggested that pDCs

modulate T cell responses by expression of PD-L1, production of IL-10 and induction of T cell apoptosis (Thompson and Knolle, 2010; Racanelli and Rehermann, 2006; Crispe, 2003).

Kupffer cells

Kupffer cells are resident macrophages in the liver and represent the largest macrophage population in the body. They can be derived from circulating monocytes or develop from yolk sac-derived cells, the precursors in organs (Racanelli and Rehermann, 2006; Knolle and Thimme, 2014). Their location in hepatic sinusoids enables them to interact with circulating T cells, NK and NKT cells. Kupffer cells are the dominant hepatic APC population that presents lipid antigens in a CD1d-restricted manner to NKT cells. Moreover, they express the high-affinity Fc receptor for IgA and complement receptors with which they can efficiently remove the complement-coated bacteria. Kupfer cells can exert both immunogenic and tolerogenic function: they are involved in tolerance against soluble antigens and liver transplants and can stimulate the suppressive activity of Treg cells. In contrast, in *Leishmania donovani*-induced granulomas and *Borrelia burgdorferi* infection, Kupffer cells induce immunity by cross-presentating parasite antigens to CD8 T cells and lipid antigens to NKT cells, respectively (Crispe 2003, Thompson and Knolle, 2010, Knolle and Thimme, 2014).

Hepatocytes

Although hepatocytes are separated from the blood stream by LSECs, stellate cells and Kupffer cells, they can directly present antigens to CD4 and CD8 T cells through LSEC fenestration. Although they express only low levels of MHC class I molecules, they are able to activate CD8 T cells. However, first antigen contact with hepatocytes induces T cell tolerance via clonal deletion, in contrast, when T cells first encounter antigen in lymphoid tissue, reencounter of the antigen on hepatocytes can cause immune-mediated hepatitis. Additionally, the CD1-restricted activation of natural killer T (NKT) cells by hepatocytes leads to the generation of IL-10-expressing CD8 T cells with regulatory function (Thompson and Knolle, 2010; Knolle and Thimme, 2014).

Liver sinusoidal endothelial cells

Apart from hepatocytes, LSECs are the most abundant cell type in the liver. Together they account for about 80% of the liver mass (Kim and Rajagopalan, 2010). In the sinusoids, the endothelium is characterized by fenestrations, which measure approximately 100 nm in diameter and occur with the frequency of 9-13 per μm^2, which accounts for approximately 10% of entire LSEC surface (Braet and Wisse, 2002; Knolle and Gerken, 2000). However, the passage of gold particles larger than 20 nm is prevented by extracellular matrix, inhibiting their free diffusion through fenestrae into the space of Disse. This barrier can be overcome by cells squeezing through fenestrations or by active transport across LSECs of for instance iron to be delivered to hepatocytes (Knolle and Limmer, 2003; Protzer et al., 2012).

LSECs are resident APCs and express different molecules, which are necessary for the interaction with leukocytes (for instance: CD54 and CD106) and several pattern recognition receptors (PRRs), which enable recognition of pathogens. The expression of PRRs allows them to remove non-enzymatically glycolysed proteins and other harmful molecules from the circulation. LSECs can phagocytose material up to 200 nm in size. In contrast, Kupffer cells phagocytose larger complexes, leading to a division of labor in the clearance of different pathogens. Apart from that, LSECs constitutively express co-stimulatory CD80, CD86 CD40 and ICOS-L and co-inhibitory PD-L1. Moreover, they express MHC class I and class II molecules, which are necessary for antigen presentation to CD8 and CD4 T cells, respectively (Knolle and Limmer, 2003; Knolle and Gerken, 2000; Thompson and Knolle, 2010).

1.4.3 Antigen presentation to CD8 T cells by liver sinusoidal endothelial cells

LSECs are unique organ-resident APCs in the liver, which combine scavenger activity with cross-presentation of exogenous antigens on MHC class I molecules to CD8 T cells (Limmer et al., 2005; Diehl et al., 2008). Intravenous injection of $Alexa^{647}$ -labeled ovalbumin (OVA) was followed by its accumulation in hepatic cells (i.e. LSECs), whereas little accumulation in spleen or lungs was observed. Direct comparison of LSECs and DCs from liver or spleen showed that LSECs are more efficient in taking up and cross-presenting OVA to $H2K^b$-OVA specific CD8 T cells. Although the uptake via mannose

receptor is essential for cross-presentation in DCs, the mannose does not seem to be involved in LSECs (Schurich et al., 2009; Höchst et al., 2012).

Cross-presentation of antigens to naive CD8 T cells by mature DCs leads to their differentiation into CTLs, which produce IL-2 and IFNγ (Kurts, 2010; Cui and Kaech, 2010; Williams and Bevan, 2007). However, CD8 T cells primed by LSECs develop a unique differentiation state. Within 18 hours LSEC-stimulated CD8 T cells upregulate activation markers and Granzyme B expression (GzmB), comparable to DC-stimulated CD8 T cells (Diehl et al., 2008; Böttcher et al., 2014). However, in contrast to DC-stimulated T cells, GzmB expression declines within 48 hours back to baseline. Interestingly, these GzmB-positive LSEC-stimulated CD8 T cells possess cytotoxic function as they killed target cells in an antigen-specific fashion (Böttcher et al., 2014). However, longer LSEC stimulation (i.e 3-5 days) under non-inflammatory conditions induces non-responsiveness of CD8 T cells, characterized by lack of IL-2 or IFNγ production after restimulation (Limmer et al., 2000; Diehl et al., 2008). Importantly, CD8 T cell proliferation and expansion within the first 72 hours of LSEC- and DC-stimulated CD8 T cells is similar, but at later time points LSEC-stimulated T cells do not expand to the same extent. LSEC-primed T cells are $CD25^{low}CD44^{high}CD62L^{high}$ enabling them to recirculate through secondary lymphoid organs. The induction of this unique functional state in CD8 T cells by LSEC is mediated by co-inhibitory PD-L1, which is expressed on LSEC and further induced during contact with CD8 T cells (Diehl et al., 2008). Priming of CD8 T cells by LSEC does not cause their deletion but instead generates an antigen-experienced CD8 T cell population that possesses memory-like properties: they can generate recall responses and give rise to effector CTLs that can control the infection, indicating that T cell priming by LSECs contributes to antipathogen immunity (Diehl et al., 2008; Böttcher et al., 2013).

1.5. Small GTPases

The organization of many fundamental cellular processes, like intracellular signaling and vesicular trafficking, is regulated by small guanine nucleotide-binding proteins of the Ras superfamily (Goldberg, 1998; Kolanus, 2007; Gillingham and Munro, 2007).

All small GTPases share a common biochemical mechanism and act as molecular switches (Fig. 3) (Wennerberg et al., 2005). Activation and inactivation of each member

is regulated by GTP binding and GTP hydrolysis, respectively, and this process is regulated by guanine exchange factors (GEFs) (catalysis of GDP into GTP), and GTPase-activating proteins (GAPs) (catalysis of GTP hydrolysis) (Donaldson and Jackson, 2011; Kolanus, 2007; Wennerberg et al., 2005; Shin and Nakayama; 2004).

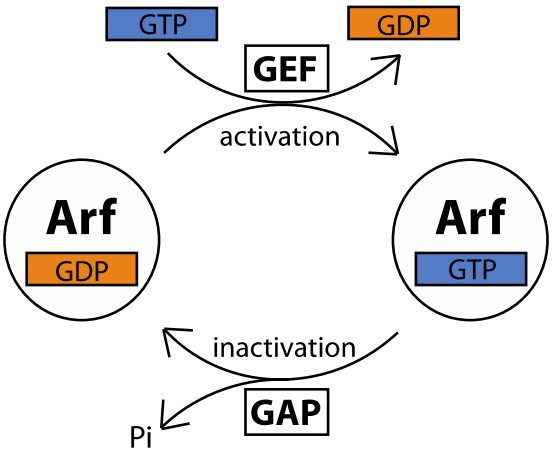

Figure 3. Schematic GDP-GTP cycle of Arf (Shin and Nakayama, 2004; modified).

General regulation of Arf activation and inactivation. An inactive form of Arf, GDP-bound, is converted to active, GTP-bound, form through GDP-GTP exchange catalyzed by a GEF. Upon interaction of active form of Arf with effector molecules, such as coat proteins and lipid kinases, GTP is hydrolyzed to GDP with a help of a GAP.

1.5.1 Arf family of small GTPases

ADP-ribosylation factor (Arf) GTPases are crucial regulators of secretion, endocytosis, phagocytosis and signal transduction (Burd et al., 2004). Figure 4 shows the structure of Arfs; GDP-GTP cycle changes the conformation of the protein by causing a loop of beta sheets between switch regions, called the interswitch, to move away from GTP binding site. A distinguishing structural feature of Arfs separating them from other GTPase proteins is their N-terminal amphipathic helix, where a myristoyl group, that can mediate membrane binding, is attached. The myristoylation of N-terminus results in replacement of methionine at the position 2 with glycine. Upon GTP-binding, the myristoylated N-terminal amphipathic helix is displaced from hydrophobic pocket and

can be inserted into the membrane (Gillingham and Munro, 2007; Donaldson and Jackson, 2011).

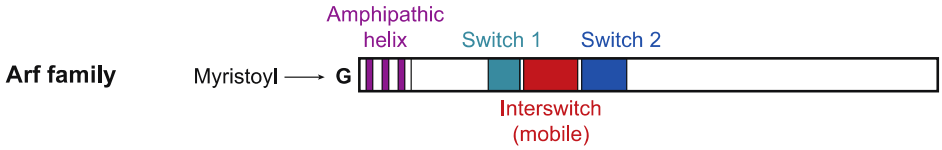

Figure 4. Schematic structure of Arf protein (Gillingham and Munro, 2007).

The Arfs have switch regions that change confirmation upon binding of GTP regions. Furthermore, they contain N-terminal amphipathic helix, which is often myristoylated.

There are six mammalian ARF proteins, which are divided in three classes: Class I (Arf1, Arf2, Arf3), Class II (Arf4 and Arf5) and Class III (Arf6) (Donaldson and Jackson, 2011). Arf1 and Arf6 are the most characterized Arf proteins. Arf1 is located at the Golgi compartment and mediates transport of the early secretory pathway from Golgi into endoplasmic reticulum (ER). In addition, it modulates the Golgi structure by stimulation of spectrin and actin skeleton at the Golgi membrane (D'Souza-Schorey and Chavrier, 2006). Arf6 primarly acts at the plasma membrane. Many studies show its contribution in cell spreading, Rac-induced ruffling, cell migration and wound healing (Donaldson, 2003). Moreover, Arf6-GFP recruits ARNO (cytohesin-2) to the plasma membrane for activation of Arf1 and regulates actin remodeling (Cohen et al., 2007; Boshans et al., 2000).

1.5.2 Small GTPase exchange factors

Because inactive GDP-bound Arfs are primarily cytosolic, their activation by GEFs is crucial for their function in membrane trafficking. Arf-GEFs possess a Sec7 domain, which is responsible for their activity and a pleckstrin homology domain (PH), important for membrane association and N-terminal coiled-coil domain (CC), which is responsible for the interaction with cellular-binding partners. The best-characterized Arf-GEFs are the cytohesins. The cytohesin family consists of four members: cytohesin-1, -2, -3 and -4 (Casanova, 2007; Kolanus, 2007; Shin and Nakayama, 2004).

Cytohesin-1 interacts with a β2-integrin (LFA-1), which mediates its activation and GEF activity. Moreover, overexpression of cytohesin-1 in Jurkat cells facilitates adhesion of LFA-1 to ICAM-1. More detailed studies revealed that cytohesin-1 expression in DCs is crucial for β2-integrin adhesion and for bone marrow DC (BMDC) migration into lymph nodes *in vitro* and *in vivo* (Weber et al., 2001; Quast et al., 2009). Cytohesin-2 interacts with Arf6 at the plasma membrane. Although cytohesin-2 and cytohesin-3 are very closely related (80% identity) they have different functions in β1 integrin recycling. Knockdown of cytohesin-2 causes decrease of cell adhesion, migration and spreading, whereas cytohesin-3 knockdown enhances these processes. Additionally, cytohesin-3 acts upstream of PI3K activity in insulin signaling (Oh and Santy, 2010; Coehn et al., 2007; Kolanus, 2007). Cytohesin-4 is less characterized than other family members. Like other cytohesins, it is not inhibited by Brefeldin A and shows GEF activity with Arf1 and Arf5 but not with Arf6 (Ogasawara et al., 2000).

1.5.3 Arl4 family

The Arl4 family consists of Arl4a, Arl4c and Arl4d. They can be distinguished from the other members of the Arf family by the C-terminal extension of 10-15 basic residues and a short insertion in the loop between the two switch regions. Similar to the Arf family, most Arl4s have an N-terminal myristoyl group, which is only exposed in the GTP-bound form (Hofmann et al., 2007; Pasqualato et al., 2002). Furthermore, it contains a C-terminal nuclear localization signal (NLS) (Lin et al., 2000).

Arl4a is distributed to the plasma membrane, cytosol and *trans*-Golgi network (TGN) (Lin et al., 2011). Arl4a can regulate actin remodeling via recruitment of cytohesin-2 to the plasma membrane and Arf6 activation (Li et al., 2007, Hoffmann et al., 2007). However, more recent studies revealed that Arl4a-induced cytoskeletal remodeling is Arf6-independent (Patel et al, 2011). Arl4a is the only Arl4 family member that interacts with golgin GCC185 in a GTP-dependent manner and recruit CLASPs, a family of microtubule binding proteins, to the Golgi membrane (Lin et a., 2011).

Arl4c, together with Arl4a and Arl4d, can recruit the C-terminal PH domains of cytohesin-1, cytohesin-3 and cytohesin-4 to the plasma membrane (Hofmann et al., 2007). Recent studies showed that expression of Arl4c is induced by stimulation with both Wnt3a and epidermal growth factor (EGF) resulting in epithelial tubular structure

formation (Matsumoto et al., 2014). The same group suggested that Arl4c could be a therapeutic target in lung and colorectal carcinoma, as Arl4s small interfering RNA (siRNA) injection inhibited tumor growth (Fujii et al., 2014).

Arl4d contains an N-terminal myristoylation site, two switch sites and a NLS (Fig. 5).

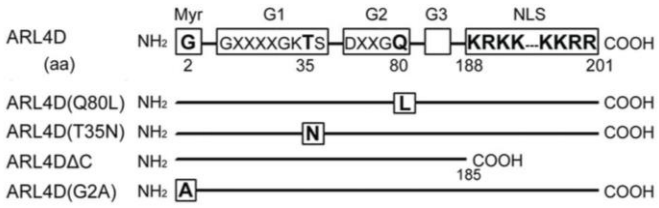

Figure 5. Schematic structure of wild type Arl4d and its mutants (Li et al., 2007).

Arl4d(T35N) - putative GTP-binding-defective; exist only in inactive form (GDP-bound);
Arl4d(Q80L) -putative GTP-bound form; exist only in active form (GTP-bound);
Arl4dΔC - lacks last 16 amino acids (aa) at C-terminus (NLS); no nuclear localization;
Arl4d(G2A) – N-myristoylation-deficient mutant; no membrane localization.

Human ARL4D interacts with cytohesin-2, particularly ARL4D WT, ARL4D(Q80L) and ARL4D(G2A) but not with ARL4D(T35N) or ARL4DΔC, demonstrating that this interaction is nucleotide dependent and requires the C-terminal NLS. Similar to other GTPases, localization of Arl4d at the plasma membrane is GTP- and myristyolation-dependent (Li et al., 2007). Furthermore, ARL4D recruits cytohesin-2 to the plasma membrane. The C-terminal polybasic c domain and the PH domain of cytohesin-2 are necessary for its relocation to the plasma membrane. Interestingly, cytohesin-2 does not catalyze nucleotide exchange on ARL4D but on ARF6. More detailed studies revealed that ARL4D activates ARF6 through cytohesin-2 that modulates actin remodeling and cell migration (Hofmann et al., 2007; Li et al., 2007).

Valproic acid (VPA) is involved in neuritogenesis and protection of the neurons upregulates Arl4d expression and the Arl4d-cytohesin-2-Arf6 signaling unit is involved in VPA-dependent neurite growth (Yamauchi et al., 2009).

Apart from the plasma membrane, the cytosol and the nucleus, Arl4d can also be found in the mitochondria. In fact, studies revealed that myristoylated GTP-defective ARL4D(T35N) is tightly associated with the inner membrane of the mitochondria. It not only alters the membrane potential but also causes mitochondrial fragmentation, indicating that ARL4D(T35N) might play a role in mitochondrial dynamics (Li et al., 2012).

2 Objectives

The adaptive immune system is initiated when CD8 T cell recognize antigen presented on the surface of APCs. Recognition of the antigen requires physical contact after which the immunological synapse is formed. This specific structure serves as a site of the signaling exchange that leads to T cell activation or inhibition. Depending on cell phenotype and the outcome of the interaction, different types of IS are observed.
In the liver, the soluble antigens are cross-presented to CD8 T cells on the surface of non-professional APCs, liver sinusoidal endothelial cells. Liver-primed CD8 T cells differentiate into nonresponsive cells that possess memory-like function upon infection. This unique differentiation state depends on the delivery of co-inhibitory signals from PD-L1 on LSECs surface to PD-1 on CD8 T cell surface. However, the further mechanism of PD-L1/PD-1 signaling has not been investigated.

The aim of this work was to better characterize the unique interaction between CD8 T cells and LSECs that has not been observed in any other organ. Therefore, the following questions were addressed:

- What kind of immunological synapse is formed at CD8 T cell-LSEC contact site?
- Does PD-L1 signaling have an impact on immunological synapse formation?
- Is nonresponsive state of liver-primed CD8 T cells reversible by co-stimulation?
- Are there other inhibitory molecules downstream of PD-1 involved in the induction of nonresponsiveness?

3 Material and Methods

3.1 Material

3.1.1 Equipment

Equipment	Name (Company)
Autoclave	Belimed, Cologne
AutoMACS	Miltenyi, Bergisch Gladbach
Camera EMCCD	ImagEM C9100-13 (Hamamatsu Photonics, Japan)
Cell counting chamber	Neubauer (La Fontaine via Labotec, Göttingen)
Cell culture plates	24-well Corning Cellbind®, flat (Corning Incorporated Life Sciences, Lowell/USA); 24-well/48-well/96-well, F- /U-base (TPP, Trasadingen/CH)
Cell sorter	FACSAriaIII™ (Becton Dickinson, Heidelberg)
Centrifuges	Multifuge 3s-r, Biofuge fresco, Biofuge Pico (Heraeus, Hanau)
Cover slips	Round (Marienfeld, Lauda-Königshofen)
ELISA reader	Mithras LB940 (Berthold Technologies, Bad Wildbad)
ELISA washer	(Nalge Nunc International, via neoLab, Heidelberg)
Flow cytometer	Canto II, LSRFortessa™ (Becton Dickinson, Heidelberg)
Fridge (+4°C)	Economic cooler (Bosch, Stuttgart); Liebherr premium, Liebherr comfort (Liebherr, Biberach)
Freezer (-20°C)	Liebherr comfort (Liebherr, Biberach)
Freezer (-80°C)	Hera freeze (Heraeus, Hanau)
Incubators	Hera cell, Hera cell 240 (Heraeus, Hanau)
Illumination system	MT20E (Olympus, Japan)
Light Cycler	LightCycler® 480 II (Roche, Penzberg)
Microscope	FluoView 1000 and IX81 (Olympus, Japan)
Pipettes	0.5-10µl, 2-20µl, 20-200µl, 100-1000µl (Eppendorf, Hamburg)
Perfusion pump	Masterflex (Cole-Parmer Instrument Company via Novodirect, Kehl/Rhein)

Petri-dishes	10 cm (Greiner bio-one, Solingen)
Preperation instruments	Labotec, Göttingen
Shaking water bath	GFL® 1092 (GFL®, Burgwedel)
Sieves, steel	University of Bonn, Department „Feinmechanik“
Slides	26x76mm (Marienfeld via Labomedic, Bonn)
Workbench, sterile	Hera safe (Heraeus, Hanau)

3.1.2 Chemical and Reagents

Chemical/Reagent	Company
Agarose, electrophoresis grade	Invitrogen, Karlsruhe
Avidin/Biotin Blocking Kit	Invitrogen, Karlsruhe
Bovine serum albumin (BSA)	Roth, Karlsruhe
Brefeldin A	eBioscience, USA
CollagenR solution	Serva, Heidelberg
Electrophoresis System	Mini-Protean®, Bio-Rad, Munich
DABCO	Sigma-Aldrich, Steinheim
DMEM Medium	Gibco BRL, Karlsruhe
Dimethylsulfoxid (DMSO) ($(CH_3)_2OS$)	Merck, Darmstadt
Donkey serum	Jackson Immunoresearch, USA
EDTA ($C_{10}H_{12}N_2O_8$)	Roth, Karlsruhe
Ethanol, absolut ($C_2H_4O_2$)	Applichem, Darmstadt
Fetal bovine serum (FCS)	PAA, Pasching, Austria
GBSS	PAA, Pasching, Austria
Ionomycin	Sigma-Aldrich, Steinheim
L-Glutamine (200 mM) ($C_5H_{10}N_2O_3$)	Cambrex, Verviers, Belgium
beta-mercaptoethanol ($HS(CH_2)_2OH$)	Sigma, Deisenhofen
Monensin	eBioscience, USA
Nycodenz	Axis-Shield, Norway
Ovalbumin (OVA)	Serva, Heidelberg
Pancoll	PAN Biotech, Aidenbach
Paraformaldehyde (PFA, $H(-OCH_2)n-OH$)	Fluca, Buchs
PBS	Biochrom, Berlin

Penicillin (10,000 U/ml)/Streptomycin (10 mg/ml)	PAA, Pasching, Austria
Percoll	GE Healthcare
Phorbol-12-myristat-13-acetat (PMA)	Sigma-Aldrich, Steinheim
ProlongGold	Invitrogen, Karlsruhe
RPMI 1640 Medium	Gibco BRL, Karlsruhe
SDS	Applichem, Darmstadt
Semi-dry Blotter	TE77, Amersham via GE Healthcare, Freiburg
Sodium azide (NaN_3)	Sigma, Deisenhofen
Sodium hydroxide (NaOH)	Merck, Darmstadt
TMB-Substrate	Pierce, Bonn
Tris ($C_4H_{11}NO_3$)	Roth, Karlsruhe
Tris-Buffered Saline (TBS)	Applichem, Darmstadt
Triton X-100	Promega, USA
Trypan Blue	Serva, Heidelberg
Tween-20	Merck, Darmstadt

3.1.3 Antibodies

3.1.3.1 Flow cytometry

Antigen	**Isotype**	**Clone**	**Company**
CD4	Rat IgG2a κ	RM4-5	eBioscience
CD8α	Rat IgG2a κ	53.6-7	BioLegend
CD25	Rat IgG1 κ	PC61.5	eBioscience
CD44	Rat IgG2b	IM7	eBioscience
CD45.1	Rat IgG2a κ	A20	eBioscience
CD45.2	Rat IgG2a κ	104	eBioscience
CD62L	Rat IgG2a κ	MEL-14	eBioscience
CD90.1 (Thy1.1)	Rat IgG2a κ	HIS51	eBioscience
CD127	Rat IgG2a κ	A7R34	eBioscience
CD279 (PD-1)	Hamster IgG	J43	eBioscience
IL-2	Rat IgG2a κ	JES6-5H4	eBioscience
IFNγ	Rat IgG1 κ	XMG1.2	eBioscience

Isotype control	Rat IgG1 κ	eBRG1	eBioscience
Isotype control	Rat IgG2a κ	eBRG2	eBioscience
KLRG1	Hamster IgG	2F1/KLRG1	BioLegend

Antibodies were directly fluorochrome labeled. Depending on fluorochrome-conjugate, antibodies were used in following dilutions:

- FITC, Alexa488 1:100
- PE, APC, PercpCy5.5, PE-Cy7, eFluor 450, BV421, Pacific Blue, BV650 1:200/1:300

3.1.3.2 ELISA

Antigen	**Isotype**	**Clone**	**Conjugate**	**Company**
IFNγ	Rat IgG1	R46A2	Purified	eBioscience
IFNγ	Rat IgG1	XMG1.2	Biotin	eBioscience
IL-2	Rat IgG2a	JES6-1A12	Purified	eBioscience
IL-2	Rat IgG2b	JES6-5H4	Biotin	eBioscience

3.1.3.3 Functional antibodies

Antigen	**Isotype**	**Clone**	**Company**
CD28	Golden Syrian Hamster IgG	37.51	eBioscience
Isotype control	Golden Syrian Hamster IgG		eBioscience
CD3		145-2C11	Institute of Molecular Medicine, Bonn
CD28		PV-1	Institute of Molecular Medicine, Bonn

3.1.3.4 Immunofluorescence

Primary antibodies

Target	**Host**	**Clone**	**Conjugate**	**Company**
TCRβ	Armenian Hamster IgG	H57-597	Biotin	eBioscience
CD11a	Rat IgG2a	I21/7	Purified	Southern Biotec

Secondary antibodies

Target	Host	Clone	Conjugate	Company
Rat	Goat	H+L	Cyanine3 (Cy3)	Jackson Immunoreserach
Biotin	Streptavidin		Cyanine5 (Cy5)	Jackson Immunoreserach
Armenian Hamster	Goat	H+L	AlexaFluor488	Molecular Probes
Rat	Goat	H+L	AlexaFluor488	Molecular Probes

3.1.3.5 Western Blot antibodies

Primary antibodies

Antigen	Conjugate	Company
β-actin	Purified	Santa Cruz Biotechnology
CD3ζ	Purified	Proteintech Europe
pCD3ζ	Purified	BD Bioscience
Lck	Purified	Cell Signalling Technologies
pLck	Purified	Cell Signalling Technologies

Secondary antibodies

Antigen	Conjugate	Company
Rabbit	HRP	Santa Cruz Biotechnology
Goat	HRP	Santa Cruz Biotechnology

3.1.4 Beads

Antibody-coated beads	Company
Anti-CD8 (MACS)	Miltenyi, Bergisch Gladbach
Anti-CD146 (MACS)	Miltenyi, Bergisch Gladbach
Anti-CD11c (MACS)	Miltenyi, Bergisch Gladbach

Fluorochrome-coated beads	Company
CountBright™ absolute counting beads	Invitrogen, Karlsruhe

3.1.5 Kits

All kits were used according to manufacturers instructions provided by the manual.

Name	Company
CD8α Isolation Kit	Miltenyi, Bergisch Gladbach
LIVE/DEAD Fixable NearIR Dead Cell Stain Kit	Invitrogen, Karlsruhe
RNeasy® Mini Kit	Qiagen, Hilden
SuperScript®VILO™	Invitrogen, Karlsruhe

3.1.6 Enzymes

Name	Company
Collagenase	Sigma, Steinheim and Roche, Basel
Peroxidase	Pierce, Bonn

3.1.7 Cell culture media

LSEC medium	DMEM high Glucose (4500 mg/l) 10% (v/v) FCS 10^5 U Penicillin 0.1 g/l Streptomycin 2 mM L-Glutamine
T cell medium	RPMI 1640 8% (v/v) FCS 10^5 U Penicillin 0.1 g/l Streptomycin

	2 mM L-Glutamine
	50µM β-mercaptoethanol

3.1.8 Buffers

ACK Lysis Buffer	16.58 g NH_4Cl
	2 g $KHCO_3$
	74.4 mg EDTA
	2000 ml H_2O
	pH 7.2-7.4
EDTA (0,5 M)	186.1 g EDTA
	approx. 20 g NaOH
	1000 ml H_2O
	pH 7.8-8.0
ELISA Blocking Buffer	0.5% (w/v) BSA in PBS
ELISA Coating Buffer	0.1 M $NaHCO_3$, pH 8.2
ELISA Washing Buffer	0.05% (v/v) Tween-20 in PBS
FACS Buffer	PBS
	1% (v/v) FCS
	2 mM EDTA
	0,02% (w/v) NaN_3
GBSS (Gey's balanced salt solution)	5 mM KCl
	1,6 mM $CaCl_2$
	0,9 mM $MgCl_2$
	0,3 mM $MgSO_4$
	0,2 mM KH_2PO_4

	1,7 mM Na_2HPO_4 (pH 7,4)
	2,7 mM $NaHCO_3$
	5,5 mM D(+)-Glukose
	50 mM HEPES
	pH 7,4
Liver Perfusion Buffer	0.01 g L- Aspartic acid
	0.02 g L-Threonine
	0.03 g L-Serine
	0.04 g Glycine
	0.05 g L-Alanine
	0.13 g L-Glutamic acid
	0.13 g L-Glutamine
	3.6 g D(+)-Glucose
	3.6 g D(-)-Fruktose
	67.4 g Sucrose
	0.22 g KCl
	0.1 g NaH_2PO_4* H_2O
	0.1 g $MgCl_2$* 6 H_2O
	2.4 g HEPES
	2.0 g $NaHCO_3$
	1000 ml H_2O
	0.05% (v/v) Collagenase
MACS Buffer	PBS
	1% (v/v) FCS
	2 mM EDTA
	pH 7,2
PBS	80 g/l NaCl
(phosphate buffered saline)	0.2 g/l KCl
	1.44 g/l $NaHPO_4$*2 H_2O

	0.2 g/l KH_2PO_4 pH 7.4
Spleen Perfusion Buffer	GBSS 0.5% (v/v) Collagenase
TBS (10x) (tris buffered saline)	200mM Tris 1.26M NaCl pH 7.6
TBS/T	TBS 0.1% (v/v) Tween 20
Western Blot: Lysis Buffer	20 mM Tris-HCl (pH 7,5) 150 mM NaCl 1 mM EGTA 1 mM EDTA 2.5 mM sodium pyrophosphate 1 mM β-glycerophosphate 1 mM sodium vanadate 1% (v/v) Triton X-100
Western Blot: Loading Buffer	0,58 M Sucrose 4% (w/v) SDS 0,04% (v/v) Bromphenol blue 62,5 mM Tris/HCl 60 mg/ml DTT pH 6,8
Western Blot: SDS-Running buffer	3 g Tris/HCl 14,4 g Glycin 1 g SDS 1000 ml H_2O

3.1.9 Animals

Experimental animals were kept under SPF (specific pathogen free) conditions in The House of Experimental Therapy (HET) or Institute of Molecular Medicine and Experimental Immunology (IMMEI) at the University Hospital Bonn.

Mouse strain	Description
Arl4d$^{tm1a(EUCOMM)Wtsi}$	Knockout of Arl4d molecule
PD-L1$^{-/-}$	Knockout of PD-L1 (B7H1) molecule
PD-1$^{-/-}$	Knockout of PD-1 molecule
C56BL/6	Inbred strain expressing the MHC I haplotype H-2^{b} (wild type mouse)
OT-I	Mouse strain bearing transgenic TCR on CD8 T cells, recognizing OVA$_{257-264}$ peptide on H2-K^{b} molecules
Arl4d OT-I	Crossed Arl4d$^{tm1a(EUCOMM)Wtsi}$ with OT-I mouse strain CD8 T cells of these mice are Arl4d-deficient and specific recognize OVA$_{257-264}$ peptide on H2-K^{b} molecules
CD45.1 OT-I	Crossed CD45.1 with OT-I mouse strain. Cells of these mice express CD45.1 that is used as a congenic marker to distinguish them from wild type (CD45.2) cells
Arl4d CD45.1 OT-I	Crossed Arl4d$^{tm1a(EUCOMM)Wtsi}$ with CD45.1 OT-I mouse strain
CD90.1	Cells of these mice express CD90.1 that is used as a congenic marker to distinguish them from wild type (CD90.2) cells

3.1.10 Recombinant viruses

Name	Description
Ad-GOL	Recombinant adenovirus expressing GFP, Ovalbumin and Luciferase driven by CMV promoter. Provided by

	Dr. Dirk Wohlleber (Institute of Molecular Immunology, Munich)

3.1.11 Primers

Name	Company
Arl4d TaqMan® Expression Assay (#Mm01249825_m1)	Life Technologies, Darmstadt
IL-2 TaqMan® Expression Assay (#Mm00434256_m1)	Life Technologies, Darmstadt

3.1.12 Software

Name	Application	Company
Cell-R	Microscopy data	Olympus
Excel 2011	Data analysis	Microsoft
FACS Diva V8.0.1	FACS measurement	BD Bioscience
FlowJo Version 9	FACS data analysis	Tree Star
Illustrator CS3	Graphic design	Adobe
ImageJ	Microscopy image analysis	NIH, USA
Microwin 2000 V4.37	ELISA analysis	Mikrotek Laborsystem
Prism5	Statistics and graphic design	Graph Pad Software
Word 2011	Documentation	Microsoft

3.2 Methods

3.2.1 Isolation of primary cells

All experimental animals were sacrificed by cervical translocation. Afterwards the body surface was cleaned with 70% ethanol and the body cavity was opened under semi-sterile conditions using surgical instruments.

3.2.1.1 LSEC isolation

In order to isolate liver sinusoidal endothelial cells (LSECs), the digestion of the liver tissue is required and was performed as follows. The portal vein (*Vena porta*) was first cannulated followed by the perfusion of the liver with perfusion buffer at the speed of 4 ml/min for 10-20 seconds. Blood was pumed out via *Vena cava* that had been opened at the start of perfusion. The liver was perfused until it turned yellow and transferred into the GBSS buffer, gallbladder was cut carefully. Afterwards collected livers were transferred into petri dish and all fluids were removed. The organs were minced using scissors, transferred into 50 ml tube and resuspend in 3ml GBSS containing 0,05% Collagenase per liver. The cell suspension was incubated for 15 min in 37^0C while shaking (240rpm). After incubation, digested tissue was passed through a 250µm steel sieve, washed with GBSS and centrifuged (1500 rpm, 10 min, 20^0C). The organ mass was resuspended in 1 ml fresh GBSS and transferred into 15 ml tube. Next, 1.23 fold 30% (v/v) warm (37^0C) Nycodenz was added. The cell suspension was mixed thoroughly and overlaid with 500-1000µl GBSS in order to prevent LSECs from drying out after centrifugation. The gradient centrifugation was performed for 20 min at the speed of 1400xg without brakes. The white-ring cell layer was collected in 1 ml MACS buffer, transferred into 50 ml tube and washed with MACS buffer (1500 rpm, 10 min). The purification of LSEC was performed using magnetic cell separation (MACS). Afterwards the cells were resuspended in LSEC medium at the concentration of $1*10^6$/ml and cultured in Corning Cellbind® 24-well or 96-well plates ($0,5*10^6$ and $0,2*10^6$ cells per well, respectively). For microscopy imaging non-coated 24-well plates were used. Each well contained glass cover slip, which had been coated with collagen (CollagenR solution, 1:10 dilution in distilled water) prior to LSEC isolation. One day after seeding, LSECs were washed with warm PBS containing 2% FCS in order to get rid of dead cells and debris. On day 2 or 3 after isolation, LSECs were used for further experiments.

3.2.1.2 Isolation of liver-associated lymphocytes

In order to isolate lymphocytes from the liver, organs were collected in GBSS and passed through 250µm steel sieve. Cells were washed with GBSS (1500 rpm, 10 min), resuspended in 10ml 40% Percoll solution (40% Percoll in PBS, v/v) and underlaid with 2 ml Pancoll solution. The gradient centrifugation was performed at the speed of 800xg for 20 min without brakes. Afterwards the upper layer containing hepatocytes and dead cells was discarded and the interface containing lymphocytes was collected for the *in vitro* stimulation.

3.2.1.3 Isolation of splenic CD8 T cells

In order to isolate CD8 T cells, spleens were collected in T cell medium and passed through 250µm steel sieve. Cells were washed ones (1500 rpm, 10 min), taken up in warm T cell medium and transferred into separation columns (syringes filled with 0.6g nylon wool per 10ml). After 45 min incubation time at 37^0C, columns were washed with T cell medium (2x syringe volume) and flow through containing lymphocytes was collected into 50 ml tube (other cells like macrophages and DCs adhered to the nylon wool). Cells were washed ones with T cell medium and onces with MACS buffer (1500 rpm, 10 min). CD8 T cells were purified using magnetic cell separation (MACS) and used for further experiments. When OT-I CD8 T cells were isolated, OT-I mice were injected (i.p.) 2 days before isolation with 300µg anti-NK1.1 antibodies in order to deplete NKT cells.

3.2.1.4 Isolation of splenic DCs

In order to isolate DCs, spleens were collected in PBS. Afterwards organs were transferred into petri dish and injected with warm spleen perfusion buffer and incubated for 20 min at 37^0C. Next, spleen were passed through steel sieves and washed with MACS buffer (1500 rpm, 10 min). $CD11c^+$ DCs were purified using magnetic cell separation (MACS) and used for further experiments.

3.2.1.5 Isolation of cells from the blood

In order to isolate cells from the blood, 32µl of blood were taken from the tail vein and transferred into PBS. After centrifugation (3000rpm, 5 min), cell pellets were

resuspended in ACK lysis buffer and incubated for 10 min at RT. Subsequently, cells were centrifuged (3000rpm, 5 min) and cell pellets were resuspended in FACS buffer and stained for FACS analysis.

3.2.1.6 Isolation of splenocytes

In order to isolate splenocytes, spleens were collected in PBS and passed through 250µm steel sieve. Cell suspension was washed in PBS (1500 rpm, 10 min), resuspended in FACS buffer and stained for FACS analysis.

3.2.2 Magnetic cell separation (MACS)

In order to purify the desired cell population from the whole organ, MACS seperation was performed. Cell suspension was incubated for 15 min in 4^0C with desired antibody-coated beads (3.1.4 or 3.1.5) in MACS buffer (positive selection) or in two steps (negative selection): first step for 10 min and second step for 15min, both in 4^0C. Afterwards, cells were washed (1200 rpm, 10 min) in MACS buffer to remove the unbound beads. Cell suspension was resuspend in 3ml MACS buffer and passed through nylon sieve. Depending on the used beads either positive or negative selection (program POSSEL or DEPLETE) was performed on AutoMACS (Miltenyi).
In order to obtain specific cell populations, the following protocols were used:

Cell type	Beads	Selection
LSEC	24µl anti-CD146/liver	POSSEL
CD8 T cells	20µl anti-CD8/spleen	POSSEL
CD8 T cells	50µl/100*10^6 cells biotin-antibody cocktail; 100µl/100*10^6 cells anti-biotin beads	DEPLETE
DC	20µl anti-CD11c/spleen	POSSEL

3.2.3 Cell culture

All isolated cells were cultured at the following conditions:

- temperature – 37^0C
- relative humidity – 90%
- CO_2 – 5%

3.2.3.1 Antigen-specific stimulation of CD8 T cells by either LSEC or DC

2-3 days mature LSECs were used for further experiments, when they were 85-100% confluent. $1*10^6$ or $2*10^5$ isolated CD8 T cells were added to each well with LSECs in 1000µl T cell medium or 200µl (24-well plate and 96-well plate, respectively) and cocultred for the indicated time points. DCs were freshly isolated at the same day as CD8 T cells, mixed 1:2 and cocultured in 1000µl T cell medium (24-well plate) for the indicated time points. In all experiments, for antigen-specific stimulation of CD8 T cells, OVA was applied at a concentration of 100µg/ml.

3.2.3.2 Stimulation of CD8 T cells with antibodies

Prior to CD8 T cell isolation, 96-well plate was coated with anti-CD3 (2µg/ml) and anti-CD28 (10µg/ml) in PBS. After 2 hours of incubation at 37^0C, plate was washed three times with PBS. $2*10^5$ CD8 T cells were cultured in 200µl T cell medium for indicated periods of time.

3.2.3.3 Restimulation of CD8 T cells

CD8 T cells from co-culture or *in vivo* experiments were restimulated with PMA (5ng/ml) and Ionomycin (200ng/ml) in T cell medium for 4 hours at 37^0C. In addition, Brefeldin A and Monensin (1:1000) were added to prevent the secretion of cytokines to the medium. Afterwards, CD8 T cells were washed once with T cell medium and once with FACS buffer (1500 rpm, 10 min) and stained intracellularlly for FACS analysis.

3.2.3.4 Calculation of the cell number

The cell number was determined using Neubauer Cell Chamber. 10µl of the cell suspension was mixed with 90µl Trypan Blue and transferred into the chamber. Non-stained cells (live cells) in 4 big squares were counted. The calculation was performed using the following formula:

$$total\ cell\ number\ \left(\frac{1}{ml}\right) = \frac{counted\ cell\ number}{4} \times 10(dilution) \times 1000(chamber\ factor)$$

3.2.4 Antigen-specific stimulation of CD8 T cells *in vivo*

3.2.4.1 Adoptive transfer

Sorted naive OT-I CD8 T cells from spleens were adoptively transferred by intravenous injection (i.v.) at the amount of $8*10^5$ cells/mouse.

3.2.4.2 Infection with the recombinant Adenovirus

One day after adoptive transfer, mice were infected with non-replicating AdGOL. The virus was diluted in NaCl solution and injected i.v. at the amount of $5*10^6$ PFU/mouse.

3.2.4.3 Analysis of CD8 T cell response

Cells from blood (3-8 days after infection), spleen (8 days after infection) and liver (8 days after infection) were isolated as described in 3.2.1.5, 3.2.1.6 and 3.2.1.2, respectively. In order to track adoptively transferred cells, cells were stained for the indicated congenic markers (CD45.1, CD45.2 or CD90.1) and measured by FACS. Additionally, cells were stained with antibodies against CD8, CD44, CD62L, KLRG1 and CD127 in order to determine development of effector cells after infection.
Eight days after infection splenocytes and liver-associated lymphocytes were restimulated as described in 3.2.3.3 and stained intracellulary for IL-2 and IFNγ.

3.2.5 Flow cytometry

3.2.5.1 Staining of the surface markers

In order to stain markers expressed on the cell surface, 10^5-$5*10^6$ cells were stained in in 96-well plate or FACS tubes containing 50µl and 500µl FACS buffer with specific antibodies, respectively. Cells were incubated for 15 min at 4^0C. Afterwards cells were washed two times in FACS buffer (2 min, 1600rpm), resuspended in 100-200µl FACS buffer and measured on FACS Canto II or LSRFortessa™ (BD Bioscience).

3.2.5.2 Intracellular staining of cytokine production

After restimulation, as described in 3.2.3.3, cells were washed in FACS buffer (2 min, 1600rpm) and stained for surface molecules (3.2.5.1). Next, cells were washed once (2 min, 1600rpm) and fixed in 100µl PFA (4% w/v in PBS) for 10 min at RT. After washing once with FACS buffer and once with 1x PERM Buffer (eBioscience, 2 min, 1600rpm), intracellular staining was performed in 96-well plates in PERM Buffer containing specific antibodies for 30 min on ice. After incubation time, cells were washed once with PERM Buffer, once with FACS buffer and resuspended in FACS buffer. For every staining an isotype control staining was applied.

3.2.5.3 Live/Dead staining

In order to distinguish between live and dead cells, specific Live/Dead staining is required. Depending on the experiment two different fluorophores were used:

- Hoechst 33258: added prior to measurement at final concentration 10µg/ml
- LIVE/DEAD Fixable NearIR Dead Cell Stain Kit: added during staining with surface markers at the concentration of 1:1000

All cells positive for the indicated fluorophores were considered as dead cells and were excluded from the analysis.

3.2.5.4 FACS sorting for adoptive transfer

Spleens were collected and mashed through metal sieve. Next, CD8 T cells were isolated from whole splenocytes using the „CD8α T cell isolation Kit". In order to sort pure naive CD8 T cell population, cells were stained in 500µl MACS buffer for CD8, CD44 and CD62L for 15 min at 4^0C. CD8 T cells were sorted at 4^0C into 15 ml tubes filled with 2ml T cell medium.

3.2.5.5 Cell number determination by FACS

In order to determine cell number, 5000 CountBright™ absolute counting beads were added to each sample prior to acquisition on FACS CantoI or LSRFortessa™ (BD Bioscience). The calculation was performed using the following formula:

$$cell\ number(sample) = \frac{counted\ cells}{counted\ beads} x5000(added\ beads)$$

To calculate cell number in the organ, total cell number was multiplicated with the respective dilution factor.

3.2.6 ELISA

In order to determine the cytokine concentration in supernatants, the sandwich enzyme linked immunosorbent assay (ELISA) was performed as follows. 96-well plate were coated either 1 hour in 37^{0}C or overnight in 4^{0}C with 50µl/well ELISA-Coating Buffer containing primary antibodies (1:500). Next, plates were washed three times with ELISA-Washing buffer and blocked with 100µl/well ELISA-Blocking buffer for 30 min at RT. After three subsequent washing steps, 50µl/well cell culture supernatant was added to each well and incubated for 1 hour at 37^{0}C. Additionally, blank controls (medium alone) and standard controls (titreted 1:4) were included. Plates were incubated for 1 hour at 37^{0}C or overnight at 4^{0}C. After three times of washing, secondary biotin-coupled antibodies were added (1:500) and plates were incubated for 1 hour in 37^{0}C). Next, plate was washed three times and incubated with 50µl/well streptavidin conjugated horseradish peroxidase (POX, 1:1000 in PBS) for 30 min at 4^{0}C. After three times of washing, 80µl/well TMB was added. A few minutes later, optical density (OD) was measured using an ELISA reader.

3.2.7 Microscopy

3.2.7.1 Immunofluorescence staining

Cells were cultured on coverslips (see 3.2.1.1). At the indicated time periods, coverslips were fixed with 4% PFA (w/v in PBS) on ice for 10 min. Next, washed three times with 1xTBS and blocked with 1% BSA + 5% donkey serum (Jackson Immunoresearch) for 30 min at RT. After three times of washing with 1xTBS, cells were stained with primary antibodies in 1% BSA and incubated for 1 hour at RT in the dark. Next, coverslips were washed three times with 1xTBS and stained with secondary antibodies in 1% BSA for 30 min at RT in the dark. Then, coverslips were washed two times with 1xTBS and one time with distilled water. After washing, coverslips were mounted in a one drop of Prolong Gold (Invitrogen) + anti-fade reagent DAPCO (Sigma-Aldrich).
Antibodies used for staining are listed in 3.1.3.4. The following dilutions were used:

- rat anti-CD11a 1:100
- biotin TCRβ 1:50
- anti-rat Alexa 488 1:200
- streptavidin Alexa488 1:200
- anti-rat cy5 1:200
- streptavidin cy3 1:200

During staining for TCRβ an additional step (between first washing with 1xTBS and blocking with 1% BSA + 5% donkey serum) was included: coverslips were incubated with Biotin Block solution A (Invitrogen) for 15 min, washed one time with 1xTBS and incubated with Biotin Block solution B (Invitrogen) for 15 min. After three times of washing with 1xTBS staining was continued as described above.

3.2.7.2 TIRF and confocal microscopy

In order to investigate the immunological synapse formed at the CD8 T cell-LSEC interface, total internal reflection fluorescence (TIRF) microscopy and confocal microscopy were used.

TIRF and epifluorescence microscopy was performed using an Olympus XI81 equipped with 60x 1.49 NA Apochromat objective and an EMCCD camera (16 x 16 μm^2 pixel size; ImagEM C9100-13, Hamamatsu Photonics). In addition, 2x and 1.6x supplementary magnifying lens were also used during imaging resulted images with 83.3 nm pixel size.

For illumination, the device is coupled with both an illumination system MT20E and a 488 nm laser (LAS/488/20, Olympus) for epifluorescence and TIRF microscopy modus, respectively. The system was operated using the Olympus CellR software (Olympus, Japan).

Confocal microscopy was performed using an Olympus FluorView™ FV1000 microscope equipped with an UPlanSApo 60x NA 1.35 objective (Olympus, Japan). For confocal illumination 543 nm laser line (cy3) and 633 nm laser line (cy5) were used. Recording was performed using Fluoview 3.0 software (Olympus, Japan).

3.2.7.3 Autocorrelation analysis

In order to calculate cluster size autocorrelation analysis was performed using the ImageJ program. Squared regions of interest (ROI) with a size of 45 pixels x 45 pixels were placed on the contact size. Then the selected ROI was duplicated to generate the reference ROI and correlated with the original image yielding a correlation coefficient of 1. Afterwards, the ROI was displaced pixel-wise up to 7 pixels and duplicated simultaneously on each shifted position and correlated with the reference ROI to calculate the correlation coefficient after each displacement. The operation was performed in all four directions (up, down, right, left) and the four values were averaged. The calculated values were plotted against the number of pixel shift yielding an autocorrelation decay curve for the respective ROI. Autocorrelation curves from individual cells were averaged for one independent experiment.

3.2.8 Gene expression array

Gene expression array has been performed in cooperation with Institute of Pathology, University Hospital in Bonn, by Dr. Lukas C. Heukamp and was performed as described (Biermann et al., 2007) . In short, for the analysis $1*10^6$ CD8 T cells from co-culture with LSECs were used. We performed RNA isolation using „RNeasy Mini Kit“ (Qiagen) according to manufacturer's recommedations and the further analysis was perfomed in Institute of Pathology. The RNA quality was assessed by Agilent Bioanalyzer 2000 (Agilent Technologies, Palo Alto, CA, USA) and only sample with RIN (RNA integrity number) values > 8 were used for the analysis. Probe preparation, hybridization, image generation and analysis were performed according to the manufacturer's guidelines for the AB1700 Microarray system. Autogridding, basic quality control, feature extraction, background correction, spot and spatial normalization were carried out with the Applied Biosystems 1700 Chemiluminescent Microarray Analyzer according to the manufacturer's instructions. The bioinformatic data were normalized by quantile normalization and transformed to log2 scale, using Bioconducter (http://www.bioconductor.org/docs/faq/)R software and the AB1700 Data Analysis script (Yongming, Andrew Sun, Applied Biosystems).

3.2.9 Western Blot

Cells from coculture were collected and lysed in WB Lysis Buffer. Afterwards cell lysetes were taken up in WB Loading buffer and incubated 5 min in 95^0C. The protein concentration was measured by BioRad DC assay. Next, electrophoresis chamber was filled with SDS-loading buffer. The equal amounts of the protein were transferred on SDS-poliacrylamide gel. Further, the gel was blotted on PVDF membrane. The protein was detected using proper primary antibodies diluted in TBS/T with 5% (w/v) BSA and incubated overnight in 4^0C. Afterwards, the membrane was washed and HRP conjugated secondary antibodies were added and incubated for 1 hour. HRP was detected via „ELC plus Western blot detection system" accroding to the manufacturer's guidelines.

3.2.10 Real-time PCR

RNA isolation was performed using the „RNeasy Mini Kit" (Qiagen) according to manufacturer's recommedations. 1µg RNA was transcribed using the SuperScript®VILO™ kit (Invitrogen) into cDNA. To analyse Arl4d and IL-2 expression Arl4d TaqMan® Expression Assay (#Mm01249825_m1) and IL-2 TaqMan® Expression Assay (#Mm00434256_m1) were used. Real-time PCR was performed using the LightCycler®480 II (Roche Diagnostics) for 40 cycles (95^0C for 15s and 60^0C for 1 min). GAPDH was used as reference gene.

4 Results

4.1 The immunological synapse formed by CD8 T cells and LSEC is not affected by PD-L1/PD-1 interaction

4.1.1 Contact of CD8 T cell with LSEC results in multifocal immunological synapse formation

Antigen recognition by T cells and their activation initiate adaptive immune responses.

Direct contact of T cell and APC results in immunological synapse (IS) formation, which consists of TCR-pMHC clusters (cSMAC), surrounded by adhesion molecules (pSMAC) (Alarcon, 2011; Thauland and Parker, 2010; Monks, 1998). So far several types of IS have been described: a classical bull's eye synapse, a multifocal synapse and a kinapse (Dustin, 2009; Alarcon, 2011). To investigate what kind of IS characterizes the LSEC-CD8 T cell interaction, we co-cultured naïve $H2K^b$-OVA specific CD8 T cells with OVA-loaded LSEC on collagen-coated coverslips for 30 and 60 minutes, to visualize early time points of IS formation (Fig 6A). Afterwards the cells were fixed and stained for TCRβ (green), which is associated with the cSMAC, and the LFA-1 subunit CD11a (red), which is associated with the pSMAC. Then the T cell-APC contact site was visualized using confocal microscopy. We found that antigen-specific interaction of CD8 T cells with LSECs results in TCRβ and CD11a cluster formation. TCRβ and CD11a clusters did not overlap and were spread all over the contact area, indicating that multifocal immune synapse was formed (Hailman et al., 2002; Brossard et al., 2005). As the CD8 T cells upon antigen recognition presented by LSECs stop migrating (von Oppen et al., 2009), we did not observe a kinapse.

4.1.2 PD-L1/PD-1 signaling rapidly interferes with TCR signal transduction

We have previously discovered that CD8 T cells primed in the liver under noninflammatory conditions by antigen presenting LSEC develop nonresponsiveness. Thus, they are not able to perform immediate cytotoxic

functions or to produce cytokines (Diehl et al., 2008; Böttcher et al., 2013) upon restimuation. Furthermore, interaction of CD8 T cells with antigen-presenting LSECs induces PD-L1 expression on these APCs and the unique CD8 T cell state is PD-L1-dependent (Diehl et al., 2008, Schurich et al., 2010).

It is reported that PD-1 expression is induced on activated T cells, B cells and NKT cells (Sharpe et al. 2007, Agata et al. 1996). As PD-1 expression on LSEC-primed CD8 T cells has not been investigated, we co-cultured wild type CD8 OT-I T cells with LSEC and we analyzed PD-1 expression for indicated times by flow cytometry (Fig 6B).

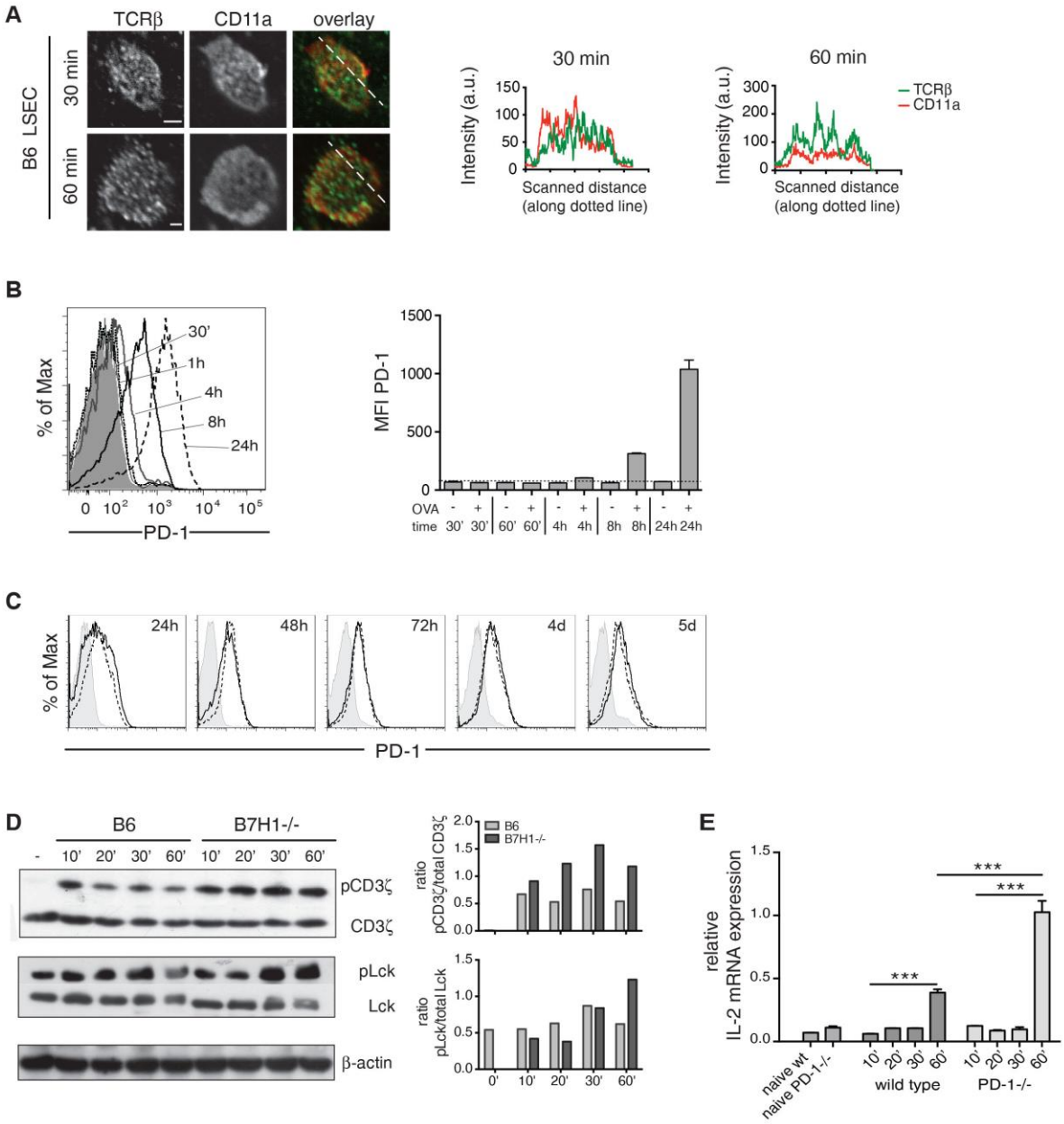

Figure 6. Naive CD8 T cell-LSEC interaction resembles a multifocal synapse.

A: OVA-loaded B6 were cultured with naïve OT-1 CD8 T cells and after the indicated times cells were fixed and stained for TCRβ (green) and the LFA-1 subunit CD11a (red) and analyzed by confocal microscopy. Line-scans show signal intensities (arbitrary units) along the dotted lines for TCRβ (green) and CD11a (red) in the overlay. Scale bar shows 10 µm. Representative data from 3 independent experiments are shown. Images are shown at arbitrary scaling. **B**: Naïve OT-1 T cells were co-cultured with B6 LSEC with or without OVA for the indicated times and stained for CD8 and PD-1. The histogram shows PD-1 expression over time gated on viable CD8 T cells. Filled grey histogram represents isotype control staining. Bar graph shows mean fluorescence intensity (MFI) of PD-1. **D:** OT-1 CD8 T cells were cultured with antigen-presenting wild type or PD-L1 $(B7H1)^{-/-}$ LSEC for the indicated times after which cell lysates were probed for protein expression by western blot as indicated and quantified. **E**: Wild type or PD-$1^{-/-}$ OT-1 CD8 T cells were cultured with antigen-presenting LSEC for the indicated times after which IL-2 mRNA levels were determined by real time PCR. Representative data from at least 3 independent experiments are shown. Data are shown as mean +/- SEM. Significance was calculated by ANOVA. *p≤0.05, **p≤0.01, ***p≤0.001.

PD-1 expression was antigen-dependently induced within 1-4 hours of T cell-APC interaction reaching a maximum at 24 hours (Fig 6B), indicating co-inhibitory signaling to T cells via PD-L1 on LSECs could occur early and was retained for at least 5 days (Fig. 6C).

It was shown that PD-1 down-modulates TCR signaling by inhibiting the TCR-associated phosphorylation of CD3ζ and ZAP70 (Sheppard et al., 2004; Dai et al., 2014). As we observed continuous expression of PD-1 on LSEC-stimulated CD8 T cells we wondered whether TCR proximal signaling is inhibited. For this reason, we co-cultured naïve CD8 T cells with either B6 or B7H1$^{-/-}$ (PD-L1-deficient) LSECs and performed western blot analysis. As shown in Fig. 6D, TCR signaling was detected within the first 10 minutes by phosphorylation of the CD3ζ chain. Furthermore, CD3ζ chain phosphorylation was attenuated over time in B6 LSEC-primed CD8 T cells. Interestingly, phosphorylation of CD3ζ and Lck, which is required for CD3ζ phosphorylation, was enhanced in the absence of PD-L1/PD-1 signaling as soon as 30' to 60', indicating that early attenuation of TCR proximal signaling in LSEC-stimulated CD8 T cells is PD-L1/PD-1-dependent.

PD-1 signaling has been shown to inhibit IL-2 production in T cells (Carter et al., 2002). We found that within 60' of LSEC stimulation IL-2 mRNA induction in naïve PD-1$^{-/-}$ CD8 T cells was significantly increased as compared to the wild type CD8 T cells, indicating that PD-1 signals are rapidly translated into differential response as early as 30'-60' after antigen-dependent stimulation by LSECs (Fig 6E).

Changes in TCR signal strength can lead to changes in immune synapse cluster formation: weaker proximal TCR signaling correlated with smaller TCR clusters (Yokosuka et al., 2005). Hence, we further studied whether the observed increase in TCR signaling strength in the absence of PD-L1-dependent signals influences IS formation. Thus, we cocultured naïve OT-I CD8 T cells with OVA-loaded PD-L1-deficient LSEC for the indicated times and stained for TCRβ and CD11a as depicted in Fig. 6A. As shown in Fig. 7, confocal microscopy revealed that also here a multifocal IS was formed. Taken together, formation of a multifocal synapse upon direct antigen-specific contact of CD8 T cell with LSEC is not influenced by PD-L1 signals.

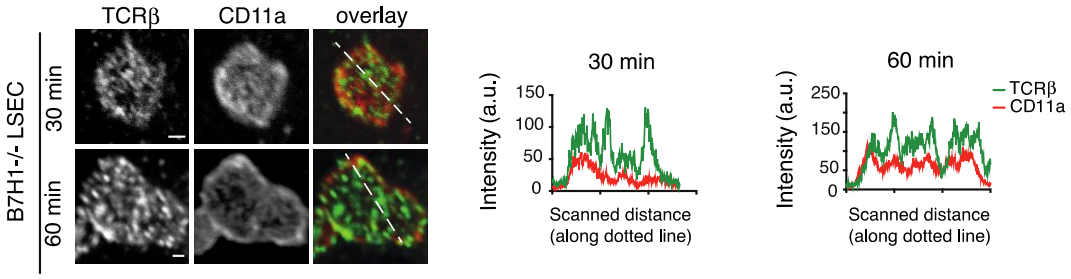

Figure 7. The absence of PD-L1 signaling did not prevent multifocal synapse formation.

OVA-loaded PD-L1 (B7H1)$^{-/-}$ LSECs were cultured and stained as in Fig. 6A and analyzed by confocal microscopy. Scale bar shows 10 μm. Images are shown at arbitrary scaling.

4.1.3 LSEC-mediated PD-L1 signals do not affect TCRβ and CD11a cluster formation

Although we found that PD-L1 signaling did not influence the spatial distribution of TCRβ and CD11a clusters within the interface between LSECs and T cells, we were interested whether the size and density of the individual TCRβ and CD11a clusters in the membrane were altered due to the lack of PD-L1 expression on LSECs. To visualize single TCRβ or CD11a protein clusters in the T cell membrane, we used total internal reflection fluorescence (TIRF) microscopy (Fig. 8). Using TIRF, we could perform a more detailed quantitative analysis of cluster density and size.

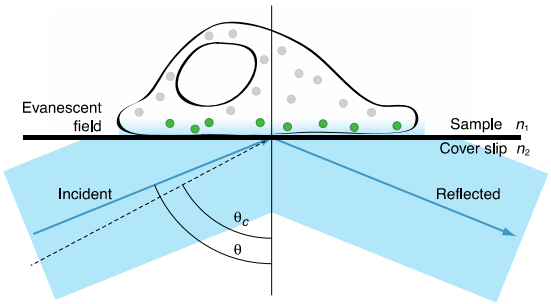

Figure 8. Schematic view of TIRF illumination principle (Mattheyses et al., 2010).

The excitation beam enters at the incident angle θ, which is bigger than critical angle θ_c. While excitation beam is reflected off the coverslip, evanescent field is formed on the other side of coverslip, where fluorophores are excited (green points). By means of TIRF fluorophores can be exited in a cellular environment very near the plasma membrane (within <100 nm) while intracellular fluorescence is reduced resulting in clear imaging of the contact area (Mattheyses, 2010; Axelrod, 2001).

LSECs are very thin at the T-cell-LSEC contact, and immunostained TCRβ and CD11a clusters in the membrane of naïve CD8 T cells can be excited by an evanescent wave that penetrates the LSECs. Using TIRF microscopy we also found single non-overlapping TCRβ and CD11a clusters at the T-cell/LSEC interaction plane, confirming the confocal data, which showed that a multifocal immune synapse is formed. Furthermore, PD-L1/PD-1 signaling did not alter the type of synapse and it did not change over the time period analyzed (Fig. 9A).

We further investigated the average cluster size of the TCRβ and CD11a clusters by means of autocorrelation analysis (see Material and Methods) (Fig. 9B). Here, we could not detect differences in cluster size of either molecule analyzed in synapses including PD-L1-dependent signalling or in synapses without (Fig. 9C). In addition, we did not observe differences in cluster density in the T cell membrane upon LSECs interaction (Fig. 9D).

Taken together, the TIRF microscopy data indicate that although LSEC-mediated PD-L1-dependent signals lead to early changes in downstream TCR signaling events in naïve CD8 T cells, it does not affect the phenotype of the immune synapse formed between LSECs and T cells.

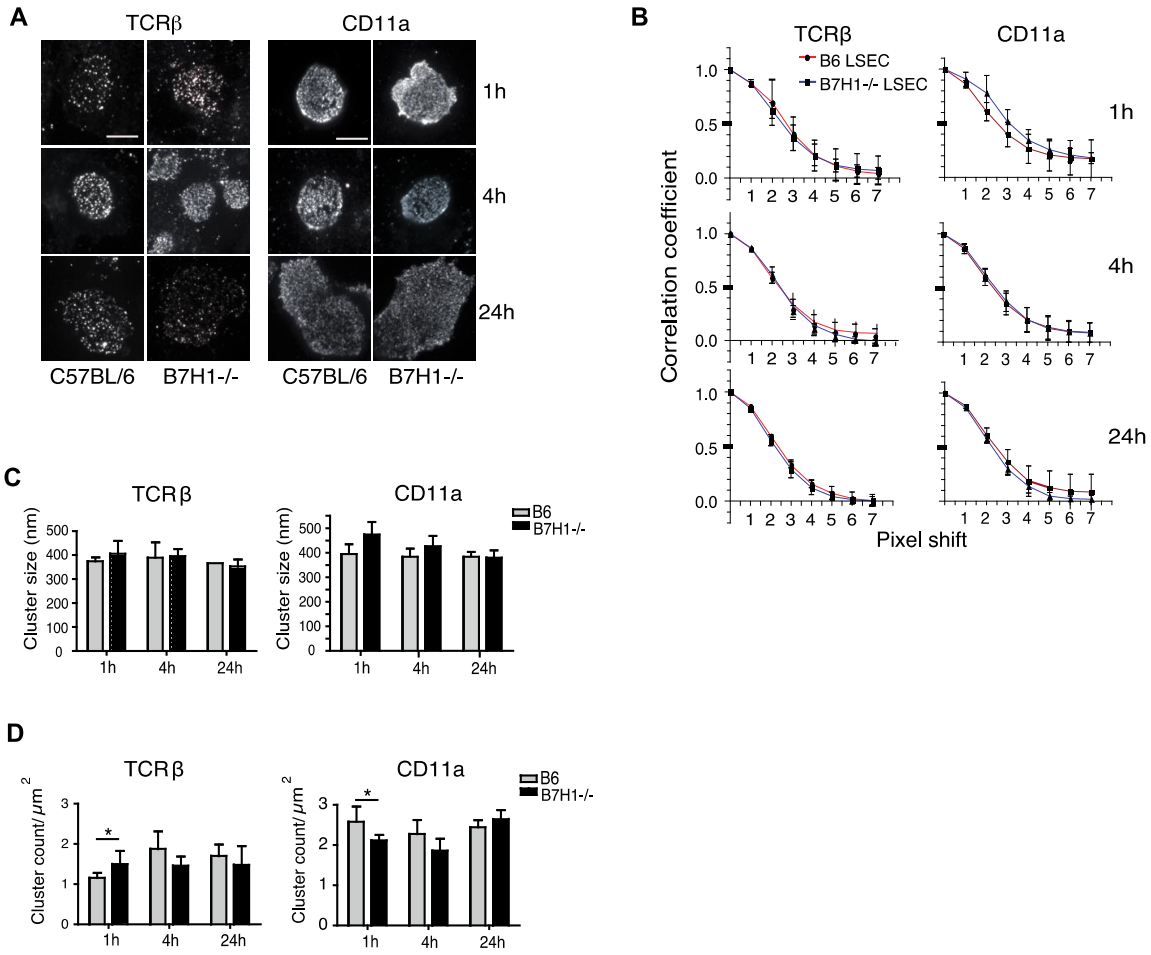

Figure 9. TCRβ and CD11a distribution in naïve CD8 T cell/LSEC interaction is not affected by PD-L1-dependent signals.

A: OVA-loaded B6 and PD-L1 $(B7H1)^{-/-}$ LSEC were cultured with naïve OT-1 CD8 T cells and after the indicated times cells were fixed and stained for TCRβ and CD11a and analysed by TIRF microscopy. Scale bar shows 6 μm. **B**: TCRβ and CD11a cluster sizes were examined by autocorrelation analysis: the approximate average half object size is proportional to the pixel shift leading to a correlation coefficient of 0.5 (n = 5 cells; values are given as mean ± SD; one pixel corresponds to 83.3 nm). **C:** Statistical analysis of B. **D**: Clusters were counted within a 14,051μm² area/T cell and cluster density is given as clusters per μm² (n=5). Data are representative for 3 independent experiments. Data are shown as mean +/- SD. Significance was calculated by Student t-test. *p≤0.05.

4.2. PD-L1/PD-1 signaling represses IL-2 production by LSEC-stimulated CD8 T cells

It was previously discovered that CD8 T cells, which had been primed in the liver under noninflammatory conditions by antigen-presenting LSECs develop nonresponsiveness, and are thus not able to perform immediate cytotoxic functions or to produce cytokines (Diehl et al., 2008; Böttcher et al., 2013). Furthermore, CD8 T cells primed by PD-L1$^{-/-}$ LSEC produce more IL-2 in comparison to CD8 T cells primed by B6 LSEC, indicating the role of PD-L1 in dampening of IL-2 production (Schurich et al. 2010; Diehl et al., 2008). To confirm that PD-L1-mediated effects were induced via PD-1 signaling we co-cultured PD-1$^{-/-}$ OT-I T cells with OVA-loaded LSECs and analyzed cytokine production by ELISA (Fig 10A). Indeed, we observed increased levels of IL-2 and IFNγ when PD-1 on T cells was lacking. Similarly, increased IL-2 production by T cells was observed when PD-L1 on LSECs was lacking (Fig. 10B).

These results suggest that LSECs utilize the regulatory PD-L1/PD-1 signaling pathway to dampen IL-2 production by CD8 T cells, thereby preventing their full activation.

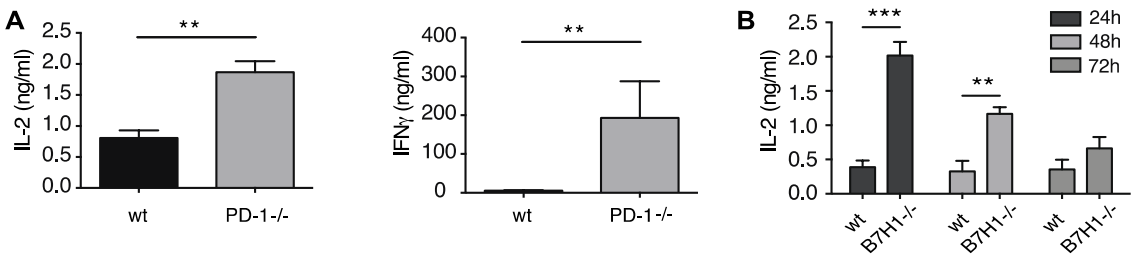

Figure 10. PD-L1/PD-1 signaling suppresses IL-2 production in LSEC-primed T cells.

A: Wild type or PD-1$^{-/-}$ OT-1 CD8 T cells were cultured with B6 LSEC for 4 days and restimulated with plate-bound anti-CD3ε antibodies. After 24h IL-2 and IFNγ content in the supernatant was determined by ELISA. **B**: OT-1 CD8 T cells were cultured with antigen-presenting LSEC from B6 or PD-L1 (B7H1)$^{-/-}$ mice for the indicated times and the IL-2 concentration in the supernatant was determined by ELISA at the indicated time points. Data are depicted as mean +/- SEM. Data are representative from 3 independent experiments. Significance was calculated by ANOVA. **p≤0.01, ***p≤0.001.

4.3 Co-stimulatory CD28 signaling does not prevent LSEC-mediated CD8 T cell non-responsiveness after prolonged co-inhibitory PD-L1/PD-1 signaling

Initially, LSEC-stimulated CD8 T cells upregulate costimulatory markers and proliferate to the same extent as CD8 T cells primed by DC. Nevertheless, they do not sustain the expression of activation markers but downregulate it with time (Diehl et al., 2008; Böttcher et al., 2014). In order to investigate whether this phenomenon was dependent on co-stimulatory/inhibitory signaling, we investigated the kinetics of the IL-2 receptor, CD25 on T cells primed by wild type LSECs PD-L1$^{-/-}$ LSECs and DCs (Fig. 11A). We could observe that CD25 expression on T cells activated by PD-L1$^{-/-}$ LSECs and DCs remains high in contrast to T cells activated by wild type LSECs where CD25 expression is downregulated within 48h. It has been reported that CD8 T cells require sustained TCR signaling to fully develop into functional effector cells with sustained CD25 expression (van Stipdonk et. al., 2003). In contrast, CD8 T cells that received brief TCR stimulus were less receptive to IL-2 (CD25 expression decreased after 24h) and less efficient in killing (van Stipdonk et. al., 2003).

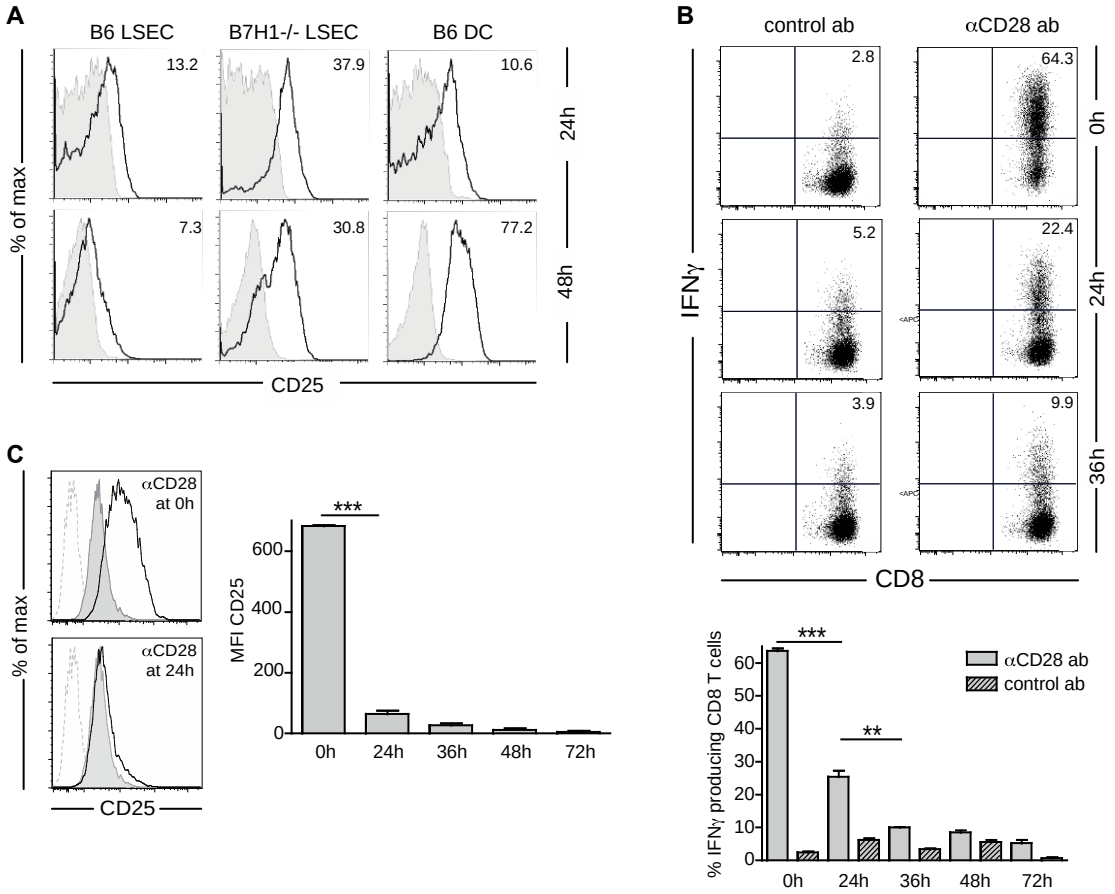

Figure 11. CD28 co-stimulation cannot reverse the induction of LSEC-primed CD8 T cells after PD-1 signal integration over time.

A: OT-1 CD8 T cells were co-cultured with antigen-presenting B6, PD-L1 $(B7H1)^{-/-}$ LSEC or B6 DC for the indicated times and stained for CD8 and CD25. Grey filled lines: isotype control, black lines: CD25. Histograms show viable CD8 T cells. Numbers indicate geometric mean of CD25. **B**: OT-1 CD8 T cells were co- cultured with antigen-presenting LSEC for 4 days, after which they were restimulated with PMA/ionomycin and 4 h later stained for CD8 and IFNγ. Anti-CD28 antibodies (10 mg/ml) or isotype control antibodies were added to the co-cultures at the indicated times. Bar graph shows percentages of IFNγ-producing CD8 T cells upon restimulation at day 4 after CD28 abs or control abs were added at the indicated times. **C:** OT-1 CD8 T cells were co- cultured with antigen-presenting LSEC for 4 days, after which they were stained for CD8 and CD25. Anti-CD28 antibodies (5 mg/ml) or isotype control antibodies were added to the co-cultures at the indicated times. Histograms show CD25 expression on viable CD8 T cells, black line: with anti-CD28; filled grey: with control antibody; dotted: unstained. Bar graph shows CD25 mean fluorescence intensity at day 4 on viable CD8 T cells co-cultured with LSEC and anti-CD28 antibodies added at the indicated times. Representative data of 3 independent experiments are shown. Data are depicted as mean +/- SD. Significance was calculated by student t-test. *p≤0.05, **p≤0.01, ***p≤0.001.

PD-1 expression on LSEC-primed CD8 T cells is sustained for at least 5 days (Fig. 6C), indicating that LSEC-primed T cells stay receptive to co-inhibitory signaling for the whole period of time. Therefore, we hypothesized that the LSEC-mediated unique differentiation of naïve CD8 T cells requires integration of co-inhibitory signals over time. To investigate this, we attempted to prevent the induction of an LSEC-primed state in CD8 T cells by adding co-stimulatory anti-CD28 antibodies to the CD8 T cell-LSEC co-culture at different time points during co-culture. After 4 days CD25 expression and IFNγ production by CD8 T cells was assessed (Fig 11B and C). When co-stimulation through CD28 was provided at early time points (0h or 24h), CD8 T cells expressed CD25 and produced IFNγ, thus nonresponsiveness has been prevented. However, when CD28 co-stimulation was provided at 36h into the co-culture, CD8 T cells were not able to produce IFNγ upon restimulation. Overall, lack of cytokine production correlated with the lack of CD25 expression.

Taken together, these results indicate that co-inhibitory PD-1 signals in LSEC-primed T cells are integrated within 24 hours. After this time CD28 co-stimulatory signals cannot prevent the induction of nonresponsiveness of CD8 T cells primed by LSECs.

4.4 Expression of small GTPase Arl4d in LSEC-primed CD8 T cells is PD-L1-dependent

Priming of naïve CD8 T cells by LSECs leads to development of T cells that are unable to perform effector function (Limmer et al., 2000). We could show that this unique state of CD8 T cells primed by LSECs is PD-L1/PD-1-dependent. In our group, gene expression analysis of *in vitro* generated LSEC-primed and DC-primed CD8 T cells was performed. Fig. 12 shows exemplary genes involved in T cell function, such as CD25 (IL-2Rα), CD122 (IL-2Rβ), granzyme B, IFNγ, T-bet, neuropilin 1 and Eomes. Genes involved in T cell activation (CD25, CD122, IFNγ, granzyme B) were not detected in LSEC-primed T cells, confirming previous findings that these cells are quiescent (Diehl et al. 2008, Böttcher et al., 2013). Moreover, we observed upregulation of Eomes expression, confirming the data of Böttcher et al. that LSEC-primed CD8 T cell show memory-like phenotype. Interestingly, one of the gene significantly induced in LSEC-primed T cells was the small GTPase Arl4d, however,

its function in T cells remains to be elucidated.

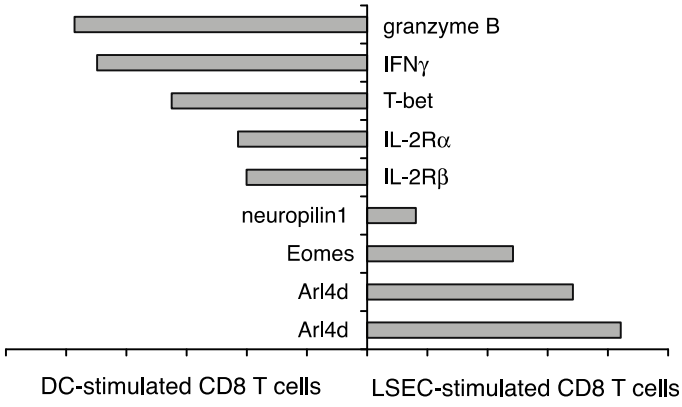

Figure 12. Arl4d expression is not detected in DC-stimulated CD8 T cells but upregulated in LSEC-primed CD8 T cells.

Naïve OT-I CD8 T cells were cocultured with OVA-loaded LSEC or DC for 4 days. Cells were harvested and gene expression analyzed as described in the materials & method section. Graph shows the relative expression of the indicated genes.

In order to validate the induction of Arl4d, we co-cultured CD8 T cells with B6 LSECs, PD-L1$^{-/-}$ LSECs and DCs and performed real-time PCR analysis. We observed a significant increase in expression of the small GTPase, Arl4d in nonresponsive B6 LSEC-stimulated CD8 T cells as compared to activated DC-stimulated CD8 T cells (Fig. 13). The induction of Arl4d mRNA did not occur in T cells stimulated by PD-L1$^{-/-}$ LSECs suggesting that Arl4d expression is induced in LSEC-primed CD8 T cells in a PD-L1-dependent fashion.

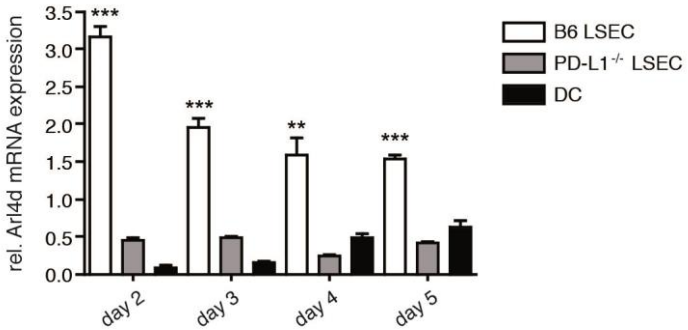

Figure 13. PD-L1-dependent expression of Arl4d in LSEC-primed CD8 T cells.

Naïve OT-I CD8 T cells were coculture with OVA-loaded B6 LSEC, PD-L1 $(B7H1)^{-/-}$ LSEC and DC for the indicated time points. Graph show mRNA Arl4d levels relative to naïve T cell mRNA levels (which were set as 1). Data are depicted as mean +/- SEM. Significance was calculated by student t-test. **p≤0.01, ***p≤0.001.

These data suggest that Arl4d could be differentially expressed in naïve, nonresponsive and activated CD8 T cells. To confirm our results, we stimulated *in vitro* naïve CD8 T cells with anti-CD3 and anti-CD28 antibodies for indicated time points and performed real-time PCR for Arl4d (Fig. 14). Again, the data analysis revealed a downregulation of Arl4d mRNA in stimulated CD8 T cells in comparison with naïve CD8 T cells. Taken together, *in vitro* co-culture and antibody-stimulation results suggest that upon delivery of co-inhibitory signals by LSECs, Arl4d expression is upregulated. In contrast, upon delivery of co-stimulatory signals by DC, PD-L1-deficient LSECs or anti-CD3/CD28 antibodies *in vitro*, Arl4d expression is downregulated.

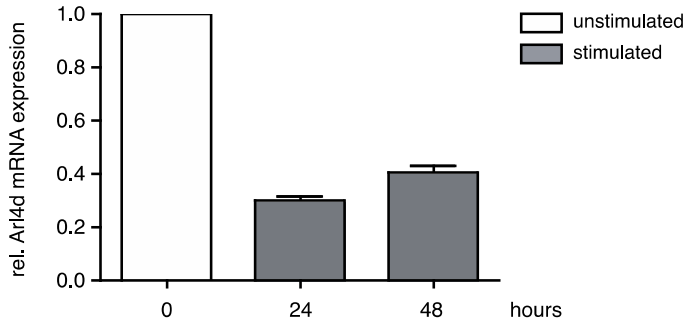

Figure 14. Arl4d expression is downregulated in activated CD8 T cells.

Naïve CD8 T cells were cultured on coated plate with anti-CD3 (2 µg/ml) and anti-CD28 (10 µg/ml) for the indicated time points. Graph shows Arl4d mRNA levels relative to naïve T cell mRNA levels (set as 1). Data are depicted as mean +/- SEM.

4.5 The Arl4d knockout mouse serves as a proper tool to study small GTPase function

As mentioned above, PD-L1/PD-1 signaling decreased CD8 T cell activation, cytotoxicity and inhibited IL-2 production. Interestingly, our findings on Arl4d expression (Fig. 12 and 13) suggest that Arl4d is induced downsteram of co-

inhibitory PD-L1/PD-1 signaling. So far Arl4d has been reported to regulate actin remodeling via Arf6 and cytohesin-2, it can be targeted to the mitochondria where it alters mitochondrial membrane potential or it can participate in neurite formation (Li et al. 2007; Li et al. 2012; Yamauchi J. et al. 2009). However, to date there are no data concerning the role of Arl4d in T cell function.

In order to investigate in detail the role of Arl4d in CD8 T cell immune regulation *in vitro* and *in vivo*, we obtained the Arl4d$^{tm1a(EUCOMM)Wtsi}$ mouse strain, which was generated by the Welcome Trust Sanger Institute in United Kingdom (Fig 15). Heterozygous mice obtained from the Sanger Institute were further bred to produce homozygous Arl4d knockout mice, which were used to study the role of Arl4d in CD8 T cell function.

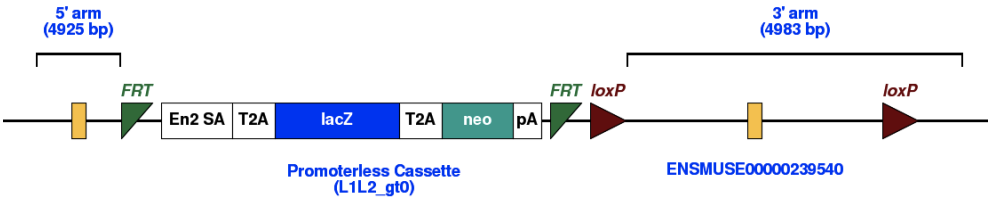

Figure 15. Schematic view of the "knock-out first" Arl4d$^{tm1a(EUCOMM)Wtsi}$ allele.

Arl4d gene has been targeted by insertion of the L1L2_gt0 cassette, composed of FRT-flanked lacZ/neomycin sequence, in chromosome 11 upstream of the critical exon. Additionally, loxP sites flank the critical exon (Welcome Trust Sanger Institute, MGI Direct Data Submission. 2010).

First, we characterized these mice in steady state and analyzed the lymphoid compartment. For this purpose, splenocytes from Arl4d$^{-/-}$ and wild type mice were stained for CD4 and CD8 and analyzed by flow cytometry. We found that the distribution of CD4 and CD8 T cells in the spleen of Arl4d knockout animals was comparable with wild type controls (Fig 16A). Moreover, also CD8 T cell percentages in the blood of Arl4d-deficient mice were not altered (Fig. 16B). As shown in Fig. 13, Arl4d expression depends on co-inhibitory PD-L1 signaling. PD-L1- and PD-1-deficient mice develop autoimmunity, therefore, it was important to study whether Arl4d-deficiency already influences the activation state of T cells in steady state. Therefore, we stained for commonly used surface markers to distinguish naïve from activated or memory CD8 T cells: CD44, CD25 (IL-2 receptor) and CD62L (L-

selectin). Expression levels of CD62L, a marker for naïve and central memory T cells, as well as the activation markers, CD44 and CD25 did not reveal major differences between Arl4d-deficient CD8 T cells and wild type CD8 T cells (Fig 16C, D and E). Taken together these data indicate that Arl4d deficiency neither affects the distribution nor the phenotype of CD8 T cells under homeostatic conditions.

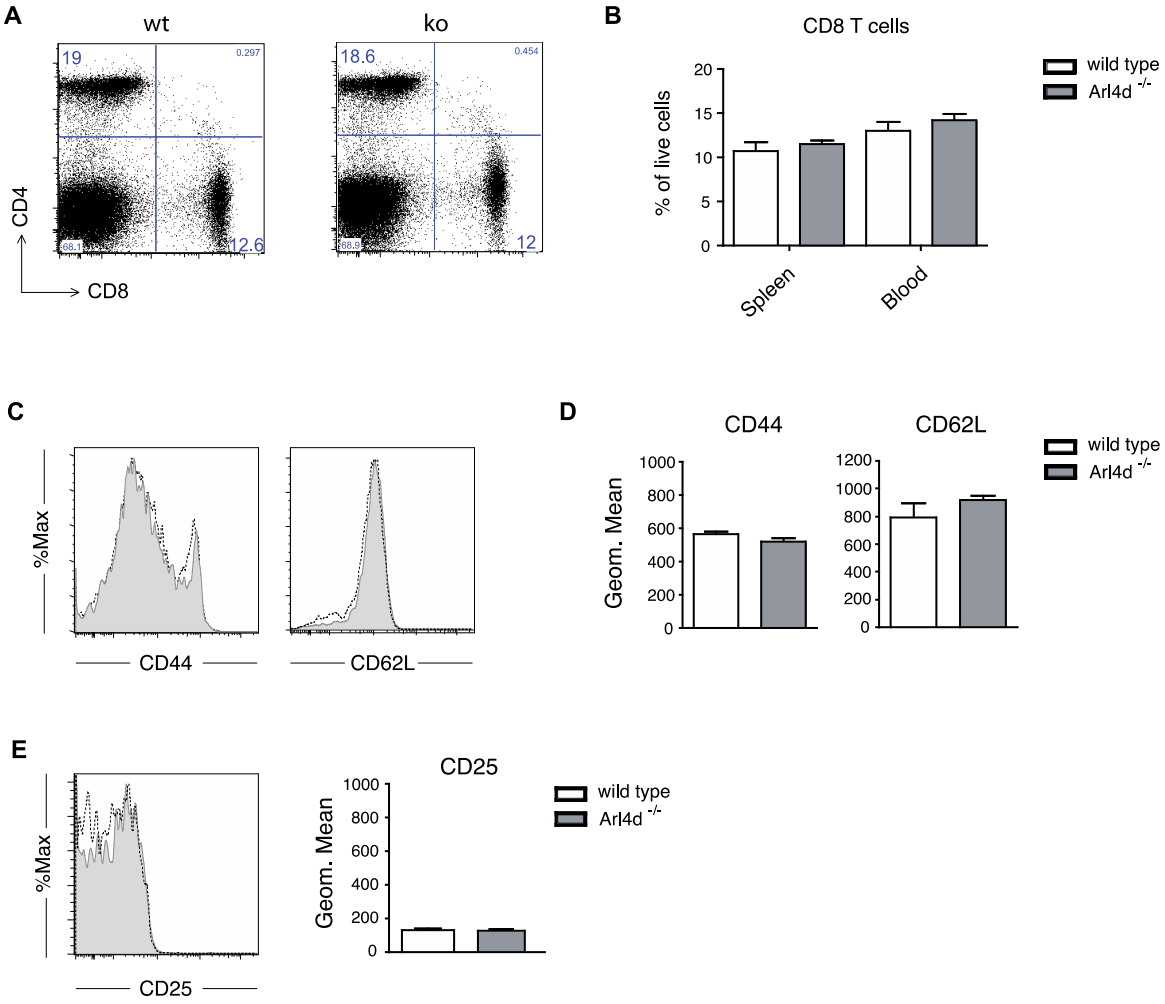

Figure 16. Arl4d-deficiency has no impact on CD8 T cell phenotype in steady state.

A: Arl4d-deficient and wild type splenocytes were stained for CD4 and CD8 and shown as percentages of live cells. Representative plots of one mouse from three are shown. **B:** Bar graph show percentages of CD8 T cells among live cells in the spleen and blood. **C:** Splenocytes were stained for CD8, CD44 and CD62L. The histograms show CD44 (left) and CD62L (right) expression on CD8 T cells. Dotted line shows wild type and filled gray line knockout splenocytes. **D:** Bar graphs show CD44 (left) and CD62L (right) geometric mean. **E:** Splenocytes were stained for CD8 and CD25. The histogram shows CD25 expression on CD8 T cells. Bar graph shows geometric mean of CD25. Data are shown as mean +/- SEM. Three mice per group were analysed. Data are representative for at least 2 independent experiments.

4.6 Arl4d deficiency leads to enhanced anti-viral CD8 T cell immune response

4.6.1 Arl4d dampens IL-2 production in CD8 T cells *in vitro*

LSEC-mediated nonresponsiveness of CD8 T cells depends on PD-L1 signaling, due to attenuation of IL-2 production (Diehl et al., 2008; Schurich et al., 2010). Interestingly, we could show that Arl4d expression is induced in LSEC-stimulated CD8 T cells and its expression is dependent on PD-L1 signals (Fig. 13). Based on these findings, we next investigated whether Arl4d plays a role in dampening of IL-2 production in CD8 T cells. For this purpose, naïve wild type and Arl4d$^{-/-}$ CD8 T cells were stimulated with plate-bound anti-CD3 and anti-CD28 antibodies for 48 hours. Supernatants were collected after 24 and 48 hours and ELISA was performed to assess the IL-2 production. We observed an increased production of IL-2 by Arl4d-deficient CD8 T cells compared to wild type CD8 T cells (Fig. 17). These data indicate that via induction of Arl4d, IL-2 production is inhibited in stimulated CD8 T cells *in vitro*.

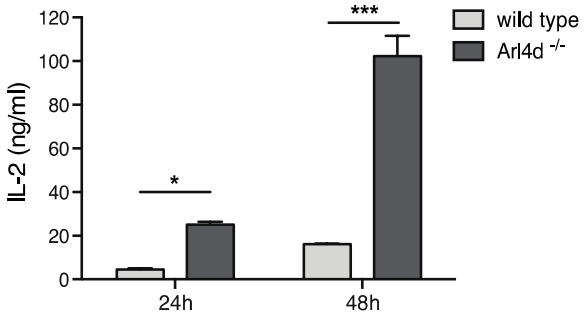

Figure 17. Arl4d deficiency leads to enhanced IL-2 production.

Arl4d$^{-/-}$ and wild type CD8 T cells were stimulated with anti-CD3 (2 µg/ml) and anti-CD28 (10 µg/ml) for the indicated time points. Data are shown as mean +/- SD. Graph show representative data from one out of two independent experiments. Statistical significance was calculated by Student's t-test. *p≤0.05 , ***p≤0.001.

4.6.2 Arl4d attenuates primary anti-viral CD8 T cell immunity *in vivo*

IL-2 plays an important role in CD8 T cell immune responses (Malek, 2008). It can drive development of naïve CD8 T cells into effector and memory cells upon antigen stimulation (Joshi et al., 2007; Pipkin et al., 2010; Liao et al., 2013).

To evaluate whether the increased IL-2 production by Arl4d-deficient CD8 T cells *in vitro* (Fig. 18) has an impact on the generation of a local immune response *in vivo*, we sorted either CD45.2$^+$ Arl4d-deficient or CD45.2$^+$ wild type naïve OT-I CD8 T cells and adoptively transferred them into CD45.1 congenic animals. Importantly, different congenic markers on transferred (CD45.2) and endogenous (CD45.1) CD8 T cells allow tracking transferred T cells during analysis. One day after transfer CD45.1 animals were infected with a non-replicating recombinant adenovirus expressing ovalbumin, GFP and luciferase (AdGOL) that preferentially infects hepatocytes. Starting from day 0 we studied accumulation of the transferred CD8 T cells in the blood by flow cytometry. Both Arl4d-deficient and wild type transferred CD8 T cells started to recirculate in the blood of AdGOL infected animals from day 3 onward. Both an increased total number and percentages of CD45.2$^+$ Arl4d-deficient CD8 T cells as compared to wild type CD8 T cells was found, starting from day 4 till day 8, indicating increased expansion of Arl4d-deficient CD8 T cells in the blood in response to viral infection (Fig. 18A and B).

During infection naïve antigen-specific CD8 T cells expand and differentiate into effector cells (Joshi et al., 2007). Moreover, it has been shown that IL-2 signals during primary immune response affect differentiation of CD8 T cells into short-lived effector cells (SLEC) (Pipkin et al., 2010). As we observed that Arl4d affects IL-2 production *in vitro*, this led us to examine whether Arl4d could affect effector T cell differentiation *in vivo*. For this reason, we analyzed the accumulation of KLRG1+ (a marker for SLEC) CD8 T cells in the blood of infected mice. Indeed, we found that a higher percentage of transferred Arl4d-deficient T cells expressed KLRG1+ as compared to the wild type controls starting at day 4 until day 8 after infection (Fig. 18C). Hence, Arl4d deficiency leads to enhanced development of effector T cells early during infection.

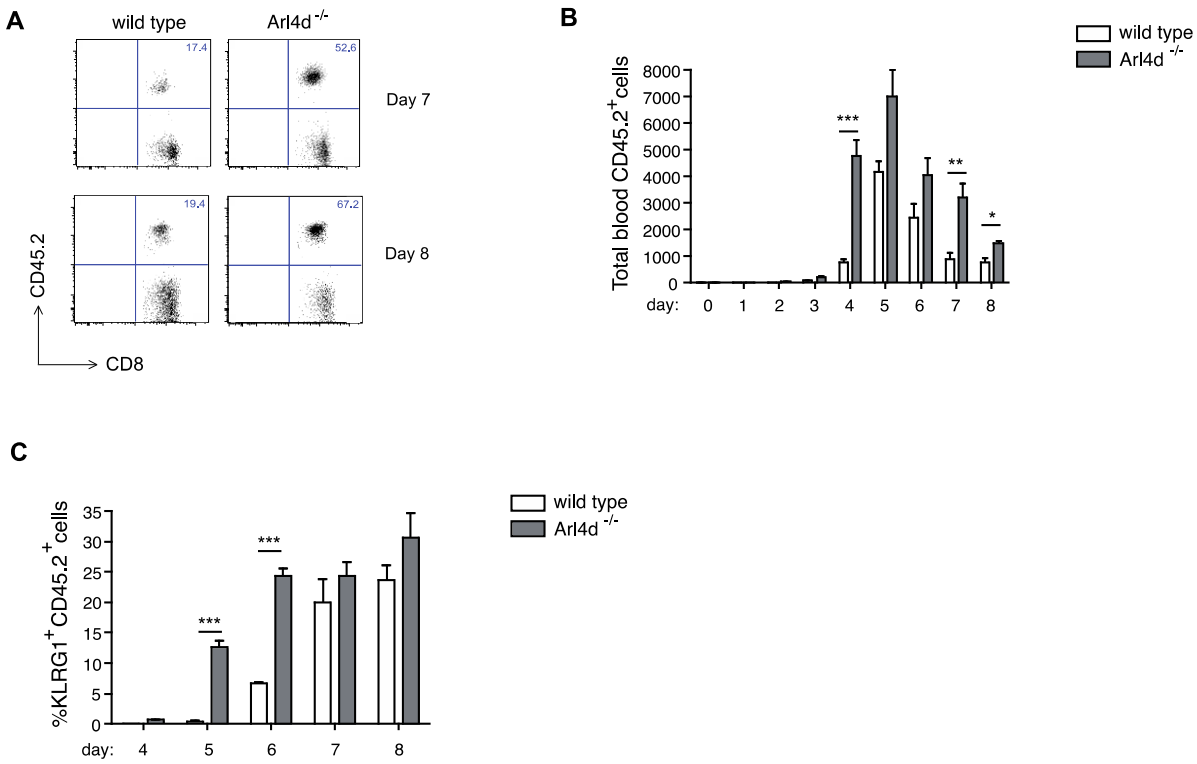

Figure 18. Increased expansion of Arl4d-deficient CD8 T cells in the blood during viral infection.

$8*10^5$ CD45.2+ Arl4d-deficient or wild type CD8 T cells were adoptively transferred into CD45.1 congenic animals. One day after transfer, mice were infected with AdOVA ($5*10^6$ PFU/mouse). **A:** Blood of CD45.1 infected mice was taken every day starting from day 0 and the cells were stained for CD8 and CD45.2 and analyzed by flow cytometry. Representative plots show CD45.2+ CD8 T cells accumulation in the blood of one mouse per group at day 7 and day 8. Numbers indicate percentages. **B:** Total numbers of transferred CD45.2+ either Arl4d ko or wild type CD8 T cells were analysed by flow cytometry in the blood of CD45.1+ infected mice at indicated times. **C:** Blood cells from B were stained additionally for KLRG1 and analysed by flow cytometry. Graph shows percentages of CD45.2+ SLEC in the blood of CD45.1 infected mice. Data from one experiment with 4 mice per group are shown. Data are presented as mean +/- SEM. Significance was calculated by Student's t-test. *p≤0.05, **p≤0.01, ***p≤0.001.

To determine the expansion, phenotype and function of the transferred T cells in the organs, CD45.1 mice were sacrificed eight days after AdGOL infection and spleens and livers were collected for analysis. Similar to the results obtained from the blood (Fig. 18B), increased amounts of transferred Arl4d-deficient CD8 T cells accumulated in the liver at day 8 after AdGOL infection (Fig. 19A). Additionally, we found increased amounts of Arl4d-deficient T cells in the spleen as compared to wild type T cells (Fig. 19B). Thus, Arl4d-deficiency not only leads to enhanced expansion

of CD8 T cells in the blood, but also in spleen and liver eight days after viral infection, indicating that Arl4d functions to restrict effector T cell generation *in vivo*.

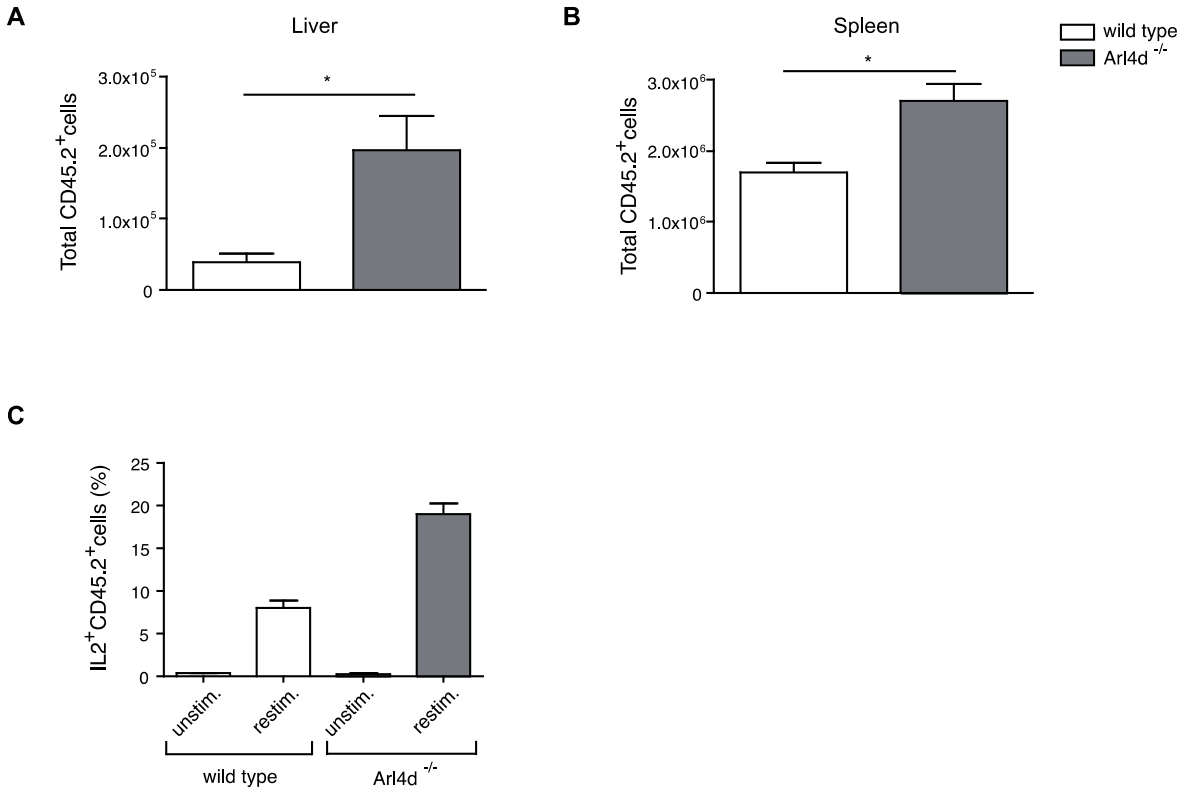

Figure 19. Arl4d dampens IL-2 production *in vivo*.

A: At day 8 liver-associated lymphocytes and splenocytes were stained for CD8 and CD45.2 and analyzed by flow cytometry. Bar graph show total number of $CD45.2^+$ cells per organ. **B:** At day 8 splenocytes were stained and analysed as in A. Bar graph show total number of $CD45.2^+$ cells per organ. **C:** Splenocytes were restimulated or not with PMA/Ionomycin for 4 hours and stained for CD8, CD45.2 and IL-2. Bar graph show percentages of IL-2 producing $CD45.2^+$ CD8 T cells. Data from one experiment with 4 mice per group are depicted. Data are shown as mean +/- SEM. Significance was calculated by Student's t-test. *$p \leq 0.05$, **$p \leq 0.01$, ***$p \leq 0.001$.

To determine the functionality of Arl4d-deficient and wild type CD8 T cells after AdGOL infection, splenocytes were restimulated with PMA/Ionomycin for 4 hours. We observed that Arl4d-deficient CD8 T cells produce increased amounts of IL-2 upon restimulation compared to wild type controls (Fig 19C), indicating that Arl4d regulates IL-2 production not only *in vitro* (Fig. 17), but also *in vivo*.

In summary, these data demonstrate that Arl4d inhibits expansion of virus-specific CD8 T cells. Moreover, Arl4d limits effector CD8 T-cell development and IL-2 production in response to viral infection.

To further investigate whether Arl4d-deficiency conveys an advantage in competition with Arl4d proficient T cells under the same inflammatory conditions, we co-transferred equal amount of Arl4d$^{-/-}$ and wild type naïve CD8 T cells into one recipient mouse before infection with AdGOL.

Therefore, we sorted CD45.1^{+} Arl4d-deficient and B6 Thy1.1 (CD90.1^{+}) wild type naïve OT-I CD8 T cells and adoptively transferred them in a 1:1 ratio into a single C57BL/6 (CD45.2^{+}, CD90.2^{+}) recipient. Of note, one additional congenic marker (CD90.1) on the wild type CD8 T cells had to be used in order to enable tracking of transferred wild type and knockout CD8 T cells in one animal. Again, one day after the T cell transfer, C57BL/6 mice were infected with AdGOL. Additionally, one group of mice was transferred with T cells but left non-infected, to confirm that transferred cells could only expand upon the antigen encounter.

In the previous experiment, we had observed that transferred CD8 T cells appeared in the blood at day 3 after infection. Therefore, we started to investigate accumulation of the transferred cells in the blood of infected and non-infected mice from day 3 onward. In contrast to the non-infected control group, both Arl4d-deficient and wild type transferred CD8 T cells started to recirculate in the blood upon AdGOL infection (Fig. 20A). Interestingly, we found increased percentages (Fig. 20B) and total numbers (Fig. 20C) of CD45.1^{+} Arl4d-deficient CD8 T cells as compared to wild type CD90.1^{+} CD8 T cells starting from day 3 till day 8, suggesting stronger expansion potential of knockout cells in competition with wild type cells in the blood of AdGOL infected mice. Additionally, transferred CD8 T cells in the blood of non-infected control mice did not proliferate, as expected.

These data confirm our previous finding that Arl4d-deficiency leads to increased expansion of CD8 T cells in the blood of viral infected mice. Importantly, the enhanced expansion of Arl4d-deficient CD8 T cells in response to infection is maintained in the presence of wild type cells that compete for the same antigen.

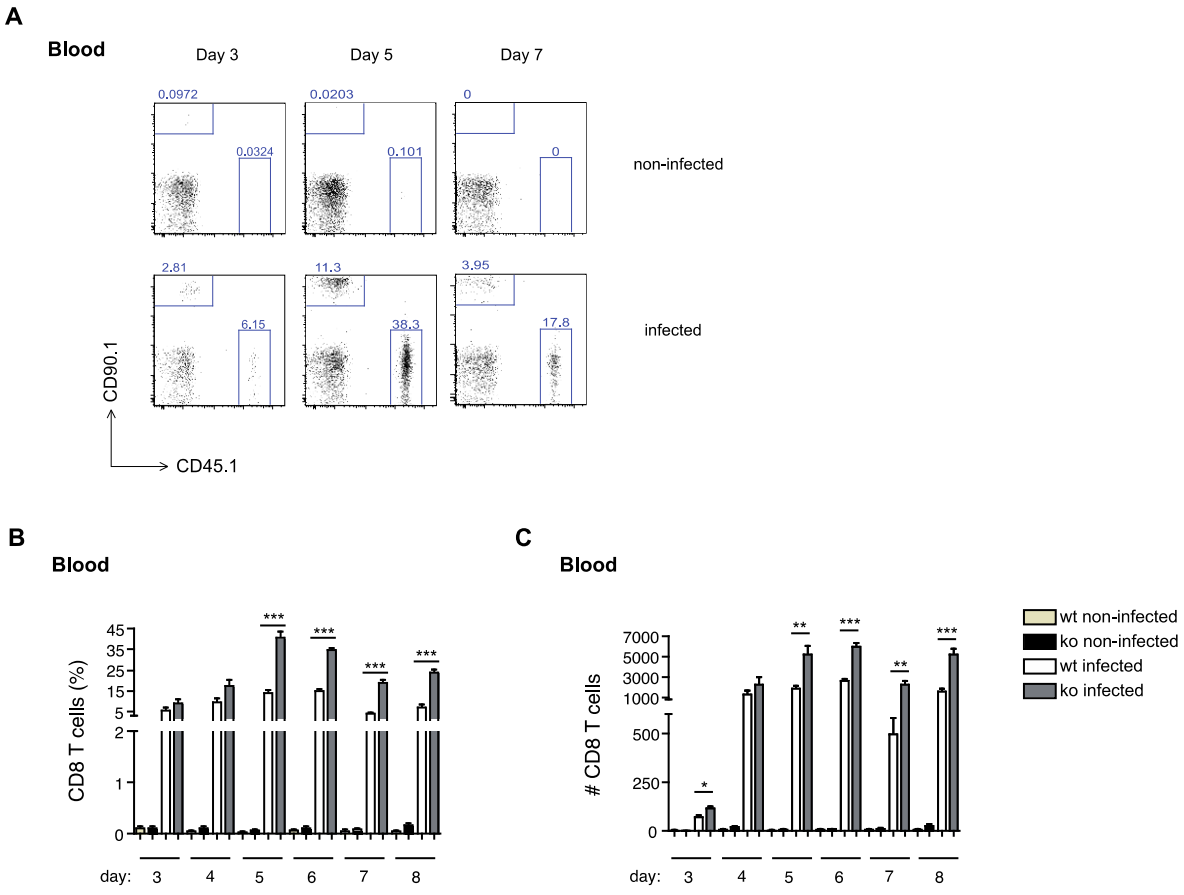

Figure 20. Arl4d-deficient CD8 T cells demonstrate a stronger potential for expansion in the blood in competition with wild type CD8 T cells in response to infection.

$5*10^5$ CD45.1$^+$ Arl4d-deficient and $5*10^5$ CD90.1$^+$ wild type OT-I CD8 T cells were mixed and adoptively transferred into B6 animals. One day after transfer, mice were infected with AdOVA ($5*10^6$ PFU). **A:** Blood of B6 infected mice was taken every day starting from day 3 and the cells were stained for CD8, CD45.1 and CD90.1 and analyzed by flow cytometry. Representative plots show distribution of CD45.1 and CD90.1 transferred cells among CD8 T cells in the blood of one mouse per group at day 3, 5 and 7. Numbers indicate percentages. **B:** Bar graph shows percentages of transferred either wild type (wt; CD90.1$^+$) or Arl4d knockout (ko; CD45.1$^+$) CD8 T cells in the blood of B6 infected mice at indicated time points after viral infection. **C:** Bar graph shows total number of transferred either wild type (wt; CD90.1$^+$) or Arl4d knockout (ko; CD45.1$^+$) CD8 T cells in the blood of B6 infected mice at indicated time points after viral infection. Data are shown as mean +/- SEM for n=3 mice in the non-infected group and n=6 mice in the infected group and represent one out of two experiments. Significance was calculated by Student's t-test. *p≤0.05, **p≤0.01, ***p≤0.001.

To evaluate accumulation and distribution of transferred CD8 T cells in the organs, eight days after AdGOL infection, we sacrificed B6 mice from the infected and non-infected groups and collected livers and spleens. As mentioned above AdGOL infects predominantly hepatocytes. Indeed, wild type and Arl4d-deficient CD8 T cells accumulated preferentially in the liver; 6,42 ± 0,47% vs. 23,37 ± 1,49% of wild type

CD8 T cells and 14,43 ± 0,85% vs. 55,67 ± 2,45% of Arl4d$^{-/-}$ CD8 T cells in the spleen and liver, respectively (Fig. 21A and B). Furthermore, compared to the wild type T cells, we found increased percentages and total numbers of Arl4d-deficient CD8 T cells at day 8 after infection in spleen and liver, confirming that Arl4d-deficiency also leads to increased expansion of CD8 T cells in peripheral organs upon viral infection (Fig. 21B and C).

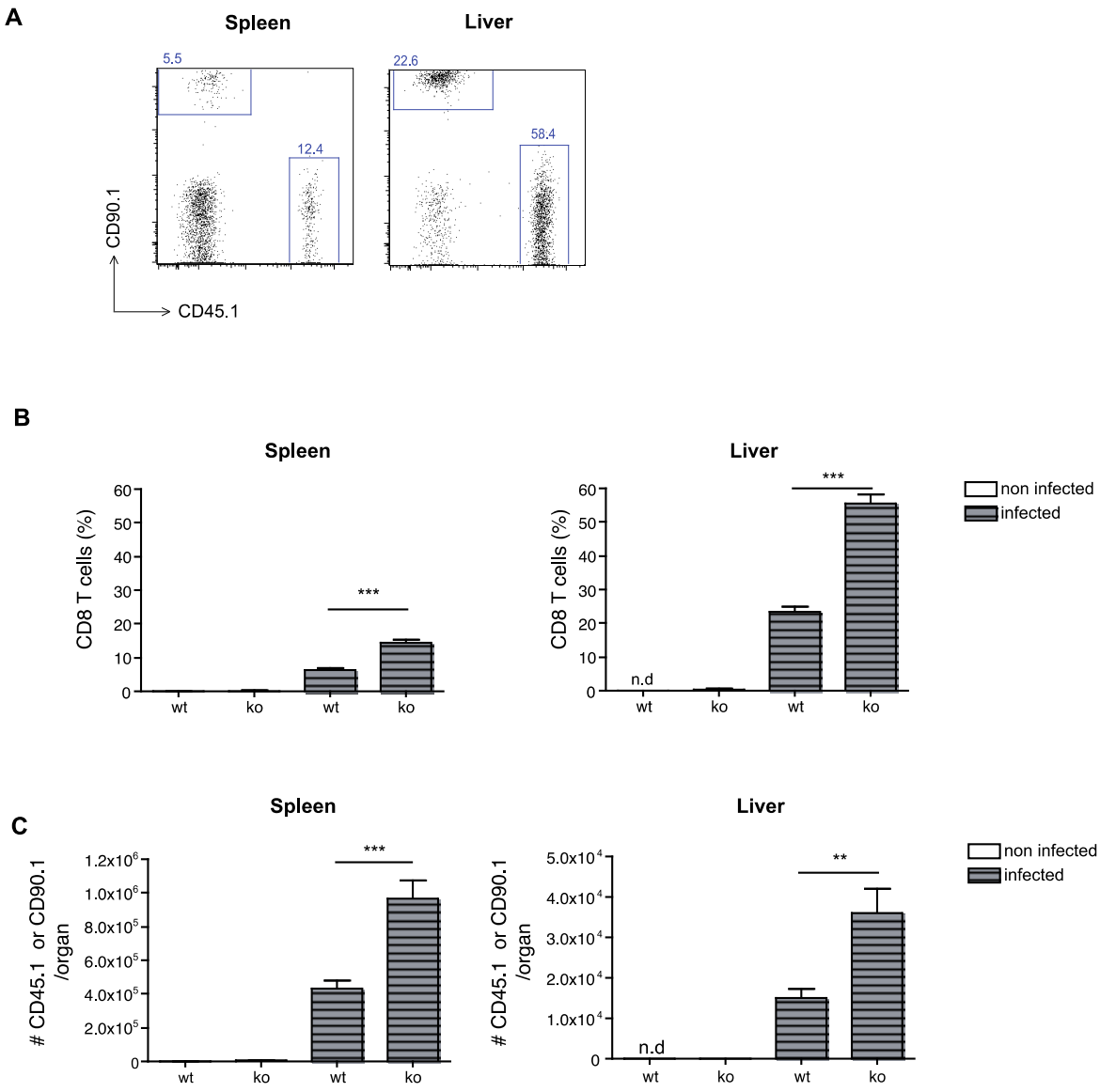

Figure 21. Increased expansion of Arl4d-deficient CD8 T cells in the organs.

Eight days after infection liver-associated lymphocytes and splenocytes were stained for CD8, CD45.1 and CD90.1. **A:** Dot plots show distribution of wt (CD90.1$^+$) and ko (CD45.1$^+$) CD8 T cells in the spleen and liver of one representative infected mouse. **B:** Bar graphs show percentages of either wild type (wt; CD90.1$^+$) or Arl4d knockout (ko; CD45.1$^+$) CD8 T cells in the spleen and liver of non-infected and infected mice. **C:** Bar graphs show total numbers of the cells in B. per organ. Data are shown as mean

+/- SEM for n=3 mice in the non-infected group and n=6 mice in the infected group and represent one out of two experiments. Significance was calculated by Student's t-test. *p≤0.05, **p≤0.01, ***p≤0.001.

4.6.3 CD8 T cells demonstrate enhanced ability for effector T cell differentiation in the absence of Arl4d

It is well known that once CD8 T cell encounter their antigen, its differentiation into effector cells is initiated (Boulet et al., 2014). We wondered whether this phenomenon is maintained when both wild type and knockout CD8 T cells compete for the same antigen during viral infection. To assess the effector CD8 T cell development in this situation we investigated the accumulation of KLRG1+ cells in the blood, starting from day 3 till day 8, and in the spleen and liver 8 days after AdGOL infection. To specifically examine the SLEC we included CD127 in the staining and we defined SLEC to be the $KLRG1^{+}$ and $CD127^{-}$ population (Kaech et al., 2003; Joshi et al. 2007) (Fig. 22A).

In the blood of AdGOL-infected mice, numbers of $KLRG1^{+}CD127^{-}$ cells among transferred Arl4d-deficient T cells were increased compared to wild type CD8 T cells in the blood (Fig. 22B). Again, similar results were obtained from the spleen and liver (Fig. 22C and D). Together, these data demonstrate that Arl4d limits SLECs development during a viral CD8 T cell response.

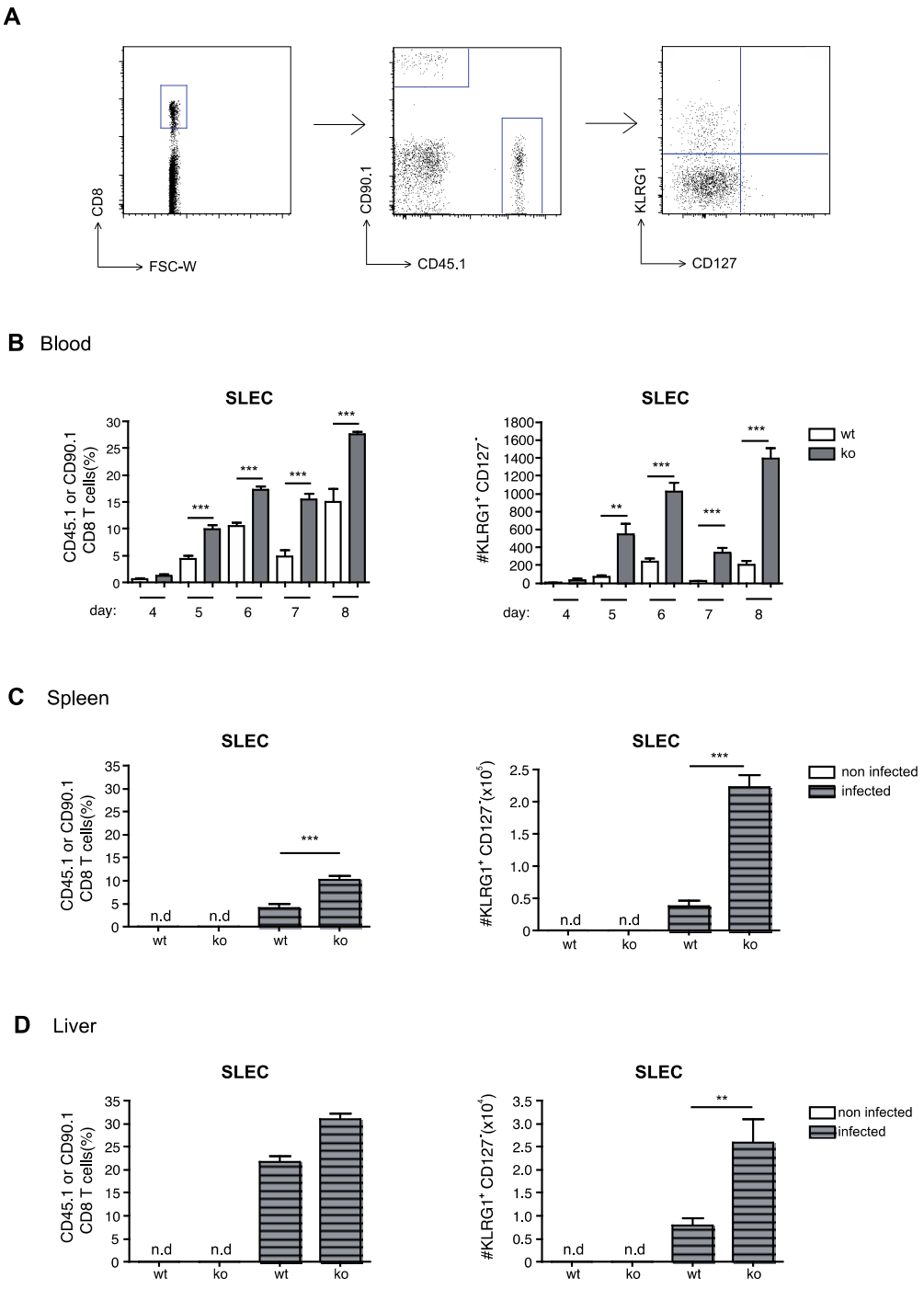

Figure 22. Arl4d inhibits effector T cell differentiation upon viral infection.

A: Gating strategy for the SLEC population identification. SLEC: $CD8^+CD90.1^+/CD45.1^+$ $KLRG1^+CD127^-$. **B:** Bar graphs show percentages (left panel) and total number (right panel) of SLEC in the blood. Bar graphs show percentages (left panel) and total number (right panel) of SLEC 8 days after AdOVA infection per spleen: C. and liver: D**.** Data are shown as mean +/- SEM for n=3 mice in the non-infected group and n=6 mice in the infected group and represent one out of two experiments. Significance was calculated by Student's t-test. *p≤0.05, **p≤0.01, ***p≤0.001. n.d – not detected.

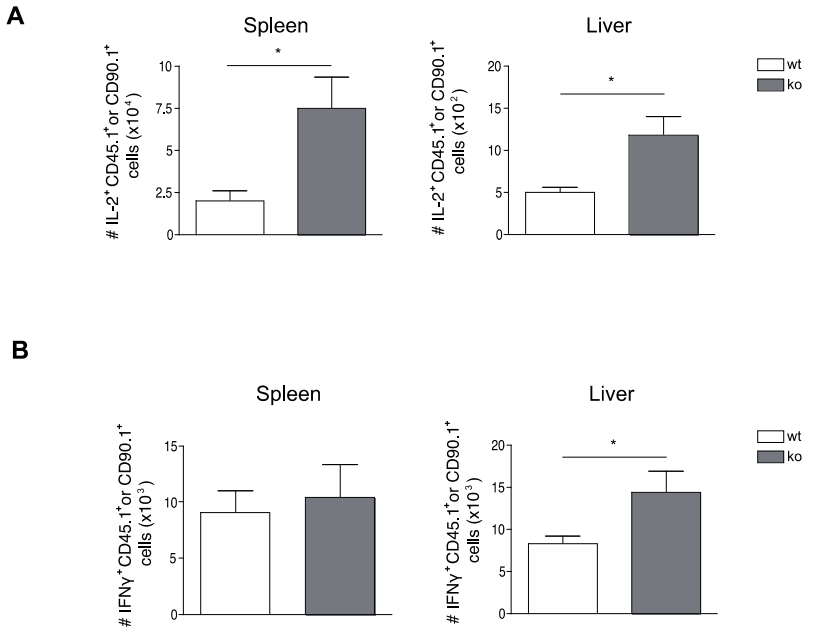

Figure 23. Arl4d dampens IL-2 and IFNγ production by CD8 T cells after restimulation.

Eight days after AdOVA infection splenocytes and liver-associated lymphocytes were restimulated with PMA/Ionomycin for 4 hours. Total number of IL-2 (A) and IFNγ (B) producing transferred either wild type (wt; CD90.1$^+$) or Arl4d knockout (ko; CD45.1$^+$) CD8 T cells per spleen (left panel) and liver (right) are shown as mean +/- SEM of n=6 infected mice and represent one out of two experiments. Significance was calculated by Student's t-test. *p≤0.05.

Next, we wondered whether increased expansion and effector T cell development of Arl4d-deficient CD8 T cells would correlate with increased IL-2 production, as it has been previously showed. Indeed, we observed increased total number of IL-2-producing Arl4d-deficient CD8 T cells after restimulation in both liver and spleen (Fig. 23A). In addition, we found increased total number of IFNγ-producing knockout CD8 T cells in liver and spleen as compared to the restimulated wild type CD8 T cells (Fig. 23B). These data indicate that Arl4d restricts the development of IL-2 and IFNγ producing T cells.

In summary, we confirmed that Arl4d inhibits expansion and effector T cell differentiation of antigen-specific CD8 T cells in response to viral infection.

Furthermore, we could show that Arl4d limits the development of IL-2 and IFNγ producing CD8 effector T cells.

5 Discussion

CD8 T cells primed by liver endothelial cells (LSECs) undergo a particular differentiation program. Initially activated, they develop into nonresponsive CD8 T cells with memory-like phenotype (Diehl et al., 2008; Böttcher et al., 2013; Böttcher et al., 2014). Previously, our group discovered that this unique state of CD8 T cells depends on delivery of co-inhibitory signaling (Diehl et al., 2008). In the present study, we further investigated the mechanism of CD8 T cell-LSEC interaction and could show that unique differentiation state of CD8 T cells requires integration of co-inhibitory PD-L1/PD-1 signaling over time, after which the nonresponsiveness of CD8 T cells cannot be prevented by CD28 co-stimulation. Furthermore, we identified the small GTPase, Arl4d to be PD-L1-dependently overexpressed in CD8 T cells primed by LSECs. Arl4d expression inhibits IL-2 production by T cells and thereby may regulate IL-2 availability. As it is PD-L1-dependently induced it might be a new downstream signaling molecule of this important co-inhibitory signaling pathway.

5.1 LSEC-CD8 T cell interaction results in multifocal synapse formation

The function of the adaptive immune system is initiated by interaction of antigen presenting cell (APC) with T cells. Upon antigen-specific contact of T cell with APC an immunological synapse (IS) is formed at the interaction site. First reports showed that the immune synapse consists of a central cluster of pMHC-TCR interactions (cSMAC) surrounded by a peripheral ring of adhesion molecules (pSMAC), which is characteristic for a classical IS (Monks et al., 1998; Grakoui et al., 1999). However, recent studies on IS formation between different types of T cells and APCs revealed additional forms such as a multifocal IS and a kinapse (Dustin, 2009). The type of IS depends on T cell differentiation state, type of APC interacting with T cell or the function of synapse (Thauland and Parker, 2010).

The classical synapse (bull's eye) is observed mostly during CTL or NK cell interaction with target cells (Krzewski and Storminger, 2008; Stinchcombe and Griffiths, 2003). In this type of IS, the cytokine granules are released in the cSMAC, whereas the pSMAC act as a gasket for efficient delivery of the lytic granules to the target cell (Beal et al., 2008; Beal et al., 2009), indicating that the type of IS is correlated with the function. In the

present study, we investigated the formation of the immunological synapse between antigen-presenting LSECs and naïve CD8 T cells. As CD8 T cells primed by LSECs do not become activated but develop into nonresponsive CD8 T cells that do not produce cytokines (Diehl et al., 2008; Schurich et al., 2010; Böttcher et al., 2013), we did not expect a bull's-eye synapse. Indeed, we did not observed a central ring of TCRβ (cSMAC) surrounded by CD11a ring (pSMAC) at the contact site of CD8 T cells and LSECs but several clusters of TCRβ and CD11a spread across the contact area, indicating a multifocal synapse (Fig. 6 and Fig. 9). The multifocal type of IS was initially described in double-positive thymocytes interacting with planar bilayers, in contrast to mature T cells that formed the classical IS on such bilayers. Those studies showed that the type of IS depends on TCR signal strength (Richie et al., 2002; Hailman et al., 2002). The fact that TCR proximal signaling is inhibited upon CD8 T cell priming by LSECs (Fig. 6) and liver-primed CD8 T cells do not produce cytokines could explain the multifocal synapse formation. However, there are several contradictory reports showing that multifocal synapse is formed between naïve CD4, CD8 and activated CD4 T cells with DCs (Brossard et al., 2005; Fisher et al., 2008; Alarcon et al., 2011; Tseng et al., 2008), in cases of strong TCR signaling. This indicates that T cells do not require a classical IS for full activation (Thauland and Parker, 2010). Furthermore, the bull's-eye synapse is not only formed as a cytotoxic synapse as this type of IS has been also observed between CD4 T cells and B cells forming an inhibitory synapse (Reichardt et al., 2007). That would suggest that not only T cell differentiation state, type of APC and TCR signal strength alone but probably all conditions together play a role in the IS formation.

As T cells are highly motile and continuously scan secondary lymphoid organs in order to detect an antigen, they can also form asymmetric motile junctions with APCs, called immunological kinapses (Dustin, 2009). However, although naïve CD8 T cells migrate intensively across LSECs *in vitro* in the absence of antigen, they stop migrating and remain arrested immediately after antigen-specific recognition on MHC I molecules on LSECs (von Oppen et al., 2009). Therefore, as expected, antigen-specific interaction of CD8 T cells and LSECs and did not lead to kinapse formation.

Taken together, the interaction between antigen-presenting LSECs and naïve CD8 T cells, which leads to silencing of immediate effector function in CD8 T cells, results in the formation of a multifocal immune synapse.

5.2 The multifocal immune synapse between LSEC-CD8 T cells is formed independently of PD-L1/PD-1

Previous findings show that upon antigen-specific LSEC-CD8 T cell interaction, the expression of the co-inhibitory molecule PD-L1 on antigen-presenting LSECs was upregulated, however no upregulation of co-stimulatory molecules CD80 and CD86 was observed. In the absence of PD-L1 on LSECs, CD8 T cells acquired full effector function and produced IL-2 upon restimulation, indicating that PD-L1 signals are required for CD8 T cell nonresponsiveness (Diehl et al., 2008). To further analyze this mechanism, we investigated PD-1 expression kinetics on LSEC-primed CD8 T cells and found antigen-specific induction of PD-1 expression early (1-4 hours) after LSEC stimulation (Fig. 6). Furthermore, consistent with the previous findings (Diehl et al., 2008) we showed that PD-L1/PD-1 signaling is required for CD8 T cell nonresponsiveness induced by LSEC-priming (Fig. 10).

In the immune synapse, PD-1 colocalizes with the TCR at the immunological synapse and forms PD-1-TCR microclusters, which are required for the inhibition of TCR proximal signaling (Pentcheva-Hoang et al., 2007; Yokosuka et al., 2012). This results in inhibition of CD3ζ and ZAP70 phosphorylation and subsequent attenuation of IL-2 production (Sheppard et al., 2004; Parry et al., 2005). Our finding that liver-primed CD8 T cells express PD-1 for at least 5 days and that PD-1 signaling attenuates TCR proximal signal strength (Fig. 6) led us to the assumption that PD-1 could have an impact on the immune synapse formation upon CD8-LSEC interaction. Therefore, we compared the IS formed between PD-L1-deficient (co-inhibitory signaling cannot be delivered) or B6 LSECs and CD8 T cells. In contrast to studies mentioned in section 5.1 (Richie et al., 2002; Hailman et al., 2002), we provide evidence that although PD-1 signals influenced TCR proximal signal strength, it did not influenced multifocal synapse formation (Fig. 7 and Fig. 9). Although CD8 T cells primed by PD-L1-deficient LSECs become activated and produce cytokines (Fig. 10), they form the same type of IS as nonresponsive B6 LSEC-primed CD8 T cells, indicating that the formation of multifocal IS upon CD8 T cell priming by LSECs is PD-L1/PD-1-independent.

Our results are consistent with a work on NK cells, which showed that NK cells formed either a cytolytic or noncytolytic (inhibitory) synapse with target cells in *in vitro* systems. In both, polyclonal IL-2 activated NK cells interacting with autologous B

lymphoblastoid cell line (BLCL) leading to NK cell inhibition, and NK cells interacting with target cells lacked self-MHC molecules, which activates NK cells, a bull's eye synapse was observed (Vyas et al., 2001; Dustin and Long, 2010). Surprisingly, nonresponsive liver-primed CD8 T cells form the same type of IS as activated DC-primed CD8 and CD4 T cells (Brossard et al., 2005; Dustin et al., 2006; Tseng et al., 2008). Hence, our and others findings indicate that the type of the synapse does not always correlate with the function.

Although the phenotype of the IS formed at the contact site of CD8 T cells and LSECs was not influenced by PD-L1/PD-1 signaling, perhaps the individual microcluster of the multifocal immune synapse could be affected. TCR proximal signals are sustained in TCR microclusters formed at the IS periphery (Varma et al., 2006), and the size of these TCR microclusters has been shown to depend on the antigen concentration and further on TCR signal strength. In the presence of decreasing the antigen concentrations, the size and density of cSMAC were reduced (Yokosuka et al., 2005). Additionally, also the size of individual TCR microclusters was proportional to the density of pMHC presented on lipid bilayers (Yokosuka et al., 2005). In our experiments we did not titrate the antigen presented by LSECs, however we observed decreased proximal TCR signaling of LSEC-primed CD8 T cells (as a result of PD-1 function) in comparison to CD8 T cells primed by PD-L1-deficient LSECs. Nevertheless, the reduced TCR signal strength, due to PD-1 signaling, did not influenced cluster size or cluster count within multifocal immune synapse (Fig. 9), indicating that both size and density of individual microclusters in the multifocal synapse is not dependent on PD-L1/PD-1 signaling.

In summary, our data indicate that although CD8 T cell stimulation by B6 or PD-L1-deficient LSECs leads to different functional outcomes, such different signaling does not affect the phenotype of the immune synapse.

We identify the multifocal synapse by staining of the cSMAC-associated molecule TCRβ and the pSMAC-associated molecule CD11a. However, we did not stain for other signaling molecules downstream from the TCR to analyze signal transduction within the synapse. Different signaling molecules are recruited to the inhibitory and cytolytic bull's eye synapse in NK cells. Within the cSMAC of the inhibitory synapses Src homology domain 2-containing protein tyrosine phosphatase 1 (SHP-1) was abundant, whereas in the cytolytic synapses no SHP-1 but several tyrosine kinases (Lck, ZAP70) were detected (Vyas et al., 2001; Vyas et al., 2002; Dustin and Long, 2010). Similar to the inhibitory

interaction in NK cells, PD-1 can recruit Src homology domain 2-containing protein tyrosine phosphatase 2 (SHP-2), which results in dephosphorylation of TCR proximal signals (Yokosuka et al., 2012). As PD-1 signals are crucial to induce the particular differentiation state of LSEC-primed CD8 T cells (Fig. 10), it is possible that by promoting recruitment SHP-2, it affects the function of other molecules, like Lck, ZAP70 or SLP-76 in the multifocal synapse at the CD8 T cell-LSEC interface.

In summary, our data indicate that although CD8 T cell stimulation by wild type or PD-L1-deficient LSECs leads to different functional outcomes, these different outcomes are not a result of alteration in immune synapse properties, but more likely due to signals further downstream of the TCR.

5.3 LSEC-primed CD8 T cell state depends on the integration of co-inhibitory signaling over a certain period of time

In the present work, we demonstrate that the differentiation state of LSEC-primed CD8 T cells depends on PD-L1/PD-1 signals. Although PD-1 can accumulate within the immune synapse and modulate TCR downstream signaling (Pentcheva-Hoang et al., 2007; Yokosuka et al., 2012), it did not affect the phenotype of the synapse or the size and density of clusters within the synapse formed between CD8 T cells and LSECs. As the immune synapse is formed within a minutes after cell-cell contact, we therefore supposed that these early events during priming do not play a role in the unique programming of liver-primed CD8 T cells. Our data show that CD8 T cells primed by LSEC upregulate PD-1 on the surface, which interacts with PD-L1 on LSECs (Diehl et al., 2008), and sustain its expression for 5 days (Fig. 6). Hence, rather the longevity of signaling than the early priming might be important for the induction of nonresponsive state of liver-primed CD8 T cells.

There are reports demonstrating that CD8 T cells need to receive sustained TCR signaling for a particular period (about twenty hours) of time in order to develop into fully differentiated effector cells and to acquire killing function (Berg et al., 1998; Iezzi et al., 1998; van Stipdonk et al., 2003). One study showed that not TCR engagement on CD8 T cells alone but sustained TCR/CD3 stimulation is required to develop TCR downstream signaling (Berg et al., 1998), in order to start Akt signaling integration that enhances transcriptional program for effector CD8 T cell development (Kim et al., 2012). The others showed that naïve OT-I CD8 T cells stimulated with OVA for four hours did

not expand to the same extent as CD8 T cells stimulated for twenty hours and showed reduced killing activity (van Stipdonk et al., 2003). As CD8 T cells require integration of the signaling in order to develop into effector cells, we supposed that LSEC-primed CD8 T cells in order to develop into nonresponsive state also could require integration of the inhibitory signaling during a distinct time period.

CD8 T cells stimulated by antigen-presenting LSECs initially increase CD25 and CD44 expression and downregulate CD62L expression and proliferate identical to CD8 T cells stimulated by DCs. However, they do not sustain activation marker expression and become $CD25^{neg}CD62L^{high}$ within 5 days after initial stimulation (Diehl et al., 2008; Böttcher et al., 2014). In the presence of PD-L1/PD-1 signaling, downregulation of CD25 expression on LSEC-primed T cells was completed within 48 hours (Fig. 11). In contrast, PD-1 expression was sustained for at least 5 days after reaching its maximum at 24 hours (Fig. 6), indicating that LSEC-primed T cells stay receptive to inhibitory signaling throughout this time. Previous findings show that augmenting the level of IL-2 in LSEC-CD8 T cell co-cultures, either by addition of exogenous IL-2 or anti-CD28 Abs at the start of co-culture, resulted in the full activation of LSEC-primed CD8 T cells (Diehl et al., 2008; Schurich et al., 2010). In order to investigate whether LSEC-primed CD8 T cells required sustained co-inhibitory signaling to fully differentiate into nonresponsive CD8 T cells, we added anti-CD28 Abs at different time points after initiation of LSEC-CD8 T cell interaction. Interestingly, we found that co-stimulation via CD28 failed to overcome the unique differentiation program of LSEC-primed CD8 T cells when introduced after 36 hours of PD-1 signal integration (Fig. 11). Thus, the key events in LSEC-induced T cell differentiation occur within 36 hours.

In summary, our studies demonstrate that development of the nonresponsiveness of LSEC-primed CD8 T cells requires integration of PD-L1/PD-1 signaling for 36 hours, after which this particular differentiation program cannot be reversed by CD28 co-stimulatory signaling.

5.4 PD-L1-dependent expression of newly discovered small GTPase in CD8 T cells

Our study shows the importance of PD-1 signal integration in induction of a quiescent state of CD8 T cells primed by LSECs. In order to further characterize these unique cells, we investigated their gene expression profile. Our results of a gene array were

consistent with the findings of Böttcher et al. showing that LSEC-primed CD8 T cells, in contrast to DC-primed CD8 T cells, do not express key genes characteristic for cytotoxic T cells like granzyme B, T-bet, IFNγ and IL-2R (Fig. 12). Furthermore, we could confirm that LSEC-primed CD8 T cells upregulate Eomes, which is characteristic for memory T cells, and Neuropilin 1 expression (Fig. 12). Taken together, we confirmed previous findings showing that LSEC-primed CD8 T cells are quiescent and display a memory-like phenotype (Diehl et al., 2008; Schurich et al., 2010; Böttcher et al., 2013). Furthermore, our analysis identified the small GTPase, Arl4d to be overexpressed in LSEC-primed CD8 T cells, whereas its expression in DC-primed CD8 T cells was absent, which we confirmed by RT PCR analysis. We further found that Arl4d is expressed in steady state in naïve CD8 T cells and upon LSEC priming its expression increases, whereas upon DC priming or antibodies stimulation it decreases (Fig. 13 and Fig. 14). Moreover, we observed that Arl4d expression in liver-primed CD8 T cells to be PD-L1 dependently induced (Fig. 13). These findings revealed that this newly discovered molecule might play a role in PD-L1/PD-1 signaling.

PD-1 inhibitory function results in attenuation of downstream signaling and dampening of IL-2 production (Francisco et al., 2010; Dai et al., 2014). SHP-2 is recruited to PD-1 on PD-1-PD-L1 binding and dephosphorylates CD3ζ, ZAP70 and further downstream PLCγ1 and ERK (Sheppard et al., 2004; Yokosuka et al., 2012). Furthermore, PD-1 inhibits PI3K/Akt pathway responsible for *IL-2* transcription and IL-2 production (Parry et al., 2005). Here, we find that Arl4d, similar to PD-1, dampens IL-2 production by stimulated CD8 T cells (Fig. 17). However, how Arl4d achieves this, it requires further investigation. Considering the molecular structure of the Arl4d GTPase, there are several possible ways in which this molecule may influence T cell function via PD-1-dependent repression of IL-2 synthesis. Arl4d is a small GTPase and can exist as a GTP- and a GDP-bound form, which in other GTPases is essential for its function. It further possesses a nuclear localization signal (NLS) for targeting to the nucleus and a myristoylation site for targeting to the plasma membrane. In its active form (GTP-bound), Arl4d has been reported to modulate actin remodeling by recruiting cytohesin-2 to the plasma membrane. Thereby, it indirectly activates Arf6, which is followed by actin reorganization and subsequent cell migration (Li et al., 2007; Hofmann et al., 2007; Yamauchi et al., 2009). In contrast, we have found Arl4d upregulation in liver-primed

CD8 T cells, which are arrested on LSECs upon antigen recognition (von Oppen et al., 2009). Furthermore, PD-1 is shown to promote CD4 T cell *in vivo* migrating upon antigen-specific interaction (Fife et al., 2009). In contrast, we showed upregulation of PD-1 expression in CD8 T cells which stop migrating upon antigen binding. These contradictory results could be explained by the fact that different cell types were investigated in different *in vitro* and *in vivo* systems. We investigated here antigen-specific stimulation of primary CD8 T cells with LSECs, whereas other investigated HEK 293T cell line (Li et al., 2007) and N1E-115 neuroblastoma cell line (Yamauchi et al., 2009) transfected with Arl4d constructs or *in vivo* stimulation of CD4 T cells (Fife et al., 2009).

The switch between a GDP-bound to a GTP-bound form of all small GTPases is catalyzed by guanine exchange factors (GEFs), cytohesins (Kolanus, 2007; Donaldson and Jackson, 2011). Cytohesin-2 and cytohesin-3 showed opposite impact on cell migration. Knockdown of cytohesin-2 resulted in reduction of cell migration, whereas knockdown of cytohesin-3 resulted in enhancement of cell migration (Oh and Santy, 2010). Cytohesin-3 is reported to be upregulated in anergic CD8 T cells that do not produce cytokines (Korthäuer et al., 2000). Arl4d recruits cytohesin-2 to the plasma membrane and indirectly promote migration (Li et al., 2007). The fact that Arl4d is upregulated in nonresponsive CD8 T cells, which do not produce IL-2, led us to the assumption that in this situation it recruits cytohesin-3, instead of cytohesin-2, and that could explain the migration stop of LSEC-primed CD8 T cells. However, it requires further investigation.

The GTP-bound form of Arl4d functions at the plasma membrane, whereas the GDP-bound form has been reported to localize to the cytosol or the nucleus (Li et al., 2007; Hofmann et al., 2007). Furthermore, Arl4d GDP-bound form has been also found in the mitochondrial inner memebrane (Li et al., 2012), one could speculate that it could interfere with T cell activation and IL-2 production via inhibition of mitochondrial function. The TCR-induced generation of mitochondrial reactive oxygen species (mROS) is crucial for T cell activation in both CD4 and CD8 T cells by activating the nuclear factor of activated T cells (NFAT) that is required for IL-2 induction (Kaminski et al., 2010; Sena et al., 2012). ROS are produced in the process called mitochondrial oxidative phosphorylation (OXPHOS) at the Complex III located at the inner mitochondrial membrane (Marchi et al., 2012). Interestingly, the inactive form of Arl4d (GDP form)

translocates to the mitochondrial inner membrane and causes disruption of the membrane potential followed by mitochondrial fragmentation (Li et al., 2012), which impairs mitochondrial function and could potentially interfere with ROS production. Such reduction of mitochondrial membrane potential can also cause a decrease in IL-2 mRNA expression (Sena et al., 2013). Thus, in its GDP-bound form Arl4d could indirectly inhibit IL-2 production by altering mitochondrial function.

Upon T cell activation, the co-stimulatory molecule CD28 plays an important role in IL-2 induction. Signalling via CD28 activates PI3K and promotes NF-κB nuclear localization where it induces *IL-2* expression (Sanchez-Lockhart et al., 2004). Moreover, transcriptional factor B lymphocyte–induced maturation protein-1 (Blimp-1) expression is induced upon TCR stimulation and IL-2 production and has been shown to act as transcriptional repressor that attenuates *IL-2* gene expression in IL-2 negative feedback loop (Martins et al. 2008; Gong and Malek, 2007). Thus, naïve Blimp-1-deficient CD4 T cells showed in steady-state higher amount of IL-2 mRNA expression in comparison to wild type CD4 T cells. Furthermore, IL-2 expression correlated inversely with Blimp-1 expression upon OVA stimulation in both CD4 (Martins et al., 2008) and CD8 T cells (Gong and Malek, 2007). As we observed dampening of IL-2 production by Arl4d and the fact that Arl4d localizes to the nucleus (Lin et al., 2000), one could speculate that Arl4d functions as transcriptional repressor of the *IL-2* gene, similar to Blimp-1, when it is localized to the nucleus.

In summary, we have described that Arl4d is induced by PD-1 signaling and inhibits IL-2 production by an as-yet unknown mechanism, which could be as diverse as modulating the inhibitory signaling pathway or inhibiting the mitochondrial function or even repressing the *IL-2* gene. In order to assess whether one or a combination of these possible mechanisms play a role, more detailed studies are required.

5.5 Composition of the peripheral lymphoid compartment in the absence of Arld4

To be able to investigate the function of Arl4d *in vivo*, we obtained Arl4d-deficient mice that were generated according to the "knock-out first" strategy from International Mouse Phenotyping Consortium (IMPC). First phenotypical analyses of these Arl4d-deficient mice revealed abnormalities in the skeletal phenotype (legacy data available from the IMPC website: http://www.mousephenotype.org), including decreased rib number, abnormal rib morphology in mutant males and decreased bone mineral content

in females. Furthermore, Arl4d-deficient mice are decreased in body weight and lean body mass. However, no overt changes in the immune system were reported by the IMPC. Our analysis of the peripheral lymphoid compartment confirmed that Arl4d-deficiency does not interfere with T lymphocyte development; distribution and numbers of CD4 and CD8 T cells in both spleen and blood were normal and Arl4d-deficient T cells did not display skewed subpopulations as measured by the activation and memory markers CD44 and CD62L (Fig. 16). This is in contrast to PD-L1-deficient mice, which have more activated CD4 T cells and increased percentages of central memory CD8 T cells (Bazhin et al., 2014). Although PD-L1 expressed on LSEC can induce Arl4d expression in CD8 T cells, PD-L1 is broadly expressed and not only signals via PD-1 but also via CD80 (Butte et al., 2007; Park et al., 2010). Therefore, the phenotypes developing due to either deficiency do not need to overlap.

In summary, our analyses showed that Arl4d had no major impact on the development of the peripheral T cell compartment in lymphoid tissues.

5.6 Function of Arl4d via regulation of IL-2 production

In the present study, we found that highly increased Arl4d expression can be found in LSEC-primed T cells, which are incapable of IL-2 secretion, and the opposite occurs in the absence of Arl4d, i.e. increased secretion of IL-2 after stimulation. Thus, Arl4d might be involved in immunological processes in which production or availability of IL-2 regulate outcome. For instance, upon antigen encounter during infection IL-2 promotes development of naïve CD8 T cells into effector cells (Pipkin et al., 2010; Liao et al., 2013) and further drives the expansion and survival of CTLs (Mitchell et al., 2010). Therefore, we analyzed the role of Arl4d in primary viral infection model and could show that Arl4d decreased accumulation and expansion of antigen-specific CD8 T cells in the blood, spleen and liver upon adenovirus (AdGOL) infection (Fig. 18). These data are consistent with studies mentioned above and indicates that Arl4d may regulate IL-2 in this model by limiting the availability of IL-2.

Nevertheless, we cannot exclude other processes that Arl4d could modulate, for instance apoptosis. After robust expansion, once the infection is cleared, 90-95% of effector CTLs die by apoptosis (Williams and Bevan, 2007; Stemberger et al., 2007). As we observed increased numbers of antigen-specific Arl4d-deficient CD8 T cells in AdGOL-infected

mice during the whole time investigated (until day 8), it is possible that those cells were less prone to apoptosis leading to their better survival on viral infection than wild type CD8 T cells. That would indicate higher intrinsic stability of Arl4d-deficient CD8 T cells and suggest that Arl4d could decrease CD8 T cell survival.

Another explanation might be an increased proliferation potential of Arl4d-deficient CD8 T cells. CD8 T cells require only short antigen stimulation (about 2h) to become active and further proliferate autonomously without the necessity of additional antigen stimulation (van Stipdonk et al., 2001; Wong and Pamer, 2001). Co-transfer of wild type and Arl4d-deficient T cells into the same recipient ensures that both T cell populations occupy the same environment and have access to the same antigen levels and pro-inflammatory cytokine surroundings. Also here Arl4d-deficient T cells expanded more than their wild type couterparts, suggesting that this increased expansion of Arl4d-deficient cells may be cell-intrinsically regulated. It is thought that expansion of CD8 T cells upon infection is driven by autocrine IL-2. Upon LCMV infection increased numbers of LCMV-specific CD8 T cells were observed in a chimeric system when augmented autocrine IL-2 signals were delivered (Cheng and Greenberg, 2002). Consistent with these data, it has been shown that antigen-specific IL-$2^{-/-}$ CD8 T cells, unable to produce IL-2, expanded to lesser extent upon viral infection as wild type CD8 T cells (Feau et al., 2011). As Arl4d-deficient CD8 T cells produce more IL-2, autocrine IL-2 may also lead to the observed enhanced expansion of CD8 T cells lacking Arl4d.

In summary, here, we provide evidence that Arl4d function to inhibit expansion of antigen-specific CD8 T cells upon adenoviral infection. Based on our findings, we speculate that modulation of autocrine IL-2 production might influence the expansion.

Following LCMV infection the majority of LCMV-specific effector CD8 T cells express KLRG1, a marker characterizing short-lived effector CD8 T cells (SLEC) (Joshi et al., 2007). These SLEC can be distinguished from memory precursors (MPEC) by their surface expression of KLRG1 and CD127 (SLEC are $KLRG1^{high}CD127^{low}$). In our study, we examined development of $KLRG1^{high}CD127^{low}$ CD8 T cells and found that both transferred wild type and Arl4d-deficient CD8 T cells developed into SLECs upon AdGOL infection. Interestingly, higher percentages and numbers of CD8 T cells expressed KLRG1 when Arl4d was lacking, indicating that Arl4d could limit effector CD8 T cell development (Fig. 22). An important role of IL-2 signals to promote differentiation of the

SLEC population has been suggested. CD25-deficient CD8 T cells (cells lacking IL-2 receptor) showed decreased development of KLRG1^{high} CD127^{low} cells at the peak of viral and bacterial infection (Obar et al., 2010; Pipkin et al., 2010). Thus, Arl4d may limit SLEC development by modulating IL-2 production during infection.
Expression of the transcription factor T-bet correlates with SLEC development and clonal expansion, whereas MPEC development depends on Eomes expression (Joshi et al., 2007; Takemoto et al., 2006). LSEC-primed CD8 T cells, in which Arl4d is overexpressed, express Eomes but not T-bet (Böttcher et al., 2013). Although we did not analyze T-bet expression in Arl4d-deficient SLEC, we did observe increased SLEC development when Arl4d was absent, suggesting that Arl4d could down modulate T-bet expression and thereby dampen effector T cell differentiation and/or expansion.

Take together, the present work shows that the unique differentiation state of LSEC-primed CD8 T cells requires integration of co-inhibitory PD-L1/PD-1 signaling for 36 hours after which this particular differentiation program cannot be reversed by co-stimulatory signaling. In such LSEC-primed T cells the small GTPase Arl4d is PD-L1-dependently induced, which may have a more general role in T cell immunity via regulating IL-2 availability. Therefore, Arl4d might play an important, as-yet undiscovered, role in the inhibitory PD-L1/PD-1 pathway and possibly serve as a modulator of CD8 T cell immune responses.

5.7 Future perspectives

In our work, we focused on the role of Arl4d in the CD8 T cells immune response on primary viral infection. After acute infection, most of the antigen-experienced CD8 T cells (90-95%) undergo apoptosis, however, a small percentage survives and forms a long-lived memory population (Obar et al., 2008; Stemberger et al., 2007; Kaech and Wherry, 2007). IL-2 signals in the primary infection are required not only for the development but also for the function of memory CD8 T cells on secondary infection (Mitchell et al., 2010; Pipkin et al., 2010). In addition, not IL-2 produced by DCs or CD4 T cells is crucial for the secondary expansion but the autocrine IL-2 produced by CD8 T cells (Feau et al., 2011). Based on our and those findings we assume that Arl4d might also affect the memory formation during primary infection and memory CD8 T cell

expansion during the secondary infection. Therefore, future studies should focus on the aspect of memory formation.

Here, we demonstrate the role of Arl4d in dampening of IL-2 production in CD8 T cells, However, we have not investigated whether Arl4d plays role in the development or functionality of other cell populations. Although Arl4d does not influence CD4/CD8 distribution both in the thymus (data not shown), spleen or blood, we have not investigated particular subpopulations, including Tregs. Natural Treg (nTreg) precursors (CD4SP $CD25^{hi}$) require IL-2 signaling for the upregulation of Foxp3 expression and their further expansion (Malek et al., 2002; Lio and Hsieh, 2008). Moreover, IL-2 is crucial for the maintenance of nTregs in the periphery and their functionality (Setoguchi et al., 2005; Fontenot et al., 2005). Apart from nTregs, IL-2 is essential for the development of Tregs from conventional CD4 T cells in the periphery (inducible Tregs, iTregs) (Almeida et al., 2002). Here besides TCR signaling, Foxp3 expression is induced by TGF-β and this process is strongly IL-2-dependent (Davidson et al., 2007). Interestingly, iTregs express high levels of PD-1 and recent studies showed the role of PD-L1/PD-1 pathway in the development of iTregs (Francisco et al., 2009). As Arl4d expression is induced on PD-L1/PD-1 interaction, it would be interesting to investigate whether Arl4d influences the development of Tregs and whether it plays a role in central and peripheral tolerance.

6 References

Alarcon, B., Mestre, D., Martinez-Martin, N. (2011). The immunological synapse: a cause or consequence of T-cell receptor triggering? Immunology *133*, 420–425.

Allenspach, E.J., Cullinan, P., Tong, J., Tang, Q., Tesciuba, A.G., Cannon, J.L., Takahashi, S.M., Morgan, R., Burkhardt, J.K., Sperling, A.I. (2001). ERM-dependent movement of CD43 defines a novel protein complex distal to the immunological synapse. Immunity *15*, 739-750.

Anderson, M.S., Venanzi, E.S., Klein, L., Berzins, S.P., Turley, S.J., von Boehmer, H., Bronson, R., Dierich, A., Benoist, C., Mathis, D. (2002). Projection of an immunological self shadow within the thymus by the aire protein. Science *298*, 1395-1401.

Arens, R., and Schoenberger, S.P. (2010). Plasticity in programming of effector and memory CD8 T-cell formation. Immunol Rev *235*, 190-205.

Babich, A., Li, S., O'Connor, R.S., Milone, M.C., Freedman, B.D., Burkhardt, J.K. (2012). F-actin polymerization and retrograde flow drive sustained PLCγ1 signaling during T cell activation. J Cell Biol *197*, 775-787.

Barber, D.L., Wherry, E.J., Masopust, D., Zhu, B., Allison, J.P., Sharpe, A.H., Freeman, G.J., Ahmed, R. (2006). Restoring function in exhausted CD8 T cells during chronic viral infection. Nature *439*, 682-687.

Bazhin, A.V., von Ahn, K., Maier, C., Soltek, S., Serba, S., Diehl, L., Werner, J., Karakhanova, S. (2014). Immunological in vivo effects of B7-H1 deficiency. Immunol Lett *162*, 273-286.

Belkaid, Y., and Tarbell, K. (2009). Regulatory T cells in the control of host-microorganism interactions. Annu Rev Immunol *27*, 551-589.

Biermann, K., Heukamp, L.C., Steger, K., Zhou, H., Franke, F.E., Sonnack, V., Brehm, R., Berg, J., Bastian, P.J., *et al.* (2007). Gene-wide expression profiling reveals new insights into pathogenesis and progression of testicular germ cell tumors. Cancer Genomics Proteimics *4*, 359-67.

Bilate, A.M., and Lafaille, J.J. (2012). Induced CD4+ Foxp3+ regulatory T cells in immune tolerance. Annu Rev Immunol *30*, 733-758.

Blum, J.S., Wearsch, P.A., Cresswell, P. (2013). Pathways of antigen processing. Annu Rev Immunol *31*, 443-73.

Boshans, R.L., Szanto, S., van Aeist, L., D'Souza-Schorey, C. (2000). ADP-ribosylation factor 6 regulates actin cytoskeleton remodeling in coordination with Rac1 and RhoA. Mol Cell Biol *20*, 3685-94.

Boyman, O., and Sprent, J. (2012). The role of interleukin-2 during homeostasis and activation of the immune system. Nat Rev Immunol *12*, 180-190.

Böttcher, J.P., Schanz, O., Garbers, C., Zaremba, A., Hegenbarth, S., Kurts, C., Beyer, M., Schultze, J.L., Kastenmüller, W., Rose-John, S., Knolle, P.A. (2014). IL6 trans-signaling-dependent rapid development of cytotoxic CD8+ T cell function. Cell Rep *8*, 1318-1327.

Böttcher, J.P., Schanz, O., Wohlleber, D., Abdullah, Z., Debey-Pascher, S., Staratschek-Jox, A., Höchst, B., Hegenbarth, S., Grell, J., Limmer, A., *et al.* (2013). Liver-primed memory T cells generated under noninflammatory conditions provide anti-infectious immunity. Cell Rep *3*, 779-795.

Braet, F., and Wisse, E. (2002). Structural and functional aspects of liver sinusoidal endothelial cell fenestrae: a review. Comp Hepatol *23*, 1.

Brahmer, J.R., and Pardoll, D.M. (2013). Immune checkpoint inhibitors: making immunotherapy a reality for the treatment of lung cancer. Cancer Immunol Res *1*, 85-91.

Brossard, C, Feuillet, V, Schmitt, A, Randriamampita, C, Romao, M, Raposo, G, Trautmann, A. (2005). Multifocal structure of the T cell–dendritic cell synapse. Eur J Immunol, *35*, 1741–1753.

Burd, C.G., Strochlic, T.I., Gangi Setty, S.R. (2004). Arf-like GTPases: not so Arf-like after all. Trends Cell Biol *14*, 687-694.

Campi, G., Varma, R., Dustin, M.L. (2005). Actin and MHC-peptide complex-dependent T cell receptor microclusters as scaffolds for signaling. J Exp Med *202*, 1031-1036.

Casanova, J.E. (2007). Regulation of Arf activation: the Sec7 family of guanine nucleotide exchange factors. Traffic *8*, 1476-1485.

Chaudhry, A., Samstein, R.M., Treuting, P., Liang, Y., Pils, M.C., Heinrich, J.M., Jack, R.S., Wunderlich, F.T., Brüning, J.C., *et al.* (2011). Interleukin-10 signaling in regulatory T cells is required for suppression of Th17 cell-mediated inflammation. Immunity *34*, 566-578.

Chen, L. (2004). Co-inhibitory molecules of the B7-CD28 family in the control of T-cell immunity. Nat Rev Immunol *4*, 336-347.

Cohen, L.A., Honda, A., Varnai, P., Brown, F.D., Balla, T., Donaldson, J.G. (2007). Active Arf6 recruits ARNO/cytohesin GEFs to the PM by binding their PH domains. Mol Biol Cell *18*, 2244-2253.

Crispe, I.N. (2003). Hepatic T cells and liver tolerance. Nat Rev Immunol *3*, 51-62.

Cui, W., and Kaech, S.M. (2010). Generation of effector CD8+ T cells and their conversion to memory T cell. Immunol Rev *236*, 151-166.

Custinger, J.M., Valenzuela, J.O., Agarwal, P., Lins, D., Mescher, M.F. (2005). Type I IFNs provide a third signal to CD8 T cells to stimulate clonal expansion and differentiation. J Immunol *174*, 4465-4469.

Dai, S., Jia, R., Zhang, X., Fang, Q., Huang, L. (2014). The PD-1/PD-Ls pathway and autoimmune diseases. Cell Immunol *290*, 72-79.

Day, C.L., Kaufmann, D.E., Kiepiela, P., Brown, J.A., Moodley, E.S., Reddy, S., Mackey, M.W., Miller, J.D., Leslie, A.j., DePierres, C., Mncube, Z., *et al.* (2006). PD-1 expression on HIV-specific T cells is associated with T-cell exhaustion and disease progression. Nature *443*, 350-354.

Davey, G.M., Kurts, C., Miller, J.F., Bouillet, P., Strasser, A., Brooks, A.G., Carbone, F.R., Heath, W.R. (2002). Peripheral deletion of autoreactive CD8 T cells by cross-presentation of self-antigen occurs by a Bcl-2-inhibitable pathway mediated by Bim. J Exp Med *196*, 947-955.

Delon, J., Kaibuchi, K., Germain, R.N. (2001). Exclusion of CD43 from the immunological synapse is mediated by phosphorylation-regulated relocation of the cytoskeletal adaptor moesin. Immunity *15*, 691-701.

Depoil, D., and Dustin, M.L. (2014). Force and affinity in ligand discrimination by the TCR. Trends Immunol *35*, 597-603.

Diehl, L., Schurich, A., Grotchmann, R., Hegenbarth, S., Chen, L., Knolle, P.A. (2008). Tolerogenic maturation of liver sinusoidal endothelial cells promotes B7-homolog 1-dependent CD8+ T cell tolerance. Hepatology *47*, 296-305.

Donaldson, J.G., Multiple roles for Arf6: sorting, structuring, and signaling at the plasma membrane. J Biol Chem *278*, 41573-6.

Donaldson, J.G., and Jackson, C.L. (2011). ARF family G protein and their regulators: roles of membrane transport, development and disease. Nat Rev Mol Cell Biol *12*, 362-375.

D'Souza-Schorey, C., and Chavrier, P. (2006). ARF proteins: roles in membrane traffic and beyond. Nat Rev Mol Cell Biol *7*, 347-358.

Duchez, S., Rodrigues, M., Bertrand, F., Valitutti, S. (2011). Reciprocal polarization of T and B cells at the immunological synapse. J Immunol *187*, 4571-4580.

Fisher, P.J., Bulur, P.A., Vuk-Pavlovic, S., Prendergast, F.G., Dietz, A.B. (2008). Dendritic cell microvilli: a novel membrane structure associated with the multifocal synapse and T cell clustering. Blood *112*, 5037-5045.

Freeman, G.J., Wherry, E.J., Ahmed, R., Sharpe, A.H. (2006). Reinvigorating exhausted HIV-specific T cells PD-1- PD-1 ligand blockade. J Exp Med *203*, 2223-2227.

Fooksman, D.R., Vardhana, S., Vasiliver-Shamis, G., Liese, J., Blair, D.A., Waite, J., Sacristan, C., Victora, G.D., Zanin-Zhorov, A., Dustin, M.L. (2010). Functional anatomy of T cell activation and synapse formation. Annu Rev Immunol *28*, 79-105.

Fujii, S., Matsumoto, S., Nojima, S., Morii, E., Kikuchi, A. (2014). Arl4c expression in colorectal and lung cancers promotes tumorigenesis and may represent a novel therapeutic target. Oncogene *34*, 4834-4844.

Francisco, L.M., Sage, P.T., Sharpe, A.H. (2010). The PD-1 pathway in tolerance and immunity. Immunol Rev *236*, 219-242.

Freiberg, B.A., Kupfer, H., Maslanik, W., Delli, J., Kappler, J., Zaller, D.M., Kupfer, A. (2002). Staging and resetting T cell activation in SMACs. Nat Immunol *3*, 911-917.

Gardner, D., Jeffery, L.E., Sansom, D.M. (2014). Understanding the CD28/CTLA-4 (CD152) pathway and its implications for costimulatiory blockade. Am J Transplant *14*, 1985-1991.

Gillingham, and A.K., Munro, S. (2007). The small G proteins of the Arf family and their regulators. Annu Rev Cell Dev Biol *23*, 579-611.

Goldberg, J. (1998). Structural basis of activation of ARF GTPase: mechanisms of guanine nucleotide exchange and GTP-myristoyl switching. Cell *95*, 237-248.

Goldstein, J.D., Perol, L., Zaragoza, B., Baeyenes, A., Maradon, G., Piaggio, E. (2013). Role of cytokines in thymus- versus peripherally derived-regulatory T cell differentiation and function. Front Immunol *4*, 155.

Goral, S. (2011). The three-signal hypothesis of lymphocyte activation/targets for immunosuppression. Dialysis & Transplantation *40,* 14-16.

Grakoui, A., Bromley, S.K., Sumen, C., Davis, M.M., Shaw, A.S., Allen, P.M., Dustin, M.L. (1999). The immunological synapse: a molecular machine controlling T cell activation. Science *285*, 221–227. Greenwald R.J., Freeman G.J, Sharpe A.H. (2005). The B7 family revisited. Ann Rev Immunol *23*, 515-548.

Hailman, E., Burack, W.R., Shaw, A.S., Dustin, M.L., Allen, P.M. (2002). Immature CD4+CD8+ thymocytes form a multifocal immunological synapse with sustained tyrosine phosphorylation. Immunity *16*, 839-848.

Hamilton, S.E., and Jameson, S.C. (2007). CD8+ T cell differentiation: choosing a path through T-bet. Immunity *27*, 180-182.

Heath, W.R., and Carbone, F.R. (2001). Cross-presentation, dendritic cells, tolerance and immunity. Annu Rev Immunol, *19*, 47-64.

Hogquist, K.A., Baldwin, T.A., Jameson, S.C. (2005). Central tolerance: learning self-control in the thymus. Nat Rev Immunol *5*, 772-782.

Hofmann, I., Thompson A., Sanderson, C.M., Munro, S. (2007). The Arl4 family of small G proteins can recruit the cytohesin Arf6 exchange factors to the plasma membrane. Curr Biol *17*, 711-716.

Höchst, B., Schildberg, F.A., Böttcher, J., Metzger, C., Huss, S., Turler, A., Overhaus, M., Knoblich, A., Schneider, B., Pantelis, D., *et al.* (2012). Liver sinusoidal endothelial cells contribute to CD8 T cell tolerance toward carcinoembryonic antigen in mice. Hepatology *56*, 1924-1933.

Huse, M. (2012). Microtubule-organizing center polarity and the immunological synapse: protein kinase C and beyond. Front Immunol *3*, 235.

Iwai, Y., Terawaki, S., Honjo, T. (2005). PD-1 blockade inhibits hematogenous spread of poorly immunogenic tumor cells by enhanced recruitment of effector T cells. Int Immunol *17*. 133-144.

Iwasaki, A., and Medzhitov, R. (2010). Regulation of adaptive immunity by the innate immune system. Science *15*, 327(5963), 291-295.

Janeway, C.A. Jr, and Medzhitov, R. (2002). Innate immune recognition. Annu Rev Immunol, *2*,197-221.

Ji, M., Liu, Y., Li, Q., Li, X.D., Zhao, W.Q., Zhang, H., Zhang, X., Jiang, J.T., Wu, C.P. (2015). PD-1/PD-L1 pathway in non-small-cell ling cancer and its relation with EGFR mutation. J Transl Med *13*, 5.

Kaczmarek, J., Homsi, Y., van Üum, J., Metzger, C., Knolle, P.A., Kolanus, W., Lang, T., Diehl, L. (2014). Liver sinusoidal endothelial cell-mediated CD8 T cell priming depends on co-inhibitory signaling integration over time. PLoS One *9*, e99574.

Kaech, S.M., Hemby, S., Kersh, E., Ahmed, R. (2002). Molecular and functional profiling of memory CD8 T cell differentiation. Cell *111*, 837-851.

Kanai, T., Totsuka, T., Uraushihara, K., Makita, S., Nakamura, T., Koganei, K., Fukushima, T., Akiba, H., Yagita, H., Okumura, K., Machida, U., Iwai, H., Azuma, M., Chen, L., Watanabe, M. (2003). Blockade of B7-H1 suppresses the development of chronic intestinal inflammation. J Immunol *171*, 4156-4163.

Keir, M.E., Liang, S.C., Guleria, I., Latchman, Y.E., Qipo, A., Albacker, L.A., Koulmanada, M., Freeman, G.J., Sayegh, M.H., Sharpe, A.H. (2006). Tissue expression of PD-L1 mediates peripheral T cell tolerance. J Exp Med *203*, 883-895.

Kim, Y., and Rajagopalan, P. (2010). 3D hepatic cultures simultaneously maintain primary hepatocyte and liver sinusoidal endothelial cell phenotypes. PLoS One *5*, e15456.

Klein, L., Hinterberger, M., Wirnsberger, G., Kyewski, B. (2009). Antigen presentation in the thymus for positive selection and central tolerance induction. Nat Rev Immunol *9*, 833-844.

Knolle, P.A., and Gerken, G. (2000). Local control of immune response in the liver. Immunol Rev *174*, 21-34.

Knolle, P.A., and Limmer, A. (2003). Control of immune responses by scavenger endothelial cells. Swiss Med Wkly *133*, 501-506.

Knolle, P.A., and Thimme, R. (2014). Hepatic immune regulation and its involvement in viral hepatitis infection. Gastroenterology *146*, 1193-1207.

Kolanus, W. (2007). Guanine nucleotide exchange factors of the cytohesin family and their roles in signal transduction. Immunol Rev *218*, 102-113.

Kurts, C., Robinson, B.W., Knolle, P.A. (2010). Cross-priming in health and disease. Nat Rev Immunol *10,* 403-14.

Kyewski, B., and Klein, L. (2006). A central role of central tolerance. Annu Rev Immunol *24*, 571-606.

Leach, D.R., Krummel, M.F., Allison, J.P. (1996). Enhancement of antitumor immunity by CTLA-4 blockade. Science *271*, 1734-1736.

Lee, K.H., Dinner, A.R., Tu, C., Campi, G., Raychaudhuri, S., Varma, R., Sims, T.N., Burack, W.R., Wu, H., Wang, J., Kanagawa, O., Markiewicz, M., Allen P.M., *et al.* (2003). The immunological synapse balances T cell receptor signaling and degradation. Science *14*, 1218-1222.

Lever, M., Maini, P.K., van der Merwe, P.A., Dushek, O. (2014). Phenotypic models of T cell activation. Nat Rev Immunol *14*, 619-629.

Li, C.C., Chiang, C.T., Wu, T.S., Pacheco-Rodriguez, G., Moss, J., Lee, F.J. (2007). Arl4d recruits cytohesin-2/ARNO to modulate actin remodeling. Mol Biol Cell *18*, 4420-4437.

Li, C.C., Wu, T.S., Huang, C.F., Jang, L.T., Liu, Y.T., You, S.T., Liou, G.G., Lee, F.J. (2012). GTP-binding-defective ARL4D alters mitochondrial morphology and membrane potential. PLoS One *7*, e43552.

Lichtenstein, T., Dufait, I., Bricogne, C., Lanna, A., Pen, J., Breckpot, K., Escors, D. (2012). PD-L1/PD-1 costimulation, a brake for T cell activation and a T cell differentiation signal. J Clin Cell Immunol S12, 006.

Limmer, A., Ohl, J., Kurts, C., Ljunggren, H.G., Reiss, Y., Groettrup, M., Momburg, F., Arnold, B., Knolle P.A. (2000). Efficient presentation of exogenous antigen by liver sinusoidal endothelial cells to CD8+ T cells results in antigen-specific T-cell tolerance. Nat Med *6*, 1348-1354.

Lin, C.Y., Huang, P.H., Liao, W.L., Cheng, H.J., Huang, C.F., Kuo, J.C., Patton, W.A., Massenburg, D., Moss, J., Lee, F.J. (2000). Arl4, an Arf-like that is developmentally regulated and localized to nuclei and nucleoli. J Biol Chem *275*, 37815-37823.

Lin, C.Y., Chiang, T.C., Liu, Y.T., Tsai, Y.T., Jang, L.T., Lee, F.J. (2011). ARL4A acts with GCC185 to modulate Golgi complex organization. J Cell Sci *124*, 4014-4026.
Liu H., Hu B., Xu D., Liew F.Y. (2003). CD4+CD25+ regulatory T cells cure murine colitis: the role of IL-10, TGF-beta and CTLA4. J Immunol *171*, 5012- 5017.

Limmer, A., Ohl J., Wingender, G., Berg, M., Jüngerkes, F., Schumak, B., Djandji, D., Scholz, K., Klevenz, A., Hegenbarth, S., Momburg, F., Hämmerling, G.J., Arnold, B., Knolle, P.A. (2005). Cross-presentation of oral antigens by liver sinusoidal endothelial cells leads to CD8 T cell tolerance. Eur J Immunol *35*, 2970-2981.

Lutz, M.B., and Schuler, G. (2002). Immature, semi-mature and fully mature dendritic cells: which signals induce tolerance or immunity? Trends Immunol *23*, 445-449.

Matsumoto, S., Fujii, S., Sato, A., Ibuka, S., Kagawa, Y., Ishii M., Kikuchi, A. (2014). A combination of Wnt and growth factor signaling induces Arl4c expression from epithelial tubular structures. EMBO J *33*, 702-718.

Mellman, I., and Steinman, R.M. (2001). Dendritic cells: specialized and regulated antigen processing maschines. Cell *10*, 255-258.

Mescher, M.F., Agarwal, I., Casey, K.A., Hammerbeck, C.D., Xiao, Z. Curstinger, J.M. (2007). Molecular basis for checkpoints in the CD8 T cell tolerance versus activation. Semin Immunol *19*, 153-161.

Metzger, T.C., and Anderson, M.S. (2011). Control of central and peripheral tolerance by Aire. Immunol Rev *241*, 89-103.

Monks, C.R., Freiberg, B.A., Kupfer, H., Sciaky, N. & Kupfer, A. (1998). Three-dimensional segregation of supramolecular activation clusters in T cells. Nature *395*, 82–86

Mueller, S.N., Gebhardt T., Carbone F.R., Heath W.R. (2013). Memory T cell subsets, migration patterns, and tissue residence. Annu Rev Immunol *31*, 137-161.

Murphy, K. P. (2012). Janewy's Immunobiology, 8th Edition.

Neefjes, J., Jongsma, M.L., Paul, P., Bakke, O. (2011). Towards a system understanding of MHC class I and MHC class II antigen presentation. Nat Rev Immunol *11*, 823-836.

Ochsenbein, A.F., Klenerman, P., Karrer, U., Ludewig, B., Pericin, M., Hengartner, H., Zinkernagel, R.M. (1999). Immune surveillance against a solid tumors fails because of immunological ignorance. Proc Natl Acad Sci USA *96*, 2233-2238.

Ohashi, P.S., Oehen, S., Buerki, K., Pircher, H., Ohashi, C.T., Odermatt, B., Zinkernagel, R.M., Hengartner, H. (1991). Ablation of "tolerance" and induction of diabetes by virus infection in viral antigen transgenic mice. Cell *65*, 305-317.

Parish, I.A., and Heath, W.R. (2008). Too dangerous to ignore: self-tolerance and the control of ignorant autoreactive T cells. Immunol Cell Biol *86*, 146-152.

Parish, I.A., and Kaech, S.M. (2009). Diversity in CD8+ T cell differentiation. Curr Opin Immunol, *21*, 291-297.

Parish, I.A., Rao, S., Smyth, G.K., Juelich, T., Denyer, G.S., Davey, G.M., Strasser, A., Heath, W.R. (2009). The molecular signature of CD8+ T cells undergoing deletional tolerance. Blood *113*, 4575-4585.

Pasqualato, S., Renault L., Cherfils J. (2002). Arf, Arl, Arp, and Sar proteins: a family of GTP-binding proteins with a structural device for 'front-back' communication. EMBO Rep *3*, 1035-41.

Patel, M., Chiang, T.C., Tran, V., Lee, F.J., Cote, J.F. (2011). The Arl4 family GTPase Arl4A complexes with ELMO proteins to promote actin cytoskeleton remodeling and reveals a versatile Ras-binding domain in the ELMO proteins family. J Biol Chem *286*, 38969-38979.

Pennock, G.K., and Chow, L.Q. (2015). The evolving role of immune checkpoints inhibitors in cancer treatment. Oncologist *20*, 812-822.

Pentcheva-Hoang, T., Egen, J.G., Wojnoonski, K., Allison, J.P. (2004). B7-1 and B7-2 selectively recruit CTLA-4 and CD28 to the immunological synapse. Immunity *21*, 401-413.

Peterson, P., Org, T., Rebane, A. (2008). Transcriptional regulation by AIRE: molecular mechanisms of central tolerance. Nat Rev Immunol *8*, 948-957.

Petrovas, C., Casazza, J.P., Brenchley, J.M., Price, D.A., Gostick, E., Adam, M.C., Precopio, M.L., Schacker, T., Roederer, M., Douek, D.C., Koup, R.A. (2006). PD-1 is a regulator of virus-specific CD8+ T cell survival in HIV infection. J Exp Med *203*, 2281-2292.

Piccirillo, C.A., and Shevach, E.M. (2004). Naturally-occuring CD4+CD25+ immunoregulatory T cells: central players in the arena of peripheral tolerance. Semin Immunol *16*, 81-88.

Probst, H.C., McCoy, K., Okazaki, T., Honjo, T., van den Broek, M. (2005). Resting dendritic cells induce peripheral CD8+ T cell tolerance through PD-1 and CTLA-4. Nat Immunol *6*, 280-286.

Protzer, U., Maini, M.K., Knolle, A.P. (2012). Living in the liver: hepatic infections. Nat Rev Immunol *12*, 201-213.

Ogasawara, M., Kim, S.C., Adamik, R., Togawa, A., Ferrans, V.J., Takeda, K., Kirby, M., Moss, J., Vaughan, M. (2000). Similarities in function and gene structure of cytohesin-4 and cytohesin-1, guanine nucleotide exchange factors. J Biol Chem *275*, 3221-3230.

Oh, S.J., and Santy, L.C. (2010). Differential effects of cytohesin 2 and cytohesin 3 on beta1 integrin recycling. J Biol Chem *285*, 14610-14616.

Qureshi, O.S., Zheng, Y., Nakamura, K., Attridge, K., Manzotti, C., Schmidt, E.M., Baker, J., Jeffery, L.E., Kaur, S., Briggs, Z., Hou, T.Z., Futter, C.E., *et al.* (2011). Trans-endocytosis of CD80 and CD86: a molecular basis for the cell-extrinsic function of CTLA-4. Science *332*, 600-603.

Quast, T., Tappertzhofen, B., Schild, C., Grell, J., Czeloth, N., Förster, R., Alon, R., Fraemohs, L., Dreck, K., Weber, C., *et al.* (2009). Cytohesin-1 controls the activation of RhoA and modulates integrin-dependent adhesion and migration of dendritic cells. Blood *113*, 5801-5810.

Racanelli, V., and Rehermann, B. (2006). The liver as an immunological organ. Hepatology *43*, 54-62.

Redmond, W.L., Marincek, B.C., Sherman, L.A. (2005). Distinct requirements for deletion versus anergy during CD8 T cell peripheral tolerance in vivo. J Immunol *174*, 2046-2053.

Redmond, W.L., and Sherman, L.A. (2005). Peripheral tolerance of CD8 T lymphocytes. Immunity *22*, 275-284.

Rodig, N., Ryan, T., Allen, J.A., Pang, H., Grabie, N., Chernova, T., Greenfield, E.A., Liang, S.C., Sharpe, A.H., Lichtman, A.H., Freeman, G.J. (2003). Endothelial expression of PD-L1 and PD-L2 down-regulates CD8+ T cell activation and cytolysis. Eur J Immunol *33*, 3117-3126.

Rudd, C.E., Taylor, A., Schneider, H. (2009). CD28 and CTLA-4 coreceptor expression and signal transduction. Immunol Rev *229*, 12-26.

Saito, T., and Yokosuka, T. (2006). Immunological synapse and microclusters: the site for recognition and activation of T cells. Curr Opin Immunol *18*, 305-313.

Sakaguchi, S., Yamaguchi, T., Nomura, T., Ono, M. (2008). Regulatory T cells and immune tolerance. Cell *133*, 775-787.

Sakaguchi, S., Wing, K., Onishi, Y., Prieto-Martin, P., Yamaguchi, T. (2009). Regulatory T cells: how do they suppress immune responses? Int Immunol *21*, 1105-1111.

Schmitt, E.G., Haribhai, D., Williams, J.B:, Aggarwal, P., Jia, S., Charbonnier, L.M., Yan, K., Lorier, R., Turner, A., Ziegelbauer, J., *et al.* (2012). IL-10 produced by induced regulatory T cells (iTregs) controls colitis and pathogenic ex-iTregs during immunotherapy. J Immunol *189*, 5638-5648.

Schurich, A. Böttcher, J.P., Burgdorf, S., Penzler, P., Hegenbarth, S., Kern, M., Dolf, A., Endl, E., Schultze, J., Wiertz, E., *et al* (2009). Distinct kinetics and dynamics of cross-presentation in liver sinusoidal endothelial cells compared to dendritic cells. Hepatology *50*, 909-919.

Schurich, A., Berg, M., Stabenow, D., Bottcher, J., Kern, M., Schild, H.J., Kurts, C., Schuette, V., Burgdorf, S., Diehl, L., Limmer A., Knolle P.A. (2010). Dynamic regulation of CD8 T cell tolerance induction by liver sinusoidal endothelial cells. Journal of immunology *184*, 4107-4114.

Schwartz, R.H. (2003). T cell anergy. Annu Rev Immunol *21*, 305-334.

Sharpe, A.H., and Freeman, G.J. (2002). The B7-CD28 family. Nat Rev Immunol *2*, 116-126.

Shin, H.W., and Nakayama, K. (2004). Guanine nucleotide-exchange factors for arf GTPases: their diverse functions in membrane traffic. J Biochem *136*, 761-767.

Sotomayor, E.M., Borrello, I., Tubb, E., Allison, J.P, Levitsky, H.I. (1999). In vivo blockade of CTLA-4 enhances the priming of responsive T cells but fails to prevent the induction of tumor antigen-specific tolerance. Proc Natl Acad SCi USA *96*, 11476-81.

Srinivasan, M., and Frauwirth, KA. (2009). Peripheral tolerance in CD8+ T cells. Cytokine *46*, 147-159.

Steinman R.M., and Nussenzweig M.C. (2002). Avoiding horror autotoxicus: The importance of dendritic cells in peripheral T cell tolerance. PNAS *99*, 351-358.

Stinchcombe, J.C., and Griffiths, G.M. (2003). The role oft he secretory immunological synapse in killing by CD8+ CTL. Semin Immunol *15*, 301-305.

Sun, J.C., and Bevan, M.J. (2003). Defective CD8 T cell memory following acute infection without CD4 T cell help. Science *11*, 339-342.

Sun, J.C., Williams, M.A., Bevan, M.J. (2004). CD4+ T cells are required for the maintenance, not programing of memory CD8+ T cells after acute infection. Nat Immunol *5*, 927-933.

Tang, Q., and Bluestone, J.A. (2008). The Foxp3+ regulatory T cell: a jack of all trades, master of regulation. Nat Immunol *9*, 239-244.

Thauland, T.J., and Parker, D.C. (2010). Diversity in immunological synapse structure. Immunology *131*, 466–472.

Thauland, T.J., Koguchi, Y., Wetzel, S.A., Dustin, M.L., Parker, D.C. (2008). Th1 and Th2 cells form morphologically distinct immunological synapses. J Immunol *181*. 393-399.

Thompson, A.W., and Knolle, P.A. (2010). Antigen-presenting cell function in the tolerogenic liver environment. Nat Rev Immunol *10*, 753-766.

Tokoyoda, K., Zehentmeier, S., Hegazy, A.N., Albrecht, I., Grün, J.R., Löhning, M., Radbruch, A. (2009). Professional memory CD4+ lymphocytes preferentially reside and rest in the bone marrow. Immunity *30*, 721-730.

Tseng, S.Y., Waite, J.C., Liu, M., Dustin, M.L. (2008). T cell-dendritic cell immunological synapses contain TCR-dependent CD28-CD80 clusters that recruit protein kinase C theta. J Immunol *181*, 4852-4863.

Tsuhima, F., Yao, S., Shin, T., Flies, A., Flies, S., Xu, H., Tamada, K., Pardoll, D.M., Chen, L. (2007). Interaction between B7-H1 and PD-1 determines initiation and reversal of T-cell anergy. Blood *110*, 180-185.

Vardhana, S., Choudhuri, K., Varma, R., Dustin, M.L. (2010). Essential role of ubiquitin and TSG101 protein in formation and function of the central molecular activation cluster. Immunity *32*, 531-540.

Varma, R., Campi, G., Yokosuka, T., Saito, T., Dustin, M.L. (2006). T cell receptor-proximal signals are sustained in peripheral microclusters and terminated in the central supramolecular activation cluster. Immunity *25*, 117-127.

Venanzi, E.S., Benoist, C., Mathis, D. (2004). Good riddance: Thymocyte clonal deletion prevents autoimmunity. Curr Opin Immunol *16*, 197-202.

Velu, V., Titanji, K., Zhu, B., Husain, S., Pladevega, A., Lai, L., Vanderford, T.H., Chennarredi, L., Silvestri, G., Freeman, G.J., Ahmed, R., Rao, R. (2009). Enhancing SIV-specific immunity in vivo by PD-1 blockade. Nature *458*, 206-210.

Vyas, J.M., Van der Veen, A.G., Ploegh, H.L. (2008). The known unknowns of antigen processing and presentation. Nat Rev Immunol *8*, 607-618.

Wan, Y.Y., and Flavell, R. A. (2007). 'Yin-Yang' functions of TGF-β and Tregs in immune regulation. Immunol Rev *220*, 199-213.

Weber, K.S., Weber, C., Ostermann, G., Dierks, H., Nagel, W., Kolanus, W. (2001). Cytohesin-1 is a dynamic regulator of distinct LFA-1 functions in leukocyte arrest and transmigration triggered by chemokines. Curr Biol 2001 *11*, 1969-1974.

Wennerberg, K., Rossman, K.L., Der, C.J. (2005). The Ras superfamily at a glance. J Cell Sci *118*, 843-846.

Williams, M.A., and Bevan, M.J. (2007). Effector and memory T cell differentiation. Annu Rev Immunol *25*, 171-192.

Yamauchi, J., Miyamoto, Y., Torii, T., Mizutani, R., Nakamura, K., Sanabe, A., Koide, H., Kusakawa, S., Tanoue, A. (2009). Valproic acid-inducible Arl4D and cytohesin-2/ARNO, acting through the downstream Arf6, regulate neurite outgrowth in N1E-115 cells. Exp Cell Res *315*, 2043-2052.

Yokosuka, T., Sakata-Sogawa, K., Kobayashi, W., Hiroshima, M., Hashimoto-Tane, A., Tokunaga, M., Dustin, M.L., Saito, T. (2005). Newly generated T cell receptor microclusters initiate and sustain T cell activation by recruitment of Zap70 and SLP-76. Nat Immunol *6*, 1253 – 1262.

Yokosuka, T., Takamatsu, M., Kobayashi-Imanishi, W., Hashimoto-Tane, A, Azuma, M., Saito, T. (2012). Programmed cell death 1 forms negative costimulatory microclusters that directly inhibit T cell receptor signaling by recruiting phosphatase SHP2. J Exp Med *209*, 1201-1217.

Yuseff, M-I., Pierobon, P., Reversat, A., Lennon-Dumenil, A-M. (2013). How B cell capture, process and present antigens: a crucial role for cell polarity. Nat Rev Immunol *13*, 475-486.

Zajac, A.J., Blattman, J.N., Murali-Krishna, K., Sourdive, D.J., Suresh, M., Altman, J.D., Ahmed, R. (1998) Viral immune evasion due to persistence of activated T cells without effector function. J Exp Med. *188*, 2205–2213.

Zhu, J., Hidehiro, Y., Paul, W.E. (2010). Differentiation of effector CD4 T cell populations. Annu Rev Immunol *28*, 445-489.

7 Abbreviations

^{0}C	Celsius grade
Ab	antibody
AdGOL	Adenovirus expressing GFP, ovalbumin and luciferase
AIRE	autoimmune regulator
APC	antigen-presenting cell
ARF	ADP-ribosylation factor
ARL	ADP-ribosylation-like factor
B7H1	B7 homolog 1
Blimp-1	B lymphocyte–induced maturation protein-1
BSA	bovine serum albumin
CD	cluster of differentiation
CCR	CC-chemokine receptor
CCL	CC-chemokine ligand
CTL	cytotoxic T lymphocyte
CTLA-4	cytotoxic T lymphocyte antigen 4
DC	dendritic cells
DMEM	Dulbeccos Modified Eagle Medium
DP	double-positive thymocyte
EDTA	Ethylendiamintetraacetat
ELISA	Enzyme-Linked Immunosorbent Assay
ER	endoplasmic reticulum
ESCRT	endosomal sorting complex required for transport
et al.	and others (*lat. et alii*)
FACS	fluorescence activated cell sorter
GAP	GTPase-activating protein
GBSS	Gey's balanced salt solution
GEF	guanine exchange factor
GDP	guanosine *diphosphate*
GTP	guanosine *triphosphate*
GzmB	granzyme B

h	hour
HRP	horseradish peroxidase
HSC	hepatic stellate cell
ICAM-1	intracellular adhesion molecule 1
IPMC	International Phenotyping Mouse Consortium
ITIM	immunoreceptor tyrosine-based inhibition motif
ITSM	immunoreceptor tyrosine- based switch motif
IFN	interferon
Ig	immunoglobulin
IL	interleukin
i.p.	intraperitoneal
i.v.	intravenous
IS	immunological synapse
ITAM	immunoreceptor tyrosine-based activation motif
l	liter
LAT	linker for activation of T cells
Lck	lymphocyte-specific protein tyrosine *kinase*
LCMV	lymphocytic choriomeningitis virus
LFA-1	lymphocyte function-associated antigen 1
LPS	lipopolysaccharide
LSEC	liver sinusoidal endothelial cells
µ	micr*o*
m	mili
M	Molar
MACS	magnetic activated cell sorter
min	minutes
mRNA	messenger ribonucleic acid
mTEC	medullary thymic epithelial cell
MHC	major histocompatibility complex
MHC I	MHC class I molecules
MHC II	MHC class II molecules
MTOC	microtubule network position microtubule organization center

n	nano
NF-κB	nuclear factor 'kappa-light-chain-enhancer' of activated B cells
NK	natural killer cells
NKT	natural killer T cell
NLS	nuclear localization signal
OD	optical density
OVA	ovalbumin
OXPHOS	mitochondrial oxidative phosphorylation
PAMP	pathogen-associated molecular pattern
PBS	phosphate buffered saline
PD-1	programmed cell death 1
PD-L	programmed cell death ligand
PFA	paraformaldehyde
PFU	plaque forming units
PI3K	phosphatidylinositol 3-kinase
PKCθ	protein kinase C-theta
PLCγ	phospolipase C-gamma
PMA	Phorbol-12-myristate-13-acetate
POX	peroxidase
PRR	pattern recognition receptor
rpm	revolutions per minute
ROI	region of interest
ROS	reactive oxygen species
RT	room temperature
s	seconds
SD	standard deviation
SEM	standard error of the mean
SHP-2	Src homology 2 (SH2)-domain-containing protein tyrosine phosphatase 2
SLP-76	Src homology 2 (SH2) domain-containing leukocyte phosphoprotein of 76 kDa
SMAC	supramolecular activation cluster

SP	single-positive thymocytes
TBS	tris buffered saline
TCR	T cell receptor
TGFβ	transforming growth factor-beta
TGN	*trans*-Golgi network
Th1	type 1 T helper cells
Th2	type 2 T helper cells
TIRF	total internal reflection fluorescence microscopy
TLR	Toll-like receptor
TNF	tumor-necrosis factor
TRA	tissue-restricted antigen
Treg	T regulatory cell
nTreg	natural T regulatory cell
iTreg	inducible T regulatory cell
VPA	valproic acid
ZAP-70	non-receptor tyrosine kinase ζ-associated protein of 70 kDa

Table of Figures

Figure 1. Immunological synapse structures 5
Figure 2. Schematic overview of liver microarchitecture. 17
Figure 3. Schematic GDP-GTP cycle of Arf (Shin and Nakayama, 2004; modified). 21
Figure 4. Schematic structure of Arf protein (Gillingham and Munro, 2007). 22
Figure 5. Schematic structure of wild type Arl4d and its mutants (Li et al., 2007)..... 24
Figure 6. Naive CD8 T cell-LSEC interaction resembles a multifocal synapse. 49
Figure 7. The absence of PD-L1 signaling did not prevent multifocal synapse formation. 51
Figure 8. Schematic view of TIRF illumination principle (Mattheyses et al., 2010). 51
Figure 9. TCRβ and CD11a distribution in naïve CD8 T cell/LSEC interaction is not affected by PD-L1-dependent signals. 53
Figure 10. PD-L1/PD-1 signaling suppresses IL-2 production in LSEC-primed T cells. . 54
Figure 11. CD28 co-stimulation cannot reverse the induction of LSEC-primed CD8 T cells after PD-1 signal integration over time. 56
Figure 12. Arl4d expression is not detected in DC-stimulated CD8 T cells but upregulated in LSEC-primed CD8 T cells. 58
Figure 13. PD-L1-dependent expression of Arl4d in LSEC-primed CD8 T cells. 58
Figure 14. Arl4d expression is downregulated in activated CD8 T cells. 59
Figure 15. Schematic view of the "knock-out first" Arl4d$^{tm1a(EUCOMM)Wtsi}$ allele. 60
Figure 16. Arl4d-deficiency has no impact on CD8 T cell phenotype in steady state..... 61
Figure 17. Arl4d deficiency leads to enhanced IL-2 production. 62
Figure 18. Increased expansion of Arl4d-deficient CD8 T cells in the blood during viral infection. 64
Figure 19. Arl4d dampens IL-2 production *in vivo*. 65
Figure 20. Arl4d-deficient CD8 T cells demonstrate a stronger potential for expansion in the blood in competition with wild type CD8 T cells in response to infection. 67
Figure 21. Increased expansion of Arl4d-deficient CD8 T cells in the organs. 68
Figure 22. Arl4d inhibits effector T cell differentiation upon viral infection. 70
Figure 23. Arl4d dampens IL-2 and IFNγ production by CD8 T cells after restimulation. 71

Acknowledgements

My sincere thanks go to Prof. Linda Diehl for giving me an opportunity to work on this interesting project. Thank you for the scientific disussions, your constant support, encouragement and trust in my work. I am greateful for your supervision and great work atmosphere that contributed to my development as a scientist.

I would like also to thank Prof. Dr. Percy Knolle for giving me an opportunity to work in his research group and for his advices during my research.
Furthermore, I would like to thank Prof. Dr. Thorsten Lang for the cooperation and for being the second reviewer of my PhD thesis; Prof. Dr. Waldemar Kolanus for the cooperation and together with Prof. Dr. Anton Bovier for reviewing my thesis.

I would especially like to thank my group member Christina Metzger. I am greatful for her constant laboratory assistance, support and for the great work atmosphere. Special thanks go also to the former group member Dr. Bastian Höchst for his advices, support during my research work and discussions on my thesis.

I would like to thank Yvonne Gäbel for her help during my research, for the great office atmosphere and our Italy trips. I would like also to thank Michaela Wittlich for working together on LSEC isolation, for her advices and great work atmosphere. Furthermore, I would like to thank all collegues from AG Knolle, AG Kurts, AG Garbi, AG Kastenmüller and AG Endl for spending a great time in the lab as well as private after work.

I would like also to thank Dr. Zeinab Abdullah, Dr. Jan Böttcher, Prof. Natalio Garbi and Prof. Wolfgang Kastenmüller for their advices and helpful discussions on my research. Furthermore, I would like to thank Andreas Dolf and Peter Wurst from Core Facility for the great help in cell sorting and helpful discussions on my FACS data.

I would like to acknowledged Dr. Yahya Homsi and Dr. Jan van Üüm from Department of Membrane Biochemistry at LIMES Institute for the great help in performing TIRF microscopy. Furthermore, I would like to thank Dr. Thomas Quast from Department of

Molecular Immunology and Cell Biology at LIMES Institute for the help in performing confocal microscopy.

My sincere thanks go to Dr. Anja Förster for her support in writing this thesis. Thank you for your corrections and helpful suggestions during the last months.

Most importantly, I would like to thank my family and friends. Does not matter if they were right next to me or 1000 km away, I felt their love and support. I especially thank my husband Daniel Mikulec for his encouregment and for believing in me. My greatest thanks go to my mother Maria Kaczmarek for giving me the freedom to choose my own way in life and support me on every step.

Thank you all!!!